Finanziato dall'Unione europea NextGenerationEU

MUR Ministero dell'Università e della Ricerca

Italiadomani PIANO NAZIONALE DI RIPRESA E RESILIENZA

Università di Foggia

Corso di Dottorato in

Biotechnology and smart practices for a sustainable management of natural resources, food and agriculture

---

XXXVIII ciclo

Integrating statistical modelling and microbial bioremediation for sustainable polluted soil management: *Pseudomonas*-based strategies within a circular economy framework

Tutor

Prof.ssa Milena Sinigaglia

Dottorando

Alessandro De Santis

Co-tutor

Prof. Antonio Bevilacqua

Anno Accademico 2024/2025

"Finanziato dall'Unione europea – Next Generation EU" - PNRR - Missione 4C2 - I.3.3 Dottorati Innovativi

TABLE OF CONTENT

Comprehensive abstract

This PhD research was developed within Mission 2, Component 1 (M2C1) of the Italian National Recovery and Resilience Plan (PNRR), focused on efficient waste management and the circular economy transition. The study was motivated by the increasing occurrence of illegally dumped urban and industrial waste in several areas of Southern Italy, particularly in the province of Foggia. Such uncontrolled disposal practices have led to the accumulation of heavy metals and other pollutants in soils, severely compromising soil quality, biodiversity, and ecological functions. These contaminated areas represent a tangible consequence of inefficient waste management and highlight the need for sustainable remediation strategies within a circular economy framework.

The main objective of the work was to design a holistic model for the sustainable management and restoration of soils impacted by illegal waste dumping, integrating statistical modelling and microbial biotechnologies. The research includes four complementary studies that progressively connect ecotoxicological assessment, microbial characterization, and functional validation of bioremediation strategies.

The first study consists of a systematic literature review (PRISMA 2020) focused on microbial heavy-metal bioremediation, especially by *Pseudomonas* spp. The analysis of 41 recent papers (2022–2025) revealed the lack of standardized methodologies and emphasized the need for quantitative models correlating metal contamination with microbial responses.

Based on these findings, a new integrated statistical index (SPERI – Standardized Potential Ecological Risk Index) was developed to evaluate soil ecological risk by combining chemical and microbiological data. Applied to soils contaminated by illegally dumped waste in the Foggia area, SPERI provided a standardized classification framework and demonstrated strong correlations between heavy metal concentration and microbiota composition.

Subsequently, one hundred indigenous *Pseudomonas* isolates were obtained from the same sites and screened for phenotypic, enzymatic, and tolerance traits under multiple chemical and environmental stresses. This analysis revealed a high degree of functional variability and the presence of strains naturally selected for multi-metal resistance.

The most promising isolates were further tested for metal removal efficiency (Cu, Pb, Cr) and identified through 16S rRNA sequencing. Several strains achieved removal rates between 70 and 90%, confirming their potential use as biological agents in sustainable soil bioremediation.

Taken together, these studies form a coherent and interconnected framework that translates theoretical evidence into applied outcomes. The result is a circular environmental management model that integrates risk assessment, microbial adaptation, and biotechnological application to foster the ecological regeneration of soils contaminated by illegal waste dumping, fully consistent with the sustainability goals and innovation principles of the PNRR M2C1.

Sommario

Questo progetto di dottorato è stato sviluppato nell'ambito della Missione 2, Componente 1 (M2C1) del Piano Nazionale di Ripresa e Resilienza (PNRR), dedicata alla gestione efficiente dei rifiuti e alla transizione verso un'economia circolare. Il lavoro nasce dalla crescente diffusione di abbandoni incontrollati di rifiuti urbani e industriali in diverse aree dell'Italia meridionale, in particolare nella provincia di Foggia. Queste pratiche illecite hanno determinato l'accumulo di metalli pesanti e altri contaminanti nei suoli, compromettendo in modo significativo la qualità del suolo, oltre che la sua biodiversità e le relative funzioni ecologiche. Le aree contaminate rappresentano una conseguenza concreta delle criticità nella gestione dei rifiuti e rendono evidente la necessità di strategie di risanamento sostenibili, in linea con i principi dell'economia circolare.

L'obiettivo principale del lavoro è stato la definizione di un modello olistico per la gestione sostenibile e il ripristino dei suoli impattati dall'abbandono illecito di rifiuti, integrando modellazione matematica e tecniche statistiche multivariate con biotecnologie microbiche. La tesi è composta di quattro studi complementari che collegano progressivamente la valutazione ecotossicologica, la caratterizzazione microbica e la validazione funzionale di strategie di biorisanamento. Nel loro insieme, questi elementi concorrono a valorizzare i siti contaminati da rifiuti prescindendo dalla logica di considerarli semplici passività ambientali, usandoli, al contrario, come serbatoi di risorse biologiche utili alla loro stessa rigenerazione, in un'ottica di gestione e valorizzazione circolare del rifiuto.

Il primo studio consiste in una revisione sistematica della letteratura secondo le linee guida PRISMA 2020, focalizzata sul biorisanamento microbico di metalli pesanti, con particolare attenzione al genere *Pseudomonas*. L'analisi di 41 articoli recenti (2022–2025) ha evidenziato la mancanza di metodologie standardizzate e la necessità di modelli quantitativi in grado di correlare i livelli di contaminazione metallica con le risposte microbiche.

Sulla base di queste evidenze, è stato sviluppato un nuovo indice statistico integrato (SPERI – Standardized Potential Ecological Risk Index) per valutare il rischio ecologico dei suoli combinando dati chimici e microbiologici. Lo SPERI, applicato ai suoli contaminati da rifiuti abbandonati illegalmente nell'area di Foggia per una prima valutazione di efficacia, ha fornito una classificazione standardizzata e ha mostrato forti correlazioni tra concentrazioni di metalli pesanti e composizione del microbiota.
Successivamente sono stati isolati cento ceppi autoctoni di *Pseudomonas* provenienti dagli stessi siti e sottoposti a screening fenotipico, enzimatico e di tolleranza in condizioni di stress chimico e ambientale. L'analisi ha evidenziato un'elevata variabilità funzionale e la presenza di ceppi naturalmente selezionati per la resistenza multi-metallo.
I ceppi più promettenti sono stati poi testati per l'efficienza di rimozione di metalli (Cu, Pb, Cr) e identificati mediante sequenziamento del gene 16S rRNA. Diversi isolati hanno raggiunto percentuali di rimozione comprese tra il 70 e il 90%, confermandone il potenziale impiego come agenti biologici per il biorisanamento sostenibile dei suoli.
Complessivamente, questi studi costituiscono un quadro coerente e integrato che traduce l'evidenza teorica in applicazioni pratiche. Il risultato è un modello di gestione ambientale circolare che unisce valutazione del rischio, adattamento microbico e applicazione biotecnologica per favorire la rigenerazione ecologica dei suoli contaminati da abbandono illecito di rifiuti, in linea con gli obiettivi di sostenibilità e con i principi di innovazione della M2C1 del PNRR.

PART I

1. General introduction

Over the past decades, the intensification of human activities has exerted increasing pressure on terrestrial ecosystems, particularly on soil, a finite and non-renewable resource essential for food security, ecosystem stability, and human well-being, as well as for health and food safety. In several regions of Southern Italy—most notably in the province of Foggia—large tracts of land have been degraded by illegal and uncontrolled dumping of urban, industrial, and agri-food waste. These practices, often conducted outside authorized management systems, have caused the accumulation of heavy metals (Pb, Cd, Cr, Cu, Zn, Ni) and persistent organic pollutants in the soil matrix. Such contamination has led to severe chemical and biological degradation, loss of fertility, and alterations in microbial biodiversity, ultimately posing risks to food safety and human health. Beyond local effects, this situation reflects broader inefficiencies in the national waste-management chain, where the absence of integrated approaches translates into both environmental and socio-economic losses. In this context, waste-impacted soils are not only endpoints of a failing waste-management chain, but they could be also potential reservoirs of biologically mediated remediation capacity that can be strategically integrated into circular waste-valorisation pathways.

The National Recovery and Resilience Plan (PNRR), established within the European Union's *Next Generation EU* framework, addresses these weaknesses through a comprehensive ecological-transition strategy. Within this plan, Mission 2 – "Green Revolution and Ecological Transition," Component M2C1 ("Efficient Waste Management and Circular Economy") promotes technological innovation and sustainability to enhance waste valorization and minimize environmental impact. The PNRR explicitly calls for actions that close the waste cycle, integrate environmental monitoring, and remediate contaminated sites. Illegal dumping and the resulting soil degradation directly contradict these objectives, representing the endpoint failure of inefficient waste management. Therefore, the restoration and

functional recovery of contaminated soils form an essential component of the circular-economy vision outlined in Mission M2C1.

From this perspective, the doctoral research presented in this thesis was designed as an activity fully consistent with the objectives of the PNRR M2C1, contributing to the development of scientific tools for sustainable waste-related soil management. The study focuses on the creation of an integrated model for assessing, classifying, and biologically restoring soils impacted by illegal waste dumping, combining statistical–ecological modelling and microbial biotechnology. By combining predictive analytics, ecological indicators, and microbial-based remediation, this research provides operational knowledge to support decision-makers and stakeholders in designing efficient, data-driven soil-recovery strategies.

Heavy metal contamination profoundly alters the soil microbiome, a fundamental component of nutrient cycling and contaminant detoxification. Yet, microorganisms exhibit remarkable adaptability: under chemical stress they activate complex resistance and detoxification mechanisms, including ion efflux, redox transformations, EPS-mediated metal sequestration, and enzymatic reduction. Harnessing these mechanisms underlies the concept of bioremediation, i.e. the use of living organisms to mitigate contamination. Within this framework, the genus *Pseudomonas* stands out for its metabolic versatility, ecological ubiquity, and demonstrated tolerance to multiple metals. The use of indigenous *Pseudomonas* strains from contaminated environments ensures environmental compatibility and exemplifies the valorization of local biological resources within a circular-economy paradigm.

The research pathway bridges the gap between environmental diagnosis and biotechnological application, translating the objectives of Mission M2C1 into tangible scientific outputs. It demonstrates that the transition from waste to resource is achievable not only through technological recycling processes but also through biological regeneration of degraded ecosystems, thereby embodying the PNRR's principles of innovation, sustainability, and territorial resilience.

More broadly, this research aligns with the strategic priorities set by the European Green Deal, the Soil Strategy 2030, and the Zero Pollution Action Plan, all of which emphasize the need for integrated frameworks capable of restoring soil functionality in waste-impacted areas. Despite the urgency of these directives, operational tools that combine ecological, microbiological, and risk-assessment perspectives remain scarce. By addressing this gap, the present work contributes to the development of science-based approaches that support both sustainable soil management and the circular re-evaluation of waste-derived environmental pressures.

Building upon these premises, the following chapter outlines the specific aims, rationale, and structure of the thesis, detailing how each research stage contributes to the overarching objectives of the national project.

PART II

2. Aims and structure of the thesis

The main goal of this PhD project was to develop and to propose a first approach for a holistic, science-based model for the management and ecological restoration of soils contaminated by illegal waste dumping, integrating quantitative risk assessment with microbial biotechnology in line with the objectives of the PNRR Mission 2, Component 1 (M2C1).

Specifically, the research has four intermediate and interconnected goals:

1. To establish the theoretical and methodological background through a systematic review of recent literature on microbial heavy metal bioremediation, identifying mechanistic insights, current limitations, and research gaps relevant to *Pseudomonas* spp.
2. To design a quantitative and reproducible index—the Standardized Potential Ecological Risk Index (SPERI)—capable of integrating chemical and biological variables to assess the ecological risk of contaminated soils and provide a standardized framework for classification and comparison.
3. To isolate and characterize indigenous *Pseudomonas* strains from multi-contaminated soils in the Foggia area, analysing their phenotypic, enzymatic, and tolerance profiles to elucidate microbial adaptation to heavy metal stress.
4. To validate the biotechnological potential of selected strains through controlled metal-removal assays (Cu, Pb, Cr) and molecular identification, demonstrating their applicability as biological agents for sustainable soil bioremediation.

These objectives collectively address the central challenges identified in Mission M2C1:

- advancing environmental monitoring and risk evaluation through predictive and data-driven tools;
- promoting resource efficiency and circular use of biological systems;
- supporting green innovation and sustainable remediation technologies that restore ecosystem functionality;

- providing a replicable methodological framework applicable to other contaminated sites nationwide.

A transversal objective of the thesis is to demonstrate that soils impacted by illegal waste dumping can be reframed from passive environmental liabilities into active reservoirs of locally adapted microbial resources, thereby embedding waste-related soil management within a broader waste-valorisation and circular-economy framework.

The thesis is organized to reflect the logical progression from theoretical synthesis to practical application:

- **Chapter 1** introduces the environmental, regulatory, and conceptual background of the research.
- **Chapter 2** (the present one) details the aims and structure of the thesis.
- **Chapter 3** presents the systematic literature review (PRISMA), establishing the scientific foundation of the project.
- **Chapter 4** describes the development and validation of the SPERI model for ecological-risk assessment.
- **Chapter 5** reports the isolation and phenotypic characterization of *Pseudomonas* strains from contaminated soils.
- **Chapter 6** focuses on the functional validation and application of selected isolates for heavy metal removal.
- **Chapter 7** provides a general discussion and concluding remarks, highlighting the implications of the findings for circular-economy strategies and future research directions.

3. Recent advances in microbial heavy metal bioremediation: mechanistic and taxonomic insights from a PRISMA-based review focused on *Pseudomonas* spp.[1]

Alessandro De Santis, Maria Rosaria Corbo, Angela Racioppo, Antonio Bevilacqua*, Milena Sinigaglia

Department of Agriculture, Food, Natural Resources and Engineering, University of Foggia, Foggia, ITALY

Abstract

Microbial bioremediation represents an ecologically sustainable solution to heavy metal pollution. Following PRISMA 2020 guidelines, this review systematically examined studies published between 2022 and 2025, retrieved from Scopus, Web of Science, and PubMed. The analysis focuses on the taxonomic distribution, mechanistic pathways, and experimental outcomes of bacterial remediation processes, particularly those involving *Pseudomonas* spp. Results demonstrate that efflux transporters, enzymatic redox systems, and biofilm formation constitute the primary adaptive mechanisms enabling detoxification of cadmium, chrome, and lead under varying physicochemical conditions. Median removal efficiencies exceeded 70% in laboratory trials, though performance decreased markedly in real soils. Despite methodological heterogeneity, *Pseudomonas* remains the most versatile genus, combining genetic plasticity with high metabolic resilience. The study highlights the need for standardized kinetic models and multi-omics integration to bridge the current gap between laboratory-scale studies and field-level implementation.

---

[1] This chapter was published on Frontiers in Microbiology De Santis, A., Corbo, M.R., Racioppo, A., Bevilacqua, A. & Sinigaglia, M. (2026). PRISMA-based review of Pseudomonas spp. in microbial heavy-metal bioremediation: mechanisms and taxonomy. Front. Microbiol. 17:1760258. doi: 10.3389/fmicb.2026.1760258

3.1 Introduction

Heavy metal contamination remains one of the most persistent environmental threats worldwide, arising primarily from industrial effluents, mining activities, intensive agriculture, and urban waste discharge. Metals such as cadmium (Cd), lead (Pb), chromium (Cr), nickel (Ni), copper (Cu), zinc (Zn), mercury (Hg), and arsenic (As) are non-degradable and can accumulate in soils and aquatic systems over time, entering the food chain and posing severe ecological and health risks (Angon et al., 2024). Their persistence leads to long-term toxicity, oxidative stress, and metabolic disruption in plants, animals, and humans. Recent assessments indicate that approximately 14–17 % of global agricultural soils are affected by excessive heavy metal concentrations, potentially exposing more than one billion people to hazardous levels (Hou et al., 2025).

To address these concerns, multiple remediation technologies have been implemented, including chemical precipitation, ion exchange, adsorption, membrane filtration, and electrochemical treatment (Shofia et al., 2025). Although these physicochemical approaches can achieve high removal efficiencies under controlled conditions, they are often limited by high costs, secondary waste generation, and reduced effectiveness in complex or heterogeneous matrices (Ilyas et al., 2024; Oladimeji et al., 2024). Moreover, they do not restore ecological balance and can disturb soil structure or microbial functionality. Consequently, sustainable alternatives based on biological processes have gained attention as self-regulating and environmentally benign solutions.

Bioremediation, that is the use of living organisms to detoxify or immobilize contaminants, has become a central component of modern environmental biotechnology. Biological systems exploit the inherent ability of microorganisms and plants to transform pollutants into less toxic or less mobile forms. Within this framework, microbial bioremediation, using bacteria and Archaea, offers significant advantages due to its adaptability, scalability, and ability to function *in situ* under

variable physicochemical conditions (Ruan et al., 2024). Recent reviews emphasize that microorganisms represent a versatile platform for heavy metal removal in both aquatic and terrestrial environments, outperforming many traditional techniques in sustainability and cost-efficiency (Firincă et al., 2025).

Microbial communities naturally interact with metals through a combination of physicochemical and metabolic processes that promote detoxification and stabilization. Although the specific mechanisms, such as surface binding, accumulation, and transformation, differ among taxa, all rely on fundamental adaptive responses that reduce metal bioavailability and toxicity (Tang et al., 2024). The overall efficiency of microbial bioremediation depends on species composition, environmental parameters (pH, temperature, redox conditions), and metal speciation. Recent studies confirm that mixed microbial consortia frequently outperform single isolates, as interspecies cooperation enhances resilience, broadens substrate range, and stabilizes performance under fluctuating conditions (Liu et al., 2023).

A growing body of literature highlights the diversity of bacterial families capable of mediating heavy metals (HMs) remediation. Bacillaceae species exhibit strong tolerance to metals such as Pb, Cd, Hg, Cr, and Ni, owing to their robust cell envelopes and ability to function under nutrient-limited conditions. Rhodococcaceae and related Actinomycetes are known for their hydrophobic surfaces and oxidative metabolism that favor metal transformation. Shewanellaceae and Geobacteraceae can reduce metal ions through extracellular electron transport, contributing to immobilization in sediments (Tang et al., 2024). In addition, the role of extracellular polymeric substances (EPS) has been increasingly recognized as a structural and functional determinant in microbial systems, enhancing metal sequestration and biofilm stability under stress (Pan et al., 2023).

Within this microbial landscape, the family Pseudomonadaceae, particularly the genus *Pseudomonas*, stands out as a cornerstone of bacterial bioremediation. *Pseudomonas* species are cosmopolitan, fast-growing, and metabolically versatile organisms that

thrive in diverse habitats, including soils, sediments, industrial effluents, and wastewater treatment plants (Ajmi et al., 2025). They are frequently isolated from multi-metal-contaminated sites and are recognized for their exceptional resistance and detoxification capacity. Recent studies have shown that *Pseudomonas aeruginosa*, *Pseudomonas putida*, and *Pseudomonas fluorescens* can tolerate and remove various metals, including Cu, Zn, Pb, and Cr, while maintaining high growth rates under stress (Zada et al., 2025). Their ecological success is attributed to their capacity to form biofilms, secrete siderophores, and regulate gene networks associated with metal homeostasis and oxidative-stress management (Dey et al., 2025). These features not only confer resilience but also make *Pseudomonas* spp. ideal candidates for bioaugmentation and biosensing applications.

Despite the substantial progress achieved in the last decade, the current scientific landscape remains methodologically fragmented. Many studies are case-specific, focusing on individual isolates, single metals, or specific experimental conditions, with limited comparability across datasets (Ghorbani & Amirahmadi, 2025). In addition, critical operational parameters such as pH, temperature, exposure time, and analytical techniques are often inconsistently reported. This heterogeneity hampers quantitative synthesis and prevents the identification of generalizable patterns linking bacterial taxa to remediation performance. Addressing these limitations requires a rigorous and transparent framework that can harmonize experimental evidence and facilitate reproducible data interpretation.

This systematic review integrates quantitative outcomes (removal efficiency and sorption capacity), environmental variables (pH, temperature, matrix), and taxonomic distribution across bacterial families, while maintaining a focused interpretative perspective on the genus *Pseudomonas*. In addition to the experimental synthesis, a bibliometric analysis was performed using VOSviewer, which enabled visualization of the most frequent keywords, co-authorship networks, and thematic clusters emerging from the recent literature. This complementary approach provided an

overview of research trends, identifying the dominant conceptual domains and highlighting the growing scientific interest toward *Pseudomonas*-mediated heavy metal remediation. By synthesizing recent empirical evidence, this work aims to identify comparative trends among bacterial groups, outline optimal conditions for heavy metal removal, and highlight knowledge gaps that can guide future mechanistic and applied research. Ultimately, the review seeks to establish a data-driven foundation for designing scalable, efficient, and ecologically sustainable microbial bioremediation strategies, positioning *Pseudomonas* as a benchmark genus within the broader bacterial community.

3.2 Materials and methods

3.2.1 Bibliometric analysis

A bibliometric evaluation was performed using VOSviewer (v. 1.6.20) based on extracted keywords. The dataset was derived from Scopus metadata exported as a tab-delimited text file and processed to map co-occurrence relationships among author and indexed keywords.

The dataset was obtained from Scopus using the following query string:

TITLE-ABS-KEY ("microbiota" OR "bacteria" OR "microorganism*") AND TITLE-ABS-KEY ("heavy metals" OR cadmium OR lead OR chromium OR nickel OR mercury OR arsenic OR copper OR zinc) AND PUBYEAR > 2000

A threshold of minimum 50 occurrences per term was applied to ensure statistical robustness. The software generated a network visualization where node size corresponds to keyword frequency, link thickness to co-occurrence strength, and color coding to cluster affiliation.

3.2.2 Review protocol and framework

This systematic review was conducted according to the PRISMA 2020 guidelines (Page et al., 2021) to ensure transparency, reproducibility, and methodological rigor.

The protocol was defined a priori and included a description of the research question, databases, search strategy, inclusion/exclusion criteria, data-extraction procedures, and synthesis methods; the checklist is available in the *Annexes* (**Table A3.1**). The primary aim was to identify, analyze, and compare recent studies (2022–2025) addressing bacterial bioremediation of toxic HMs across environmental matrices. The central research questions were:

- Which are the bacterial genera exhibiting the highest performance in removing or transforming HMs?
- What are the environmental and operational conditions (pH, temperature, matrix) optimizing removal efficiency?
- How do study design and mechanistic characterization affect data comparability?

3.2.3 Information sources and search strategy

Three major databases, Scopus, Web of Science (WoS), and PubMed, were systematically queried to identify peer-reviewed research articles and reviews published between January 2022 and June 2025. Searches were limited to English-language publications and subject categories related to environmental science, biotechnology, and microbiology. Equivalent Boolean search strings were adapted for each database to ensure semantic and structural consistency. Minor syntactic differences were due to database-specific query syntax

Before defining the final search strings, several preliminary and more permissive query combinations were tested across the three databases. These exploratory strings included broader taxonomic and functional terms (e.g., microorganism, biodegradation, pollutant removal, metalloid detoxification) to evaluate retrieval coverage and background noise. After iterative refinement, the most specific and reproducible queries were selected and applied in the final systematic search.

The final search strings, which generated the dataset used in this review (6th text string), is reported in **Table A3.2**. The last search was performed in September 2025. Reference lists of retrieved papers were manually screened to capture additional relevant studies not indexed under the same keywords.

3.2.4 Eligibility criteria study selection

Studies were considered eligible for inclusion if they met all the following criteria.

First, only original experimental research published in peer-reviewed international journals from January 2022 onward and written in English was included. Furthermore, the following relevant parameter were used as including markers:

- Studies focused on microbial bioremediation of HMs in environmentally relevant matrices (soil, water, sediment, wastewater, or sludge).
- Focus on microorganisms served as the primary remediation agents, including both single isolates, and microbial consortia.
- Studies providing quantitative evidence of metal removal, tolerance, or biosorption, reporting at least one measurable parameter like removal percentage, adsorption capacity, minimum inhibitory concentration (MIC), or initial and/or final metal concentration.
- Studies including mechanistic or molecular characterization, demonstrating the biochemical, structural, or genetic basis of metal removal.
- Reported mechanisms like extracellular polymeric substances (EPS) production, biofilm formation, redox transformation, precipitation or biomineralization, expression of resistance genes.
- Mechanistic evidence supported by instrumental analyses (FTIR, SEM/EDS, XRD, TEM) or omics-level approaches (WGS, transcriptomics, metagenomics).

- Metagenomic or microbiome studies were included only if they provided quantitative data on genes or pathways directly involved in heavy metal detoxification or resistance.

Studies were excluded if they met one or more of the following conditions:

- Plant-centered phytoremediation – experiments in which the core remediation mechanism was plant-based, even when assisted by plant growth-promoting rhizobacteria (PGPR).
- Review or theoretical papers – including reviews, mini-reviews, opinion articles, or purely conceptual frameworks without new experimental data.
- Non-metal pollutants only – investigations limited to microplastics, antibiotics, or organic contaminants not coupled with heavy metal bioremediation.
- Lack of quantitative data – studies reporting only qualitative or descriptive outcomes without explicit numerical metrics of removal or tolerance.
- Modeling or simulation only, in silico, docking, or predictive models without experimental validation.
- Duplicate or inaccessible full text, articles not retrievable or overlapping with already included datasets.

A detailed summary of all inclusion and exclusion criteria applied in this review is provided in **Table A3.3**

3.2.5 Study Selection

All records retrieved from Scopus, Web of Science, and PubMed were exported to Microsoft Excel for centralized management. Duplicate entries were identified and removed through automated matching of DOI, title, and first author fields, followed by manual verification.

Title and abstract screening were independently performed by two reviewers according to pre-established eligibility criteria. Each record was classified as Include, Maybe, or Exclude. Disagreements were resolved through discussion until a consensus was

reached. Studies marked as Maybe were retained for full-text evaluation. The entire screening workflow and decision log were managed in a structured Excel matrix to ensure transparency and reproducibility.

Inclusion criteria required that (i) bioremediation represented the primary focus of the study, (ii) the biological system consisted of bacterial isolates or microbial consortia, (iii) at least one of the target metals was Cd, Pb, Cr, Ni, Cu, Zn, Hg, or As, (iv) quantitative removal data were reported (e.g., initial and residual concentrations, percentage removal, adsorption capacity, or kinetic parameters), (v) robust analytical methods were applied (ICP-MS, AAS, ICP-OES, SEM-EDS, FTIR, or XRD), and (vi) taxonomic identification was provided at least to the 16S rRNA gene level.

Studies were excluded if they focused exclusively on phytoremediation or non-metal pollutants (e.g., dyes, hydrocarbons, pesticides), employed aquatic or wastewater systems without soil relevance, lacked quantitative outcomes, failed to identify microorganisms, or represented reviews, commentaries, or duplicated datasets.

All records (188) retrieved from Scopus (n = 98), Web of Science (n = 86), and PubMed (n = 4) were imported into Microsoft Excel for centralized management and deduplication. Duplicate entries were identified through automated DOI matching and manually verified; 28 duplicates were removed, resulting in 160 unique studies eligible for screening.

Title, abstract, and keyword screening was independently performed by two reviewers according to the inclusion and exclusion criteria reported in **Table A3.3**. After this phase, 68 studies were considered potentially relevant and retrieved for full-text assessment. Following detailed evaluation, 41 studies met all eligibility requirements and were included in the systematic review. The main reasons for exclusion were: (i) absence of quantitative data on heavy metal removal; (ii) focus on phytoremediation or non-metal pollutants; (iii) lack of taxonomic identification; and (iv) studies not performed on soil or soil-related matrices. The complete identification, screening, and inclusion process is summarized in **Figure 3.1**, which follows the PRISMA 2020 flow-

diagram structure. The corresponding PRISMA 2020 checklist is provided in the *Annexes* (**Table A3.1**).

3.2.6 Data extraction

For each included article, a structured data-extraction form was completed to capture, when applicable:

- Bibliographic metadata: authors, year, journal, DOI
- Taxonomic data: genus, species, strain code
- Target metal(s) and initial concentration
- Matrix type (soil, effluent, sludge, synthetic medium)
- Experimental conditions: pH, temperature, contact time
- Analytical techniques (AAS, ICP-OES, ICP-MS, XRF)
- Quantitative performance metrics: removal %, q_{max}, rate constants
- Mechanistic evidence (biofilm formation, EPS, enzyme assays, redox changes)

Data were independently extracted by two reviewers and cross-checked for consistency. Discrepancies were resolved through consensus.

Figure 3.1 PRISMA 2020 flow diagram summarizing the identification, screening, eligibility, and selection process for the systematic review. A total of 188 records were initially identified across Scopus (n = 98), Web of Science (n = 86), and PubMed (n = 4). After removing 28 duplicates, 160 unique records were screened based on title, abstract, and keywords. 68 full texts were assessed for eligibility, and 41 studies met all inclusion criteria and were finally included in the review. in accordance with the PRISMA 2020 statement.

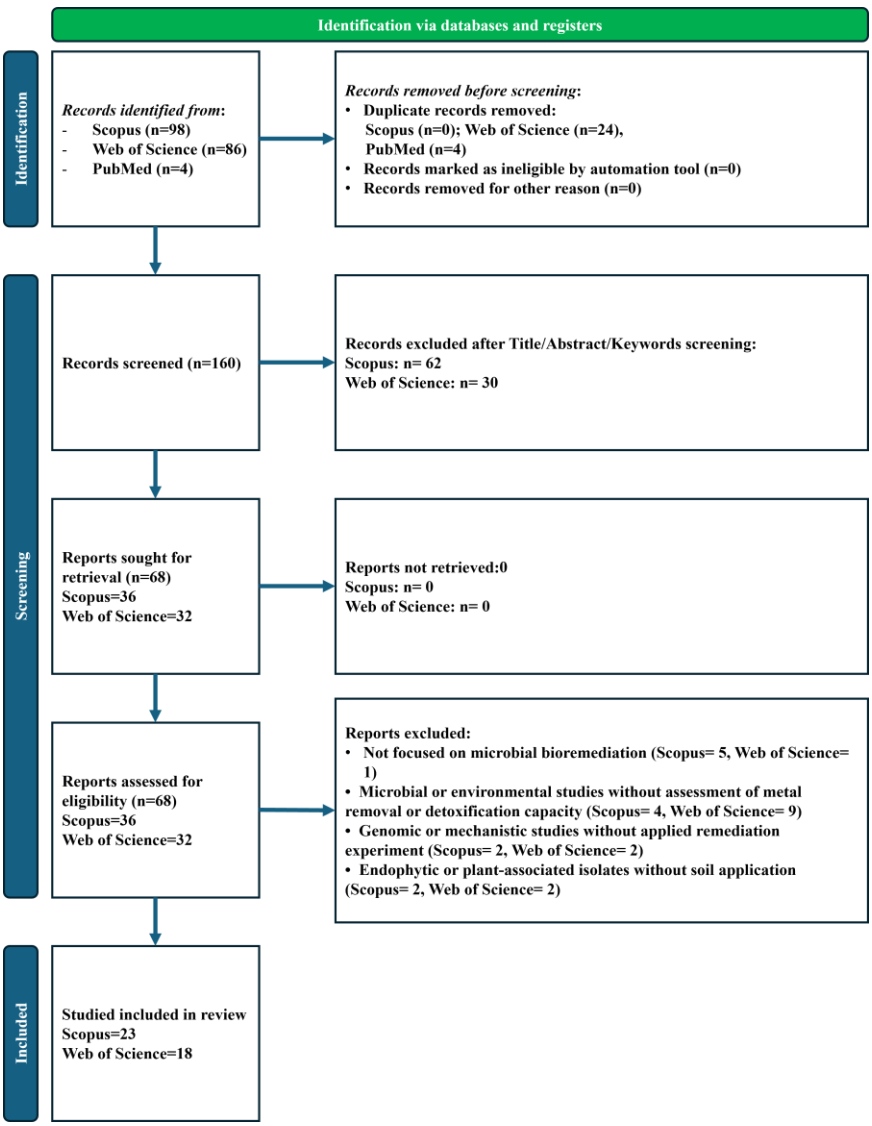

3.2.7 Quality assessment

The methodological quality of the included studies was evaluated using a modified Newcastle–Ottawa Scale (NOS) adapted for environmental and microbiological research. Each study was assessed on the following domains, as reported in **Table 3.1**. A maximum score of 10 indicated high methodological quality. Studies scoring ≥ 7 were retained for full synthesis; those below were discussed qualitatively. The results obtained by the included articles are resumed in **Table A3.4**

Table 3.1 Modified Newcastle–Ottawa Scale (NOS) criteria adapted for evaluating the methodological quality of environmental microbiology studies included in the review.

Criterion	Description	Scoring
Study design	Clear experimental setup and control conditions	0–2
Taxonomic identification	Level of bacterial identification (genus/species/strain)	0–2
Quantitative validity	Analytical precision (AAS, ICP-OES/MS, replicates)	0–2
Mechanistic characterization	Evidence of mechanism (EPS, enzymes, biofilm, redox)	0–2
Reproducibility & reporting	Complete reporting of methods and statistics	0–2

3.2.8 Data synthesis

A mixed-methods synthesis approach was applied:

- Quantitative aggregation of removal efficiencies by bacterial genus and metal type
- Qualitative thematic analysis of recurring mechanisms, experimental conditions, and ecological context

Statistical summaries (mean ± SD, range, median) and visualizations (boxplots, heatmaps) were generated in Statistica v.14 (StatSoft, Tulsa, OK).

Results were organized thematically into four domains:

1. Taxonomic distribution and frequency
2. Metal-specific performance
3. Matrix influence and environmental conditions
4. Mechanistic diversity and adaptation strategies

3.3 Results

3.3.1 Bibliometric network of keywords

The bibliometric co-occurrence analysis conducted via VOSviewer revealed a structured network of research themes within the field of microbial heavy metal bioremediation (**Figure 3.2**). Four major clusters emerged: (1) "bioremediation/HMs/removal" (red), characterised by high frequencies of nodes such as "bioremediation", "adsorption", "chromium", "biosorption"; (2) "soil pollution/microbial community" (green), containing keywords like "soil", "microbial community", "plant growth", "soil pollutants"; (3) "genetics/metabolism/bacterial taxonomy" (yellow), including "metabolism", "genetics", "*Pseudomonas*", "metal tolerance"; and (4) "environmental engineering/water/sediment" (blue), encompassing "water pollution", "sediment", "ecosystem restoration". The size of nodes (frequency of keyword occurrences) and thickness of links (co-occurrence strength) indicate that the red and green clusters are the dominant thematic domains, with "bioremediation" and "soil pollution" serving as central hubs. The dense interconnections between clusters highlight that research on microbial remediation of HMs is inherently multidisciplinary, bridging microbial physiology, soil science, pollutant removal technologies and ecosystem restoration. Notably, keywords associated with the genus *Pseudomonas* and "metal tolerance" are centrally located within the yellow cluster, thus supporting the decision to treat *Pseudomonas* as a benchmark genus in this

review. The complete list of keywords ranked by frequency and link strength is provided in **Table A3.5**.

Figure 3.2 VOSviewer network of keyword co-occurrence in microbial heavy metal bioremediation studies (2000–2025). Node size represents keyword frequency (occurrence ≥ 50) and link thickness indicates co-occurrence strength. Colors denote main thematic clusters: red (bioremediation and biosorption), green (soil pollution and microbial communities), yellow (genetics and *Pseudomonas*-related studies), and blue (environmental engineering and water/sediment remediation).

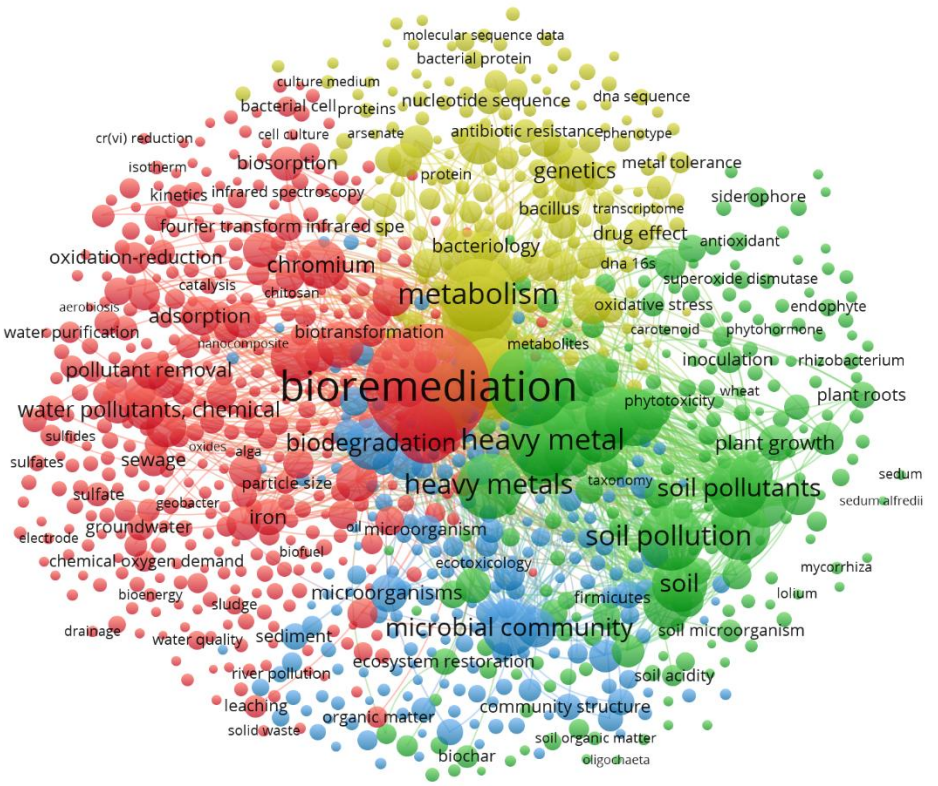

3.3.2 General overview and quantitative performance of the included studies

3.3.2.1 Dominant genera and distribution patterns

From a taxonomic standpoint, *Bacillus* spp. dominated the dataset (n=23), followed by *Pseudomonas*, *Lysinibacillus*, *Enterobacter*, and *Staphylococcus*. *Bacillus* species were the most frequently isolated from industrial or agricultural soils contaminated with Cd, Pb, or Cr, often achieving removal efficiencies above 80%. *Bacillus altitudinis* and *B. tequilensis* reached Pb removal rates close to 98% under slightly alkaline conditions (pH 7.5–8.0), whereas *B. cereus* exhibited strong Cd and Cr(VI) biosorption coupled with carbonate precipitation (Chen et al., 2025; Kaushal & Pati, 2024; Wang et al., 2025; Zuo et al., 2022). *P. aeruginosa* and *P. putida* displayed greater versatility across metal types, with efficient Cr(VI) to Cr(III) reduction (up to 95%) within 48–72 h under aerobic conditions (Dahnoun et al., 2024; Satyapal et al., 2024; Sundarraj et al., 2023). *Enterobacter* sp. further contributed through EPS-mediated binding and urease-induced mineralization of Cd, Pb, and As (Mondal et al., 2025). While mixed consortia combining *Bacillus* and *Pseudomonas* were utilized (Mungla et al., 2022), the highest efficiencies were often observed in synergistic microbial associations. For instance, the cooperation between *Bacillus thuringiensis* and *Citrobacter freundii* demonstrated a synergistic removal efficiency of 97.68% for Cd, significantly higher than the 66-88% achieved by either strain alone (Cai et al., 2025). Similarly, a bifunctional community composed of *Enterobacter* and *Bacillus* genera was constructed, which not only removed 98.0% of Cd via biomineralization (inducing CdCO3 precipitation) but also simultaneously degraded 88.3% of the organic pollutant pyrene (Lin et al., 2022). The mechanisms underpinning these synergies were linked to the induction of precipitation *via* Microbially Induced Calcite Precipitation (MICP) (Yan et al., 2024) and the upregulation of specific metabolic pathways, such as the urea cycle, which helps buffer environmental pH (Cai et al., 2025).

3.3.2.2 Metal targets and environmental context

Across contaminants, Cd and Pb were the most frequently studied metals, often investigated concurrently in co-contaminated agricultural soils (Mondal et al., 2025; Zhang et al., 2024; Zuo et al., 2022). The highly toxic hexavalent chromium (Cr(VI)) was another primary focus, particularly in studies involving industrial effluents (Elahi et al., 2022; Ye et al., 2024). Other metals, like Ni (Kashyap et al., 2022; Manikandan & Nair, 2023), Zn (Mtengai et al., 2022; Yasmin et al., 2022), and As (Mondal et al., 2025; Satyapal et al., 2024), were also investigated. The experimental contexts varied widely, from remediating agricultural soils, where the goal was often to reduce metal bioavailability and plant uptake (Dahnoun et al., 2024; Zuo et al., 2022), to the detoxification of industrial effluents (Elahi et al., 2022; Kashyap et al., 2022), and controlled aqueous laboratory systems designed to define removal mechanisms (Manikandan & Nair, 2023; Shaaban Emara et al., 2023).

3.3.2.3 Analytical approaches and experimental parameters

Analytical methods were highly consistent across the studies. Metal quantification was predominantly performed using Atomic Absorption Spectroscopy (AAS) (Bhandari et al., 2024; Dahnoun et al., 2024; Kaur et al., 2024; Surabhi et al., 2025) or ICP-MS (Cai et al., 2025; Chen et al., 2025; Liang et al., 2025). To elucidate removal mechanisms, FTIR spectroscopy was widely applied, confirming that biosorption relies on the involvement of key functional groups on the cell wall—primarily carboxyl (C=O), amino (N-H), hydroxyl (O-H), and phosphate (P=O) groups—which serve as binding sites for metal cations (Mondal et al., 2025; Yan et al., 2024; Yasmin et al., 2022). These spectroscopic findings were visually corroborated by SEM-EDS, which confirmed metal adhesion, accumulation, and morphological changes on the bacterial surface (Chen et al., 2025; Shan et al., 2024; Yan et al., 2024). Furthermore, XRD analysis was used to identify the specific crystalline nature of bioprecipitated minerals, such as $CdCO_3$ (Ghosh et al., 2024; Mondal et al., 2025; Yan et al., 2024).

3.3.2.4 Genetic determinants of metal resistance

Gene-level characterization identified bacterial tolerance determinants such as the efflux gene *chrA* and the metallochaperone *copZ* (Su et al., 2022). In plant-bacteria interaction studies, inoculation also demonstrated effects on the host plant; for example, bacterium H27 significantly reduced the expression of the plant's endogenous Cd transport genes, *HAM2* and *IRT1*, in tobacco (Gao et al., 2024). Experimental conditions were typically mesophilic, optimized around pH 6.5–8.0 (Yasmin et al., 2022, 2022) and temperatures of 28–40°C (Monga et al., 2022; Shan et al., 2024; Yasmin et al., 2022). Contact times in batch biosorption assays ranged from rapid removal within 20 hours (Zuo et al., 2022) to 5–7 days required for complete Cr(VI) reduction or maximum accumulation (Elahi et al., 2022; Su et al., 2022). Soil pot experiments assessing plant uptake necessarily lasted much longer, (e.g., 40 days) (Zhang et al., 2023).

3.3.2.5 Quantitative removal efficiencies

Quantitatively, the highest removal efficiencies were consistently recorded in systems targeting Cd, Pb, and Cr(VI) (Bhandari et al., 2024; Elahi et al., 2022; Kaushal & Pati, 2024; Lin et al., 2022; Manikandan & Nair, 2023; Mondal et al., 2025; Shaaban Emara et al., 2023). The *Bacillus* genus was a dominant and highly effective performer: *B. altitudinis* showed 96% Pb bioaccumulation efficiency (Kaushal & Pati, 2024), *B. amyloliquefaciens* achieved 99.8% Pb bioremediation (Shaaban Emara et al., 2023), and *B. cereus* removed 99% of Cr(VI) from tannery effluents (Elahi et al., 2022). Other genera also showed high potential; *Lysinibacillus cavernae* demonstrated robust Cr(VI) reduction at 76.21% under optimized conditions (Shan et al., 2024). *Pseudomonas* strains showed varied but high potential, with *P. stutzeri* immobilized on rice husk biochar removing 95% of Cd and 92% of Ni (Manikandan & Nair, 2023), although other strains showed more moderate efficiencies around 60-70% (Mtengai et al., 2022). Finally, *Enterobacter* sp. (ACP-1) achieved exceptional removal rates of

98% (Pb) and 97% (Cd) from mixed-metal solutions (Mondal et al., 2025), underscoring the high efficiencies found in non-*Bacillus* genera as well.

3.3.3 Mechanistic insights

The 41 studies reveal a consistent convergence toward six dominant functional pathways (**Figure 3.3**) governing bacterial heavy metal detoxification: EPS-mediated biosorption, biofilm-driven community resilience, enzymatic and redox transformations, biomineralization and MICP, and genetic/efflux-based regulation. These mechanisms frequently co-occur within the same strain or consortium, underscoring the multi-layered adaptability of environmental bacteria under metal stress (Manikandan & Nair, 2023; Yan et al., 2024).

Figure 3.3 Summary of the dominant heavy metal detoxification mechanisms identified across the dataset (n=41 studies), their frequency of occurrence, and the most representative bacterial genera associated with each pathway.

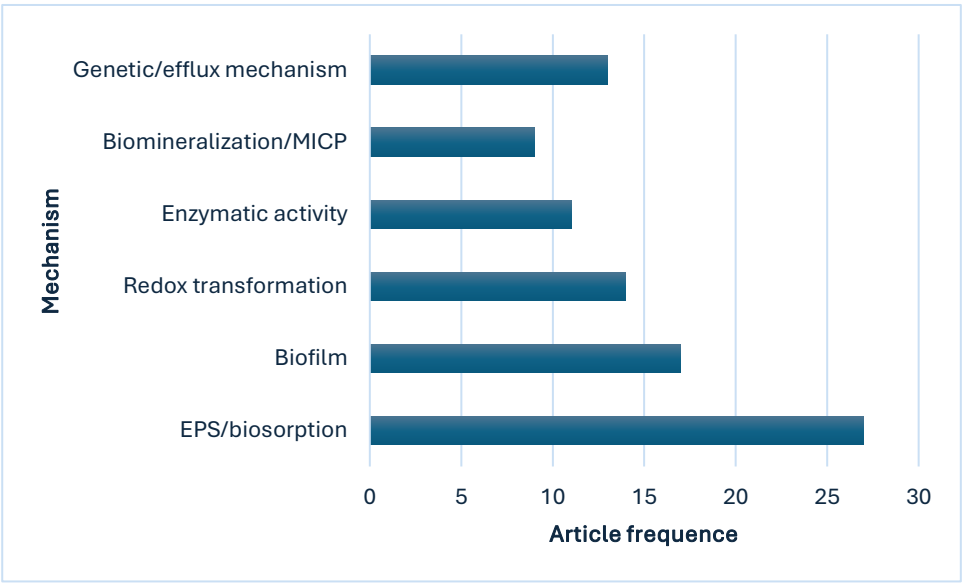

EPS-mediated biosorption represented the most widespread process, documented in more than 60% of the studies. EPS secreted by *Bacillus*, *Enterobacter*, and other species provided abundant binding sites capable of complexing Pb^{2+}, Cd^{2+}, and Ni^{2+} ions (Chen et al., 2025; Mondal et al., 2025; Wang et al., 2025). FTIR and SEM-EDS analyses consistently identified these functional groups (such as carboxyl, amino, and phosphate groups) and confirmed their participation in surface complexation (Mitra et al., 2025; Yan et al., 2024; Yasmin et al., 2022). The strong correlation between EPS density and removal efficiency explains the high performance of *Bacillus* in direct biosorption assays (with efficiencies up to 99.8% for Pb) (Bhandari et al., 2024; Shaaban Emara et al., 2023).

Biofilm formation and community-level resilience appeared in roughly 40% of the dataset, mainly among *Pseudomonas*, *Bacillus*, and mixed consortia, specifically noted in studies on fungal-bacterial and *B. subtilis* biofilms (Ghosh et al., 2024; Henagamage et al., 2022). In rhizospheric systems, microbial consortia stabilized metal ions at the root interface, reducing plant uptake by 50–80% (Gao et al., 2024; Zhang et al., 2023). The integration of EPS and biofilm mechanisms explains the persistence of microbial populations under chronic metal exposure.

Genetic and efflux-based mechanisms were confirmed through the detection of specific resistance genes (**Table 3.3**). The most clearly identified mechanisms in the dataset relate to chromium (Cr) and arsenic (As). For instance, in *P. putida*, the chromate reductase (ChrR) gene was explicitly isolated and transferred to *E. coli* to confirm its responsibility for Cr(VI) reduction (Sundarraj et al., 2023). Further genomic analysis on a *Pseudomonas/Rhodococcus* consortium (Su et al., 2022) detailed the Cr(VI) tolerance mechanism, showing it was mediated by the efflux of chromate via the chrA and copZ genes, supplemented by DNA-repaired proteases. For arsenic detoxification, increased expression of the arsenite oxidase enzyme was observed in *Pseudomonas* sp. AK9, which directly correlated with an enhanced transformation of As(III) (Satyapal et al., 2024).

Table 3.3 Most frequently reported genes and enzymes involved in heavy metal detoxification, specifying their associated metals, representative taxa, and primary function.

Gene/Enzyme	Associated metals	Representative taxa	Function
chrA	Cr(VI)	*Pseudomonas* sp. *Rhodococcus* sp.	Efflux of Cr(VI)
copZ	Cr(VI)	*Pseudomonas* sp. *Rhodococcus* sp.	Cr(VI) tolerance / Efflux
Chromate reductase (ChrR) gene	Cr(VI)	*P. putida*	Cr(VI) reduction
Arsenite oxidase (Enzyme)	As (Arsenic)	*Pseudomonas* sp.	As(III) transformation / oxidation

Redox and enzymatic transformations were identified in one-third of the papers, particularly in *Pseudomonas* and *Bacillus* isolates (Ali et al., 2022; Sundarraj et al., 2023). Cr(VI) reduction to Cr(III) was the most frequently observed process, mediated by reductase enzymes that generate insoluble $Cr(OH)_3$ or mixed chromite phases (Monga et al., 2022; Ye et al., 2024). Additional redox reactions included transformations between arsenic species (Ghosh et al., 2024; Satyapal et al., 2024). Enzymatic activities such as dehydrogenase, peroxidase, and superoxide dismutase were reported in 25% of studies, reinforcing the coupling between biochemical and physicochemical detoxification (Wang et al., 2025; Yan et al., 2024).

3.4 Discussion

3.4.1 Comparative analysis of microbial performance and mechanisms

The systematic assessment of 41 studies published between 2022 and 2025 revealed a pronounced taxonomic convergence in heavy metal bioremediation, with members of *Bacillus*, *Pseudomonas*, *Enterobacter*, and *Lysinibacillus* dominating across environmental matrices. These genera consistently exhibited high removal efficiencies

for cadmium, lead, and chromium, which aligns with the robust structural and physiological traits characteristic of Gram-positive and metabolically versatile Gram-negative bacteria.

Bacillus species showed exceptional biosorption capacities, often exceeding 100 mg g^{-1} for Pb^{2+} and Cd^{2+} (Wang et al., 2025; Ye et al., 2024), attributable to their thick peptidoglycan layers, teichoic acids, and ureolytic biomineralization potential. Conversely, *Pseudomonas* strains, particularly *P. aeruginosa*, *P. putida*, and *P. fluorescens*, displayed remarkable multi-metal tolerance, frequently sustaining growth under 500–700 mg L^{-1} of Cd or Cr while maintaining removal rates above 70 %. These outcomes confirm the broad detoxification spectrum of *Pseudomonas*, driven by both surface adsorption and intracellular sequestration. The predominance of these taxa corroborates prior evidence indicating that bacterial consortia combining *Bacillus*, as high-affinity sorbents, and *Pseudomonas*, as redox transformers and EPS producers, outperform single strains in multi-metal matrices (Cai et al., 2025; Peng et al., 2023).

Mixed consortia exhibited synergistic mechanisms in which *Bacillus* contributed carbonate precipitation and surface complexation, whereas *Pseudomonas* enhanced redox transformations through periplasmic reductases and metal-chelating siderophores. The co-occurrence of these functions yields a sequential detoxification process, whereby soluble ions are first immobilized extracellularly and subsequently converted to less mobile species within biofilms. This synergy underlines the ecological advantage of cooperative systems in natural and engineered environments.

Three dominant pathways emerged: (i) passive biosorption through carboxyl, hydroxyl, and phosphoryl moieties within the cell wall; (ii) bioaccumulation and redox transformation mediated by enzymatic systems such as chromate reductases and arsenate reductases; and (iii) biomineralization processes involving carbonate and phosphate precipitation.

Studies employing advanced spectroscopy (FTIR, XRD, SEM–EDS) confirmed the formation of $CdCO_3$, $Pb_3(PO_4)_2$, and $Cr(OH)_3$ as common end-products, providing

molecular validation for immobilization mechanisms (Kaur et al., 2024; Zhang et al., 2024). Together, these findings establish that microbial metal removal is not a single process but a sequence of coupled reactions integrating physicochemical adsorption with biologically driven transformations.

3.4.2 Environmental and operational determinants of metal removal

Bioremediation performance was highly dependent on environmental conditions, particularly pH, temperature, and substrate composition. Optimal pH values clustered between 6.5 and 8.0, where deprotonation of cell-wall ligands enhances cation binding and carbonate precipitation. Acidic conditions (pH < 5) generally reduced sorption efficiency by promoting metal solubility and proton competition, although acid-tolerant *Pseudomonas* and *Rhodococcus* bacteria maintained activity in soils contaminated with mixed metals. Temperature affected both adsorption kinetics and metabolic rates, with optimal ranges between 28°C and 35°C across most isolates. Extreme thermophiles or psychrotolerant strains were rare, confirming that mesophilic systems dominate soil remediation under temperate climates.

Matrix effects were also significant; in fact, synthetic solutions frequently yielded higher removal percentages than soil or sludge matrices due to reduced ionic competition. However, field-relevant matrices better captured the complexity of environmental constraints. In particular, studies employing real contaminated soils demonstrated that bacterial immobilization efficiency decreases 10–25 % relative to aqueous systems, primarily due to metal–clay interactions and organic matter interference (Lin et al., 2022; Zhang et al., 2024). Nonetheless, the persistence of biofilm-forming strains mitigated these losses by maintaining localized microenvironments conducive to sorption and precipitation.

Nutrient availability and carbon sources further modulated bioremediation kinetics. Simple sugars and organic acids facilitated EPS synthesis, enhancing sorption sites and metal chelation. The inclusion of urea or ammonium salts in media triggered

MICP, increasing immobilization through $CaCO_3$ lattice formation. Such findings emphasize that bioremediation efficiency arises from a balance between microbial physiology and physicochemical context, where even minor shifts in pH or nutrient status can redefine metal speciation and bioavailability.

While *Bacillus* species remain among the most efficient biosorbents due to their robust cell walls and sporulation capacity, recent evidence highlights the broader ecological and mechanistic versatility of *Pseudomonas* spp. as model organisms for heavy metal bioremediation. Comparative analyses indicate that *Pseudomonas* can operate effectively across a wider spectrum of environmental conditions, including acidic and multi-metal-contaminated soils, where *Bacillus* often exhibits reduced metabolic activity. Genomically, *Pseudomonas* is shown in the dataset to harbor a well-characterized set of resistance operons, such as chromate efflux systems (e.g., chrA) and specific reductases (Su et al., 2022; Sundarraj et al., 2023), along with stress-response regulators under quorum-sensing control (Lu et al., 2022), conferring rapid adaptability and multi-metal tolerance. From an applicative standpoint, non-spore-forming *Pseudomonas* strains develop resilient biofilms capable of maintaining metabolic activity under fluctuating redox and moisture conditions, making them suitable for continuous bioreactors and biosensor interfaces. Moreover, the genus is one of the most genomically annotated among soil bacteria, providing a reproducible framework for cross-study comparison and systems-biology modelling.

3.4.3 Functional and genetic determinants in Pseudomonas spp.

Within the analyzed dataset, *Pseudomonas* spp. consistently represented the most functionally diverse genus. Crucially, it also stands out as the most mechanistically and genetically well-characterized genus in the context of these studies, providing a clearer framework for its application compared to other taxa.

Genome-level investigations and specific gene analyses, which were reported for *Pseudomonas* more frequently than for other genera, have begun to elucidate its

extensive repertoire of resistance determinants. For example, specific genomic analyses in the dataset linked Cr(VI) tolerance directly to the function of efflux genes chrA and copZ (Su et al., 2022). This was further supported by studies isolating the specific chromate reductase (ChrR) gene from *P. putida*, confirming its central role in reduction (Sundarraj et al., 2023). Similarly, arsenic detoxification was explicitly correlated with the "increased expression of arsenite oxidase" in *Pseudomonas* sp. (Satyapal et al., 2024).

This depth of available genetic information—spanning efflux systems, enzymatic reduction, and stress-response enzymes—is complemented by its proven metabolic versatility. Mechanistically, *Pseudomonas* exhibits a dual detoxification strategy that combines:

1. Passive biosorption: via copious EPS and biofilm matrices rich in functional groups.
2. Active metabolic reduction: (e.g., Cr(VI) to Cr(III)) mediated by the reductase enzymes localized in the cytoplasmic membrane.

While other genera, such as *Bacillus*, demonstrate exceptionally high removal efficiencies (often via biomineralization or EPS sorption), the *Pseudomonas* genus offers a more complete, "benchmark" model. The combination of its broad metabolic capabilities (including redox transformations often lacking in other biosorbents), its detailed genomic annotation, and its robust stress-response mechanisms makes it a uniquely reliable and adaptable candidate for bioaugmentation.

3.4.4 Integrative interpretation and ecological implications

The evidence underscores that microbial bioremediation is a multi-layered process integrating community ecology, metal chemistry, and environmental dynamics. In terrestrial matrices, microbial assemblages restructure in response to chronic metal exposure, selecting for resistant phenotypes with enhanced EPS and biofilm production. This adaptive remodelling not only supports metal immobilization but also

contributes to soil stabilization and nutrient cycling. The co-occurrence of plant growth promoting traits, such as phosphate solubilization, indole-acetic-acid synthesis, and siderophore production, demonstrates that many remediation-competent strains simultaneously enhance soil fertility, bridging the gap between bioremediation and agroecological restoration (Gao et al., 2024; Ghosh et al., 2024). From an applied perspective, the convergence of adsorption, biomineralization, and redox conversion mechanisms across different taxa suggests that integrated consortia or sequential treatment systems can achieve superior outcomes in heterogeneous contaminated soils. Field-scale trials incorporating *Pseudomonas–Bacillus* co-inocula or biochar-supported bacterial systems have already demonstrated stable performance under fluctuating pH and moisture, supporting their scalability. However, ensuring ecological compatibility and long-term persistence remains essential to avoid unintended perturbations of indigenous microbiota. At the same time, the environmental sustainability of microbial remediation extends beyond removal efficiency. The re-establishment of soil microbial diversity and enzymatic functionality is crucial to restoring ecological services after decontamination. The capacity of *Pseudomonas* to reinstate biogeochemical cycling reinforces the dual role of these bacteria as both detoxifiers and ecological engineers.

3.4.5 Limitations and perspectives for future research

Although the present synthesis provides robust evidence on the efficiency and mechanisms of bacterial heavy metal remediation, several methodological limitations persist. The heterogeneity of experimental conditions, particularly regarding initial metal concentrations, exposure times, and analytical protocols, still hampers quantitative comparability among studies. Many works rely on batch experiments with synthetic solutions, which tend to overestimate removal rates compared with complex soil matrices. Moreover, the limited number of field-scale investigations constrains the extrapolation of laboratory findings to real environments.

Despite the rigorous application of PRISMA inclusion criteria and NOS quality assessment, several potential sources of bias remain inherent to the analyzed literature. Selection bias may derive from the restriction to English-language publications and recent years (2022–2025), which, while ensuring methodological consistency, might have excluded earlier high-quality studies. Experimental and analytical heterogeneity also contributes to variability, as differences in matrix type, initial metal concentrations, and exposure durations limit quantitative comparability across studies. Moreover, the frequent use of synthetic batch systems introduces matrix bias, often overestimating removal efficiencies relative to field conditions. Reporting bias may further arise from the incomplete disclosure of standard deviations, replicates, or negative outcomes, whereas instrumental bias stems from the use of different quantification techniques (AAS, ICP-OES, ICP-MS) with varying sensitivity. Finally, interpretation bias may occur when gene presence (e.g., *chrA*, *copZ*, *arsC*) is equated with functional expression without corroborating enzymatic or transcriptional evidence. Acknowledging these biases is essential for contextualizing the quantitative synthesis and reinforces the need for standardized protocols and transparent reporting practices in future microbial bioremediation research.

Whole-genome and transcriptomic data can elucidate the regulatory networks underlying metal resistance, enabling predictive modeling of community dynamics. Furthermore, the development of hybrid bio-technological systems, combining microbial consortia with biochar, alginate carriers, or plant roots, offers a promising avenue for enhanced stability, reusability, and ecological compatibility. Long-term monitoring of inoculated soils will be essential to evaluate persistence, horizontal-gene transfer, and ecosystem resilience following bioaugmentation. Beyond these methodological needs, several emerging directions can drive the next generation of microbial bioremediation research. Artificial-intelligence and bioinformatic approaches could be employed to design strains combination with optimized multi-metal tolerance and controlled expression of efflux and redox genes. Metagenomic-

guided restoration strategies, leveraging indigenous microbial communities from contaminated soils, may facilitate adaptive bioaugmentation and reduce ecological disturbance. Gene-editing technologies such as CRISPR-Cas could be applied to enhance or fine-tune key detoxification pathways identified in these studies, such as the chromate reductase and efflux systems (e.g., chrA), improving both specificity and kinetics of metal transformation. At the ecosystem scale, integration with digital environmental monitoring systems (IoT-based biosensors and AI-linked data platforms) could allow real-time assessment of bioremediation performance and soil health recovery. In parallel, coupling microbial remediation with carbon-capture and soil-fertility restoration processes, such as microbial-induced carbonate precipitation or biochar-assisted nutrient recycling, would align these technologies with circular-economy objectives. The transition from laboratory prototypes to field-deployable, data-driven bioremediation systems will require interdisciplinary collaboration across microbiology, materials science, and environmental engineering. Integrating high-throughput sequencing, microspectroscopic imaging, and environmental metabolomics will deepen mechanistic understanding while ensuring sustainability and safety. Microbial bioremediation stands at the intersection of biotechnology and ecological restoration. By merging advanced genomics, synthetic biology, and digital environmental sensing, future research can transform microbial bioremediation into scalable, intelligent, and self-regulating platforms for global soil detoxification and environmental resilience.

These methodological and conceptual limitations delineate both the current boundaries and the future trajectory of microbial heavy metal bioremediation research. Addressing these gaps will require not only the harmonization of experimental standards and data reporting, but also the integration of genomic, physicochemical, and digital approaches into unified predictive frameworks. Such an effort would bridge the existing divide between laboratory-scale experimentation and field-scale implementation, fostering

scalable, data-driven remediation systems that are ecologically sustainable and technologically robust.

3.5 Conclusion

Microbial bioremediation of HMs emerges as a multifactorial process governed by genetic, biochemical, and ecological interactions. Across the 41 studies analyzed, a consistent pattern highlights the dominance of *Pseudomonas* and *Bacillus* species as functional pillars of detoxification, supported by complementary mechanisms such as EPS-mediated biosorption, enzymatic redox transformations, and biomineralization. Among these, *Pseudomonas* stands out as a benchmark genus for its genomic plasticity, multi-metal tolerance, and biofilm-mediated resilience under variable environmental conditions.

The integration of these microbial traits with advanced analytical, genomic, and digital tools will enable the transition from laboratory-scale experiments to sustainable field applications. Future developments should therefore focus on standardized methodologies, long-term ecological monitoring, and the incorporation of predictive models to ensure the stability and scalability of microbially driven soil restoration.

Advanced microbial bioremediation will require the convergence of microbiology, systems biology, and environmental engineering toward a unified, data-driven framework for soil and water detoxification. Harnessing the inherent adaptability of microbial consortia, particularly *Pseudomonas*-based communities, while embedding sustainability, biosafety, and ethical governance principles will be crucial to translate current research into resilient, climate-responsive solutions. Through this integrative approach, microbial biotechnology can evolve from a remediation tool into a cornerstone of ecological restoration and circular-economy strategies.

References

Ajmi, N., Tasci, G., Saticioglu, I. B., & Duman, M. (2025). Pangenome analysis of *Aquipseudomonas alcaligenes* 67P: insights into ecological distribution, environmental adaptation, and metabolic versatility. Total Environment Microbiology, 1(2), 100010. https://doi.org/10.1016/j.temicr.2025.100010

Ali, Q., Ayaz, M., Yu, C., Wang, Y., Gu, Q., Wu, H., & Gao, X. (2022). Cadmium tolerant microbial strains possess different mechanisms for cadmium biosorption and immobilization in rice seedlings. *Chemosphere*, *303*, 135206. https://doi.org/10.1016/j.chemosphere.2022.135206

Angon, P. B., Islam, Md. S., Kc, S., Das, A., Anjum, N., Poudel, A., & Suchi, S. A. (2024). Sources, effects and present perspectives of heavy metals contamination: Soil, plants and human food chain. *Heliyon*, *10*(7), e28357. https://doi.org/10.1016/j.heliyon.2024.e28357

Bhandari, D., Sharma, P., & Dwivedi, V. (2024). Microbial bioremediation: Unravelling the potential for cleaner environments through comparative analysis. *Bioremediation Journal*, 1–9. https://doi.org/10.1080/10889868.2024.2357136

Cai, Q., Zhao, W., Wang, J., Yang, G., Amils, R., Martínez, J. M., Mateos, G., Carrasco-Ropero, I., Wu, J., & Xu, M. (2025). A cooperation mechanism between *Bacillus thuringiensis* and *Citrobacter freundii* that enhances cadmium biomineralization. *Journal of Hazardous Materials*, *488*, 137354. https://doi.org/10.1016/j.jhazmat.2025.137354

Chen, Y., Fang, Z., Iddrisu, L., Ye, J., Pan, X., Liang, Y., & Gooneratne, R. (2025). Integrated analyses of characterization and transcriptome reveal the adaptive response mechanism of *Bacillus cereus* FCHN 7–1 in cadmium adsorption. *Journal of Hazardous Materials*, *489*, 137525. https://doi.org/10.1016/j.jhazmat.2025.137525

Dahnoun, K., Djadouni, F., Essghaier, B., Naccache, C., Zitouna, N., Zehdi-Azouzi, S., BayyiĞiT, İs., Latif, H. R., Mezghani-Khemakhem, M., & Bourguiba, H. (2024). Characterization and bioremediation potential of heavy metal resistant bacteria isolated from agricultural soil. *Turkish Journal of Agriculture and Forestry*, *48*(4), 607–617. https://doi.org/10.55730/1300-011X.3205

Dey, N., Banerjee, S., & Pramanik, K. (2025). Arsenic-resistant endophytic bacteria: In-house 'plant-probiotics'. *Journal of Soil Science and Plant Nutrition*. https://doi.org/10.1007/s42729-025-02722-3

Elahi, A., Rehman, A., Zajif Hussain, S., Zulfiqar, S., & Shakoori, A. R. (2022). Isolation and characterization of a highly effective bacterium *Bacillus cereus* b-525k for hexavalent chromium detoxification. *Saudi Journal of Biological Sciences*, *29*(4), 2878–2885. https://doi.org/10.1016/j.sjbs.2022.01.027

Firincă, C., Zamfir, L.-G., Constantin, M., Răut, I., Jecu, M.-L., Doni, M., Gurban, A.-M., & Șesan, T. E. (2025). Innovative approaches and evolving strategies in heavy metal bioremediation: Current limitations and future opportunities. *Journal of Xenobiotics*, *15*(3), 63. https://doi.org/10.3390/jox15030063

Gao, Y., Zhang, X., Wang, L., Guan, E., Zhu, L., Wang, J., Kim, Y. M., & Wang, J. (2024). Contribution of Cd passivating functional bacterium H27 to tobacco growth under Cd stress. *Chemosphere*, *362*, 142552. https://doi.org/10.1016/j.chemosphere.2024.142552

Ghorbani, M., & Amirahmadi, E. (2025). Optimizing biochar for heavy metal remediation: A meta-analysis of modification methods and pyrolysis conditions. *Environments*, *12*(11), 399. https://doi.org/10.3390/environments12110399

Ghosh, P. K., Pramanik, K., Mahapatra, K., Mondal, S., Ghosh, S. K., Ghosh, A., & Maiti, T. K. (2024). Plant growth-promoting *Bacillus cereus* MCC3402 facilitates rice seedling growth under arsenic-spiked soil. *Biocatalysis and Agricultural Biotechnology*, *61*, 103405. https://doi.org/10.1016/j.bcab.2024.103405

Henagamage, A. P., Peries, C. M., & Seneviratne, G. (2022). Fungal-bacterial biofilm mediated heavy metal rhizo-remediation. *World Journal of Microbiology and Biotechnology*, *38*(5), 85. https://doi.org/10.1007/s11274-022-03267-8

Hou, D., Jia, X., Wang, L., McGrath, S. P., Zhu, Y.-G., Hu, Q., Zhao, F.-J., Bank, M. S., O'Connor, D., & Nriagu, J. (2025). Global soil pollution by toxic metals threatens agriculture and human health. *Science*, *388*(6744), 316–321. https://doi.org/10.1126/science.adr5214

Ilyas, M. F., Gill, S., Farhad, M., Hannan, F., Tauqeer, H. M., Ramzani, P. M. A., Turan, V., Virk, Z. A., & Iqbal, M. (2024). Rhizoremediation. In *Bio-organic amendments for heavy metal remediation* (pp. 389–404). Elsevier. https://doi.org/10.1016/B978-0-443-21610-7.00039-2

Kashyap, S., Chandra, R., Kumar, B., & Verma, P. (2022). Biosorption efficiency of nickel by various endophytic bacterial strains for removal of nickel from electroplating industry effluents: An operational study. *Ecotoxicology*, *31*(4), 565–580. https://doi.org/10.1007/s10646-021-02445-y

Kaur, M., Sidhu, N., & Reddy, M. S. (2024). Removal of cadmium through biomineralization using halophilic and ureolytic bacteria under saline conditions. *International Biodeterioration & Biodegradation*, *191*, 105805. https://doi.org/10.1016/j.ibiod.2024.105805

Kaushal, P., & Pati, A. M. (2024). *Bacillus altitudinis* mediated lead bioremediation for enhanced growth of rice seedlings. *Current Microbiology*, *81*(12), 410. https://doi.org/10.1007/s00284-024-03934-z

Liang, B., Feng, Y., Ji, X., Li, C., Li, Q., Zeng, Z., & Wang, Y. (2025). Isolation and characterization of cadmium-resistant *Bacillus cereus* strains from Cd-contaminated mining areas for potential bioremediation applications. *Frontiers in Microbiology*, *16*, 1550830. https://doi.org/10.3389/fmicb.2025.1550830

Lin, H., Shi, J., Dong, Y., Li, B., & Yin, T. (2022). Construction of bifunctional bacterial community for co-contamination remediation: Pyrene biodegradation and cadmium biomineralization. *Chemosphere*, *304*, 135319. https://doi.org/10.1016/j.chemosphere.2022.135319

Liu, X., Mei, S., & Salles, J. F. (2023). Inoculated microbial consortia perform better than single strains in living soil: A meta-analysis. *Applied Soil Ecology*, *190*, 105011. https://doi.org/10.1016/j.apsoil.2023.105011

Lu, L., Chen, C., Ke, T., Wang, M., Sima, M., & Huang, S. (2022). Long-term metal pollution shifts microbial functional profiles of nitrification and denitrification in agricultural soils. *Science of The Total Environment*, *830*, 154732. https://doi.org/10.1016/j.scitotenv.2022.154732

Manikandan, S. K., & Nair, V. (2023). Developing a biocatalyst showcasing the synergistic effect of rice husk biochar and bacterial cells for the removal of heavy metals. *New Journal of Chemistry*, *47*(46), 21199–21213. https://doi.org/10.1039/D3NJ02889E

Mitra, S., Dey, J., Sarkar, S., & Banik, P. (2025). Halotolerant bacteria isolated from the soils of Indian mangrove ecosystem for metal removal and NPK enhancement. *Scientific Reports*, *15*(1), 20804. https://doi.org/10.1038/s41598-025-07839-0

Mondal, S., Mondal, T., Pal, P., Mitra, S., Ghosh, S. K., Soren, T., & Maiti, T. K. (2025). Bioprotective mechanisms of *Enterobacter* sp. Against arsenic, cadmium, and lead toxicity and its potential role in soil bioremediation. *Journal of Environmental Chemical Engineering*, *13*(2), 115432. https://doi.org/10.1016/j.jece.2025.115432

Monga, A., Fulke, A. B., Gaud, A., Sharma, A., Ram, A., & Dasgupta, D. (2022). Isolation and identification of novel chromium tolerant bacterial strains from a heavy metal polluted urban creek: An assessment of bioremediation efficiency and flocculant production. *Thalassas: An International Journal of Marine Sciences*, *38*(2), 1233–1244. https://doi.org/10.1007/s41208-022-00458-w

Mtengai, K., Ramasamy, S., Msimuko, P., Mzula, A., & Mwega, E. D. (2022). Existence of a novel heavy metal–tolerant *Pseudomonas aeruginosa* strain Zambia SZK-17 Kabwe 1: The potential bioremediation agent in the heavy metal–contaminated area. *Environmental Monitoring and Assessment*, *194*(12), 887. https://doi.org/10.1007/s10661-022-10565-z

Mungla, G., Facknath, S., & Lalljee, B. (2022). Assessing the potential of mechanical aeration combined with bioremediation process in soils and coastal sediments impacted by heavy metals. *AIMS Environmental Science*, *9*(5), 692–707. https://doi.org/10.3934/environsci.2022039

Oladimeji, T. E., Oyedemi, M., Emetere, M. E., Agboola, O., Adeoye, J. B., & Odunlami, O. A. (2024). Review on the impact of heavy metals from industrial wastewater effluent and removal technologies. *Heliyon*, *10*(23), e40370. https://doi.org/10.1016/j.heliyon.2024.e40370

Page, M. J., McKenzie, J. E., Bossuyt, P. M., Boutron, I., Hoffmann, T. C., Mulrow, C. D., Shamseer, L., Tetzlaff, J. M., Akl, E. A., Brennan, S. E., Chou, R., Glanville, J., Grimshaw, J. M., Hróbjartsson, A., Lalu, M. M., Li, T., Loder, E. W., Mayo-Wilson, E., McDonald, S., … Moher, D. (2021). The PRISMA 2020 statement: An updated guideline for reporting systematic reviews. *BMJ*, n71. https://doi.org/10.1136/bmj.n71

Pan, H., Zhao, X., Zhou, X., Yan, H., Han, X., Wu, M., & Chen, F. (2023). Research progress on the role of biofilm in heavy metals adsorption-desorption characteristics of microplastics: A review. *Environmental Pollution*, *336*, 122448. https://doi.org/10.1016/j.envpol.2023.122448

Peng, C., Zhao, X., Ji, X., Wu, J., Liang, W., Song, H., Zhang, W., & Wang, X. (2023). Mixed bacteria passivation for the remediation of arsenic, lead, and cadmium: Medium optimization and mechanisms. *Process Safety and Environmental Protection*, *170*, 720–727. https://doi.org/10.1016/j.psep.2022.12.037

Ruan, Z., Chen, K., Cao, W., Meng, L., Yang, B., Xu, M., Xing, Y., Li, P., Freilich, S., Chen, C., Gao, Y., Jiang, J., & Xu, X. (2024). Engineering natural microbiomes toward enhanced bioremediation by microbiome modeling. *Nature Communications*, *15*(1), 4694. https://doi.org/10.1038/s41467-024-49098-z

Satyapal, G. K., Haque, R., & Kumar, N. (2024). Gamma irradiation in modulating arsenic bioremediation potential of *Pseudomonas* sp. AK1 and AK9. *International Journal of Radiation Biology*, *100*(6), 934–939. https://doi.org/10.1080/09553002.2024.2345137

Shaaban Emara, N., Elwakil, B. H., Zakaria, M., & Olama, Z. A. (2023). Mechanistic action of lead removal by the native isolate *Bacillus amyloliquefaciens* ON261680.1. *Arabian Journal of Chemistry*, *16*(8), 104962. https://doi.org/10.1016/j.arabjc.2023.104962

Shan, B., Hao, R., Zhang, J., Li, J., Ye, Y., Xu, H., & Lu, A. (2024). Bioremediation potential of Cr(VI) by *Lysinibacillus cavernae* CR-2 isolated from chromite-polluted soil: A promising approach for Cr(VI) detoxification. *Geomicrobiology Journal*, *41*(4), 459–473. https://doi.org/10.1080/01490451.2023.2246035

Shofia, S. I., Vickram, A. S., Saravanan, A., Deivayanai, V. C., & Yaashikaa, P. R. (2025). Sustainable separation technologies for heavy metal removal from wastewater: An upgraded review of

physicochemical methods and its advancements. *Sustainable Chemistry for the Environment*, *10*, 100264. https://doi.org/10.1016/j.scenv.2025.100264

Su, Y., Sun, S., Liu, Q., Zhao, C., Li, L., Chen, S., Chen, H., Wang, Y., & Tang, F. (2022). Characterization of the simultaneous degradation of pyrene and removal of Cr(VI) by a bacteria consortium YH. *Science of The Total Environment*, *853*, 158388. https://doi.org/10.1016/j.scitotenv.2022.158388

Sundarraj, S., Sudarmani, D. N. P., Samuel, P., & Sevarkodiyone, S. P. (2023). Bioremediation of hexavalent chromium by transformation of *Escherichia coli* DH5α with chromate reductase (ChrR) genes of *Pseudomonas putida* isolated from tannery effluent. *Journal of Applied Microbiology*, *134*(1), lxac019. https://doi.org/10.1093/jambio/lxac019

Surabhi, A., Sundaramanickam, A., Barathan, V., & Praveena, S. M. (2025). Multi-metal tolerance efficiency and bioremediation capabilities of *Bacillus aerius* from mangrove rhizosphere. *Geomicrobiology Journal*, *42*(8), 737–744. https://doi.org/10.1080/01490451.2025.2523818

Tang, H., Xiang, G., Xiao, W., Yang, Z., & Zhao, B. (2024). Microbial mediated remediation of heavy metals toxicity: Mechanisms and future prospects. *Frontiers in Plant Science*, *15*, 1420408. https://doi.org/10.3389/fpls.2024.1420408

Wang, X., Xu, W., Lu, Y., Cao, L., Tian, M., Shang, Y., Han, N., & Ding, J. (2025). Lead biosorption by *Bacillus tequilensis*: Characterization of resistance mechanisms and its potential for remediation of contaminated soil. *Journal of the Science of Food and Agriculture*, *105*(13), 7095–7102. https://doi.org/10.1002/jsfa.14408

Yan, Z., Li, Y., Peng, S., Wei, L., Zhang, B., Deng, X., Zhong, M., & Cheng, X. (2024). Cadmium biosorption and mechanism investigation using two cadmium-tolerant microorganisms isolated from rhizosphere soil of rice. *Journal of Hazardous Materials*, *470*, 134134. https://doi.org/10.1016/j.jhazmat.2024.134134

Yasmin, R., Zafar, M. S., Tahir, I. M., Asif, R., Asghar, S., & Raza, S. K. (2022). Biosorptive potential of *Pseudomonas* species RY12 toward zinc heavy metal in agriculture soil irrigated with contaminated waste water. *Dose-Response*, *20*(3), 15593258221117352. https://doi.org/10.1177/15593258221117352

Ye, Y., Hao, R., Shan, B., Zhang, J., Li, J., & Lu, A. (2024). Mechanism of Cr(VI) removal by efficient Cr(VI)-resistant *Bacillus mobilis* CR3. *World Journal of Microbiology and Biotechnology*, *40*(1), 21. https://doi.org/10.1007/s11274-023-03816-9

Zada, S., Rafiq, M., & Sajjad, W. (2025). Industrial application of extreme microbes: Harnessing the power of nature's extremophiles. *Frontiers in Microbiology*, *16*, 1697504. https://doi.org/10.3389/fmicb.2025.1697504

Zhang, L., Hu, Y., Chen, Y., Qi, D., Cai, B., Zhao, Y., Li, Z., Wang, Y., Nie, Z., Xie, J., & Wang, W. (2023). Cadmium-tolerant *Bacillus cereus* 2–7 alleviates the phytotoxicity of cadmium exposure in banana plantlets. *Science of The Total Environment*, *903*, 166645. https://doi.org/10.1016/j.scitotenv.2023.166645

Zhang, L., Wang, W., Yue, C., & Si, Y. (2024). Biogenic calcium improved Cd2+ and Pb2+ immobilization in soil using the ureolytic bacteria *Bacillus pasteurii*. *Science of The Total Environment*, *921*, 171060. https://doi.org/10.1016/j.scitotenv.2024.171060

Zuo, W., Song, B., Shi, Y., Zupanic, A., Guo, S., Huang, H., Jiang, L., & Yu, Y. (2022). Using Bacillus thuringiensis HM-311 hydroxyapatite biochar beads to remediate Pb and Cd contaminated farmland soil. Chemosphere, 307, 135797. https://doi.org/10.1016/j.chemosphere.2022.135797

4. A statistical approach to model soil microbiota versus heavy metals: a case study on soil samples from Foggia, Southern Italy[2]

Alessandro De Santis[1], Antonio Bevilacqua[1], Maria Rosaria Corbo[1], Barbara Speranza[1], Matteo Francavilla[1], Giuseppe Gatta[1], Federica Carucci[2], Milena Sinigaglia[1]

[1]Department of Agriculture, Food, Natural Resources and Engineering, University of Foggia, Foggia, ITALY

[2]Department of Agricultural and Forestry Sciences (DAFNE), University of Tuscia, Viterbo, Italy

Abstract

Heavy metal contamination undermines soil functions and food safety, while risk appraisals often rely on chemical indices that can be unstable in the presence of extremes and only indirectly reflect biological integrity. We present an integrative framework that couples standardized contamination metrics with soil microbiome profiling to deliver stable, interpretable classifications and actionable bioindicators. Twelve peri-urban soils from southern Italy were analysed for potentially toxic elements, including Arsenic (As), Cadmium (Cd), Chromium (Cr), Copper (Cu), Nickel (Ni), Lead (Pb), and Zinc (Zn) and profiled by shotgun metagenomics. We introduce a Standardized Ecological Risk index (SPERI) that preserves the ranking conveyed by conventional composites yet reduces outlier leverage. SPERI strongly agreed with Improved Potential Ecological Risk Index (IPERI) while stabilizing variance (R^2 = 0.896) and improved between-site comparability. Along the contamination gradient, community structure shifted consistently: families such as Pseudomonadaceae, Xanthomonadaceae and Rhodospirillaceae increased with risk, whereas Geodermatophilaceae and Nocardiaceae declined. Simple decision-tree

[2] This chapter was published on Scientific Reports (De Santis, A., Bevilacqua, A., Corbo, M. R., Speranza, B., Francavilla, M., Gatta, G., Carucci, F. & Sinigaglia, M. (2026). A statistical approach to model soil microbiota versus heavy metals: a case study on soil samples from Foggia, Southern Italy. Scientific Reports, 16:2586. https://doi.org/10.1038/s41598-025-32485-x)

models trained on family-level relative abundances reliably separated SPERI classes and repeatedly selected Zn- and Cd-enriched sites as primary split drivers, aligning microbial signals with chemical risk. By combining open, reproducible analytics with jointly chemical- and microbiome-informed endpoints, this workflow improves the interpretability and transferability of ecological risk assessment and supports targeted remediation and monitoring in contaminated agro-ecosystems.

Keywords: Classification and regression trees, Shotgun metagenomics; Standardized ecological risk index; Correlation; Ecological risk assessment; Microbial communities.

4.1. Introduction

Soil contamination by heavy metals (HMs) is one of the most persistent and widespread environmental threats, with significant implications for human health, agricultural productivity, and the ecological integrity of terrestrial ecosystems (Gatta et al., 2018; Nyiramigisha et al., 2021; Sodhi et al., 2022). HMs commonly found as contaminants in agricultural soils that can exert toxic effects on plants and microbial communities include cadmium (Cd), lead (Pb), chromium (Cr), arsenic (As), mercury (Hg), nickel (Ni), copper (Cu), and zinc (Zn). Among these, Cd, Pb, As, Hg, and Cr are considered highly toxic and pose serious risks to plant health even at relatively low concentrations (Rashid et al., 2023). Unlike organic pollutants, HMs are not biodegradable and can persist in the environment for decades, accumulating in soils and entering the food chain via plants and groundwater (Hama Aziz et al., 2023). These contaminants originate primarily from anthropogenic activities, including industry, intensive agriculture, vehicular traffic, and the uncontrolled disposal of solid waste (Mavakala et al., 2022; Tiabou et al., 2024; X. Xu et al., 2024).

Land-use intensification, and improper waste disposal can exacerbate the vulnerability of agricultural and peri-urban soils to HMs accumulation. In addition to these anthropogenic inputs, HMs may also derive from the natural weathering and erosion of parent material, contributing to baseline geochemical variability across sites. Previous context analyses of Foggia County (Southern Italy) promoted by Legambiente (Marvelli, 2025) have reported environmental degradation linked to illegal dumping, highlighting the need for targeted ecological risk assessment strategies.

Poor soil health can directly and indirectly affect human well-being; in fact, contaminated soils represent a vector of exposure to hazardous substances through various pathways, in particular by eating contaminated food (Brevik et al., 2020). More critically, contaminants such as Pb, Cd, and As can be taken up by crops (Khatun et al., 2022; Rashid et al., 2023), entering the food chain and potentially exceeding

regulatory thresholds. The consumption of such contaminated produce has been linked to chronic illnesses, including neurological disorders, kidney dysfunction, and carcinogenic effects (Munir et al., 2021; Patel et al., 2021; Grados et al., 2022).

Given these risks, ecological risk assessment (ERA) has emerged as a key framework for evaluating the potential ecotoxicological consequences of soil contamination. This approach provides an integrated framework to evaluate the potential ecotoxicological impact of soil contaminants (Rattner et al., 2024; Shea & Thorsen, 2012). However, traditional approaches relying solely on chemical analyses could experience a bias in capturing the complex ecological consequences of HMs pollution. Chemical data can quantify concentrations but do not reflect the actual biological functionality or ecological and health status of the soil. In recent years, attention has shifted toward integrating chemical indicators with biological metrics, in particular microbial community dynamics, which offer a more holistic and functional perspective on soil health (Bhaduri et al., 2022).

Soil microbial communities play a central role in essential ecosystem processes, including organic matter decomposition, nutrient cycling, and carbon sequestration (Naylor et al., 2022). Due to their functional roles and sensitivity to environmental gradients, microbial communities provide integrative indicators of both contamination levels and ecosystem functioning. Exposure to HMs can disrupt microbial diversity and composition, reducing functional redundancy and ecological resilience (Campillo-Cora et al., 2025; Z. Wang et al., 2025). Numerous studies have demonstrated that microbial taxonomic structure and richness are tightly linked to contamination gradients, suggesting the potential of using soil microbiota as bioindicators of ecological degradation (Ma et al., 2022; Visca et al., 2025; Wilhelm et al., 2023; Zheng et al., 2025).

To effectively integrate microbial and chemical evidence in ecological assessments, it is essential to adopt quantitative tools that translate complex environmental data into interpretable metrics. In this context, synthetic indices provide a means of

summarizing contamination levels and potential ecological risks in a standardized, comparative format.

To quantify and compare the degree of contamination across sites in a reproducible manner, several synthetic indices have been developed to condense heterogeneous chemical information into standardized metrics. The Geoaccumulation Index (Igeo) estimates HMs enrichment relative to natural background levels, distinguishing between natural and anthropogenic inputs (Ferreira et al., 2022). The Improved Potential Ecological Risk Index (IPERI) incorporates both concentration and toxicity coefficients of individual elements (Li et al., 2025), while is proposed another index, the Synthetic IPERI (SPERI), to normalize these data, and to facilitate cross-site comparisons. Their application aligns with European geochemical baselines, such as those established by the GEMAS project (Cicchella et al., 2015), and conforms to national regulatory frameworks, including the Italian Legislative Decree 152/2006 on environmental quality standards (Official Gazette of the Italian Republic, 2006).

Recent advances in metagenomics and predictive statistics have opened new ways for understanding microbial dynamics in contaminated soils. Microbial community data thus offer not only diagnostic information on the current contamination state, but also predictive insights into future shifts in soil functionality and ecological degradation. In particular, decision-tree models such as Classification and Regression Trees (C&RT) have been effectively used to correlate microbial patterns with contamination levels, enabling the identification of specific microbial taxa as potential ecological risk indicators (Ma et al., 2022; Yang et al., 2023). These integrated approaches not only offer insight into the current state of the ecosystem but also provide predictive tools for environmental monitoring and sustainable land management (De'ath & Fabricius, 2000)

While several studies have explored the effects of HMs on soil microbial diversity (Sun et al., 2022; Zhao et al., 2025) or applied synthetic indices separately to quantify ecological risk (Cao et al., 2023; Wang et al., 2023), integrated approaches that

simultaneously combine chemical contamination metrics, culture-based and metagenomic microbial data, and predictive modelling, are missing. This study seeks to fill that gap by establishing an interdisciplinary framework for ecological risk assessment that bridges the divide between environmental chemistry and microbial ecology. Specifically, the objective is to construct a unified model, and to propose an approach based on Classification and Regression Tree (C&RT) that integrates chemical indicators with microbiological data derived from both traditional culturing and high-throughput sequencing.

4.2 Methods

4.2.1 Soil sampling strategy and site selection criteria

Soil samples were collected from twelve distinct locations in the peri-urban area surrounding the city of Foggia (41°27′30.42″N, 15°33′06.77″E), within a radius of approximately 6–12 km from the urban centre. All sampling points were positioned in areas impacted by recurrent episodes of uncontrolled and illegal waste disposal documented in municipal and regional reports. These dumping activities represent the primary and most persistent source of heavy metal inputs into local soils, making this territory a suitable model for evaluating contamination patterns and testing the proposed ecological-risk indices. This activity is an exploratory action focusing on soil samples (<50 g) collected solely for methodological purposes aimed at the isolation and/or characterization of bioremediating microbiota and not an official environmental monitoring activity. Therefore, according to national and local guidelines and regulations a preliminary approval is not required.

Site selection was guided by the presence of visible indicators of anthropogenic disturbance. Soil samples were retrieved from the uppermost 0–10 cm of the soil profile using sterile sampling tools to avoid cross-contamination. At each site, five individual soil cores were collected within a 3 × 3 m area using stainless-steel corers and spatulas disinfected with 70% ethanol between collections. The five cores were

pooled into a single composite sample of approximately 0.5 kg of soil. In the laboratory, composite samples were homogenised under aseptic conditions in sterile polyethylene trays, manually cleared of coarse debris (stones and roots), and sieved through a 2-mm stainless-steel mesh. The homogenised soil was then subdivided into aliquots dedicated to physicochemical analyses, CFU enumeration, and DNA extraction, as described in the next paragraphs. All samples were kept refrigerated immediately after collection (4°C), transported to the laboratory in insulated containers, and processed within 24 hours to preserve microbial viability and community structure. This procedure was repeated twice to have biological replicates.

4.2.2 Characterisation of microbial communities

A 10 g aliquot of each soil sample was suspended in 90 mL of a 0.9% (w/v) saline solution. After mechanical homogenization for 30 minutes, the suspension was serially diluted.

The culture media (Oxoid, Milano, Italy) adopted for microbial enumeration included Plate Count Agar (PCA) both for total viable bacteria and aerobic spore-forming bacteria at 30°C for 24h. The latter preceded by a heat shock treatment at 80 °C for 10 minutes to inactivate vegetative cells. Pseudomonas Agar Base (PAB) medium supplemented with Cetrimide-Fucidin-Cephaloridine (CFC) (Oxoid), incubated at 25°C for 72h, was used to quantify *Pseudomonas* spp.

Coliform bacteria were quantified using Violet Red Bile Agar, incubated at 37 °C and 44 °C for 18-24h to differentiate between mesophilic and thermotolerant strains. Sulfite-reducing bacteria were detected on SPS medium, while Potato Dextrose Agar (PDA) was utilized for the isolation and growth of fungi. Actinomycetes were cultivated using an optimized medium (10 g/L bacteriological peptone, 5 g/L beef extract, 5 g/L NaCl, 10 g/L glycerol, 20 g/L Agar) for their recovery.

4.2.3 DNA isolation and wet lab procedures

Genomic DNA was isolated from approximately 200 mg of soil using the Chemagic™ DNA Soil 250 Kit on the Chemagic™ 360 instrument (Revvity, Waltham, MA, USA), following the manufacturer's protocol. Mechanical cell disruption was carried out using Bashing bead lysis tubes and the Omni Bead Ruptor Elite (OMNI International, Kennesaw, GA, USA) with five cycles of 1-minute bead beating at 4.2 m/s followed by 30-second resting intervals, totalling 5 minutes of lysis. Purified DNA was eluted in 90 µL of nuclease-free water.

DNA concentration was quantified using the Equalbit™ DNA BR Assay Kit (Vazyme, Nanjing, PRC) and measured on an Infinite Pro 200 F Nano+ fluorescent plate reader (Tecan, Männedorf, Switzerland). For shotgun metagenomic library preparation, the VAHTS® Universal Plus DNA Library Prep Kit for Illumina V2 with unique dual indexes (UDIs) was used according to the manufacturer's instructions. Fragment size distribution was assessed by capillary electrophoresis on the LabChip GX Touch HT system using the DNA NGS 3K Assay Kit (Revvity). Final library quantification was performed with the Equalbit 1× dsDNA HS Assay Kit (Vazyme) on the same plate reader. Libraries were pooled and diluted to 140 pM for paired-end 2×150 bp sequencing using the 300-cycle 25B Reagent Kit on the NovaSeq X Plus System (Illumina, San Diego, CA, USA).

4.2.3.1 Bioinformatic Analyses

Each sample generated more than 20 million raw reads. Demultiplexing and adapter trimming were performed using NovaSeq Control Software, while FastQ Toolkit (Illumina) was applied to remove reads with a mean quality score below 30 or a length shorter than 100 bp. Quality control of filtered reads was carried out using FastQC v0.12.1. High-quality reads were then analyzed using the DRAGEN™ Metagenomics Pipeline v3.5.13 (Illumina, BaseSpace), which includes host filtering, taxonomic classification (Kraken2 using the PlusPF-8 reference database), and relative abundance

profiling. As a second step, eukaryotic reads (including human, plant and fungal sequences) were automatically removed by the host-filtering module of the DRAGEN pipeline, and only prokaryotic reads were retained for downstream analyses. Low-abundance taxa representing less than 0.01% of total prokaryotic reads per sample were excluded to eliminate singletons, doubletons and other spurious low-frequency assignments.

Family-level classification represented the lowest taxonomic rank consistently detected across samples, whereas genus- and species-level assignments were sparse and unreliable. Therefore, all downstream analyses, including diversity metrics and C&RT modelling, were performed at the family level.

4.2.4 Physical and chemical characterization of soils

Soil samples collected from each experimental site were subjected to a comprehensive analysis of their physico-chemical characteristics. The soil pH was determined using a 1:2.5 (w/v) soil-to-water suspension, while electrical conductivity (EC) was assessed in a 1:2 (w/v) aqueous extract. Total nitrogen (N) content was quantified according to the Dumas method (Official Gazette of the Italian Republic, 1999). Available phosphorus, expressed as P_2O_5, was extracted using the sodium bicarbonate method developed by Olsen et al. (Olsen et al., 1954). Total organic carbon (TOC) content was evaluated via chemical oxidation with potassium dichromate, followed by titration with ferrous sulfate ($FeSO_4$), in accordance with the Walkley-Black procedure (Walkley, 1947). The percentage of organic matter (OM) was then estimated by multiplying the TOC value by the conversion factor 1.724. The total sulphur was quantified by a LECO Elemental Analyzer, model S832 (St Joseph, MI, USA). The particle size distribution (clay, sand, silt) was conducted by a laser diffraction analysis (Faé et al., 2019) using a Mastersizer 3000 (Malvern Panalytical LTD., Malvern, UK). Total metal composition (Al, As, B, Ba, Ca, Cd, Cr, Cu, Fe, K, Mg, Mn, Na, Ni, P, Pb, Si, Sr, Ti, V, Zn) was determined by inductively coupled plasma optical emission

spectrometry (ICP-OES, Thermo Scientific iCAP 7000 series), after microwave-assisted acid digestion of 0.5 g of air-dried soil samples with 9 mL of HNO_3 (65%) and 3 mL of HCl (37%), according to EPA Method 3051A (Link et al., 1998). Quality assurance was ensured by including blanks, duplicates, and certified reference materials (CRM) in the analytical run.

4.2.5 Ecological risk assessment

To evaluate the ecological risk potentially associated with HMs contamination in the sampled soils, a multi-index approach was applied, integrating the calculation of the Geo-accumulation Index (Igeo) (Zerizghi et al., 2022), the Improved Potential Ecological Risk Index (IPERI) (Li et al., 2025), and the Synthetic Potential Ecological Risk Index (SPERI) based on the study of Hakanson (1980). These synthetic indices were calculated for selected potentially toxic elements (PTEs), namely As, Cd, Cr, Cu, Ni, Pb, and Zn.

The Igeo was calculated as described in **Equation 4.1**:

$$\text{Igeo} = \log_2 * \left(\frac{C_n}{1.5 * B_n}\right) \textbf{(Eq. 4.1)}$$

where C_n is the measured concentration of the element in the sample and B_n is its corresponding geochemical background value obtained from GEMAS European geochemical baselines (Cicchella et al., 2015).

According to the classification originally proposed by Grattacaso et al. (2025), the geo-accumulation index (Igeo) is divided into seven contamination levels, each corresponding to a defined soil quality class: Class 0: Igeo ≤ 0 (Practically uncontaminated), Class 1: 0 < Igeo ≤ 1 (Uncontaminated to moderately contaminated), Class 2: 1 < Igeo ≤ 2 (Moderately contaminated), Class 3: 2 < Igeo ≤ 3 (Moderately to heavily contaminated), Class 4: 3 < Igeo ≤ 4 (Heavily contaminated), Class 5: 4 < Igeo ≤ 5 (Heavily to extremely contaminated), Class 6: Igeo > 5 (Extremely contaminated).

To assess the ecological risk posed by each element, the **Improved Potential Ecological Risk Index (IPERI)** was calculated as follows (**Equation 4.2**):

$$\text{IPERI} = \sum T_r^i * CF_i \text{ (Eq. 4.2)}$$

$$CF_i = \left(\frac{C_n^i}{B_n^i}\right)$$

Where CF_i is the contamination factor of the i^{th} metal, T_r^i is the toxic response coefficient (Cd = 30, Pb = 5, Cu = 5, Cr = 2, Ni = 5, Zn = 1, As = 10) (Hakanson, 1980; Li et al., 2025). The cumulative IPERI was used to classify ecological risk into the following categories: RI < 150 (low risk), 150 ≤ RI < 300 (moderate risk), 300 ≤ RI < 600 (considerable risk), and RI ≥ 600 (very high risk).

The last index SPERI, a normalized index, was calculated according to the **Equation 4.3,** as follows:

$$\text{SPERI} = \frac{1}{n}\sum_{i=1}^{n} \frac{C_i - C_i^{min}}{C_i^{max} - C_i^{min}} \text{ (Eq. 4.3)}$$

Where: n is the number of metals, C_i is the observed concentration of the i^{th} metal in the sample, C_i^{min} and C_i^{max} are, respectively, the minimum and maximum observed concentrations of the i^{th} metal across the dataset.

4.2.6 Statistics

For each sampling site, physicochemical and culture-based measurements were obtained from two independent biological samples, with all laboratory determinations performed in technical duplicate. Statistical analyses were carried out on the mean values of the two biological replicates per site.

Shotgun metagenomic sequencing, instead, was performed on one representative biological sample per site, as detailed in the Bioinformatic Analyses section. α

diversity was quantified using the Shannon and Simpson indices, and the differences among the twelve soil samples were evaluated through the Kruskal–Wallis test. In addition, relative abundance of bacterial families was analyzed either by the Wilcoxon rank-sum test (two groups) or the Kruskal–Wallis test (multiple groups). P-values were adjusted using the Benjamini–Hochberg procedure. These analyses were done through Statistica v.14 (Statsoft, Tulsa, USA)

Correlation analysis was carried out using PAST v.5.2 (Hammer et al., 2001), based on Spearman's coefficients, to evaluate potential associations between factors and identify co-occurrence trends. In addition, scatter plots were generated using Statistica v.14 to visually explore bivariate relationships between the risk indices (IPERI and SPERI), with linear regression lines and R^2 values used to confirm the strength of associations. The same software was used to develop a Classification and Regression Tree (C&RT) model aimed at classifying samples according to the combined SPERI/IPERI ecological risk category and the corresponding microbiota composition.

4.2.7 Classification and Regression Tree (C&RT) modelling

Classification and Regression Tree (C&RT) analyses were performed using Statistica StatSoft v14. The SPERI and IPERI classes were used as dependent variables in two separate models. Predictors consisted of relative abundances of bacterial families derived from the metagenomic dataset. The most dominant families across all samples (Bradyrhizobiaceae, Conexibacteraceae, Mycobacteriaceae, Xanthomonadaceae, Rhodospirillaceae, Rhodobacteraceae, Streptomycetaceae, Nocardioidaceae, Burkholderiaceae and Comamonadaceae) were selected as predictors for model construction. These values were obtained after quality filtering, host read removal and exclusion of low-abundance taxa (<0.01% of prokaryotic reads), and represent the only predictors included in the C&RT framework. In the resulting decision trees, the numeric values displayed at each splitting node represent thresholds of metagenomic

relative abundances for the bacterial families contributing most strongly to the classification.

Model construction followed the standard implementation of the C&RT algorithms in Statistica. Node splitting was based on the Gini impurity criterion, with equal misclassification costs and estimated prior probabilities. A minimum of five observations was required to form a node, and tree growth was constrained using the "prune on variance" stopping rule to prevent overfitting. Model stability and robustness were evaluated through cross-validation following Statistica's default settings.

4.3 Results

4.3.1 Microbial composition of soils

The microbiological analysis, summarized in **Table 4.1**, showed consistent abundances of Actinomycetes, *Pseudomonas* spp., and mesophilic bacteria across most soil samples, with values generally above 6.5 log CFU/g. Sample 12, however, exhibited markedly lower counts for all groups, suggesting unfavourable conditions. Aerobic spore-forming bacteria ranged from moderate to high levels, peaking in sample 3 (7.00 log CFU/g), while moulds were absent in samples 3 and 6 but present elsewhere. Anaerobic spore-formers were the less abundant overall, though sample 12 showed a relative increase for this group. Total and faecal coliforms did not exhibit any detectable growth.

Genomic profiling of microbial communities was done on both fungi and bacteria; fungi represent a significant part of microbial populations (1% or lower). However, data were variable and do not allow cluster or regression analysis with the other parameters; therefore, for modelling purposes the attention was only given to bacteria. The dataset referred to bacterial families allows to assess within-sample diversity (α-diversity), providing insights into ecosystem stability and species distribution. α-diversity analyses showed comparable patterns across all samples. The Shannon index

indicated consistently high diversity (mean ± SD: 3.8 ± 0.09), while the Simpson index (mean ± SD: 0.95 ± 0.05) confirmed low dominance and an even distribution of taxa. Together, these metrics point to a stable community structure with limited variability across the sampling sites.

Table 4.1 Microbial abundance in soil samples expressed as log-transformed colony-forming units per gram of dry soil (log CFU/g). Values represent the mean ± standard deviation for each microbial group. "ND" indicates not detected.

	Actinomycetes	*Pseudomonas* spp.	Total viable count	Aerobic spore-forming	Mould	Anaerobic spore-forming
1	7.15±0.03	6.62±0.05	6.82±0.13	6.28±0.32	4.23±0.03	2.54±0.24
2	7.10±0.06	6.77±0.21	7.00±0.14	6.75±0.30	3.94±0.24	3.32±0.32
3	6.89±0.07	6.73±0.12	6.92±0.09	7.00±0.05	ND	2.45±0.15
4	6.92±0.02	6.32±0.12	6.58±0.03	5.62±0.85	4.38±0.34	3.48±0.02
5	6.82±0.02	6.73±0.26	6.63±0.11	4.53±0.13	4.31±0.03	1.15±0.15
6	6.68±0.21	7.00±0.08	6.71±0.03	4.54±0.14	ND	2.11±0.05
7	6.70±0.11	6.93±0.02	7.01±0.03	4.59±0.16	4.15±0.07	2.13±0.05
8	6.79±0.33	6.68±0.05	6.37±0.26	4.80±0.11	4.30±0.15	1.56±0.56
9	7.10±0.09	6.74±0.08	6.72±0.18	4.82±0.02	4.74±0.04	1.80±0.20
10	7.16±0.02	6.76±0.23	6.78±0.14	4.72±0.08	4.20±0.07	1.54±0.06
11	7.28±0.07	6.72±0.58	7.20±0.09	6.24±0.26	4.07±0.01	2.57±0.27
12	4.42±0.37	4.02±0.42	4.10±0.58	4.13±0.39	4.55±0.47	3.29±0.11

α-diversity indices did not reveal significant differences among groups, indicating comparable overall richness and evenness. Consequently, these analyses were complemented with a compositional assessment restricted to dominant taxa. To minimise the impact of low abundance features only bacterial families reaching ≥1% relative abundance in at least one sample were retained. The 1% threshold was adopted as an operational criterion to define dominant taxa, balancing the exclusion of rare features with the preservation of ecologically relevant families. The stacked bar chart (**Figure 4.1**) displays the relative abundance of 22 bacterial families.

Figure 4.1 Relative abundance of bacterial families across twelve soil samples. Each bar represents one sample (from 1 to 12), and colours indicate the taxonomic affiliation at the family level. The values are presented as percentages of total reads per sample. Taxa contributing less than the 1% threshold are grouped under "Others"

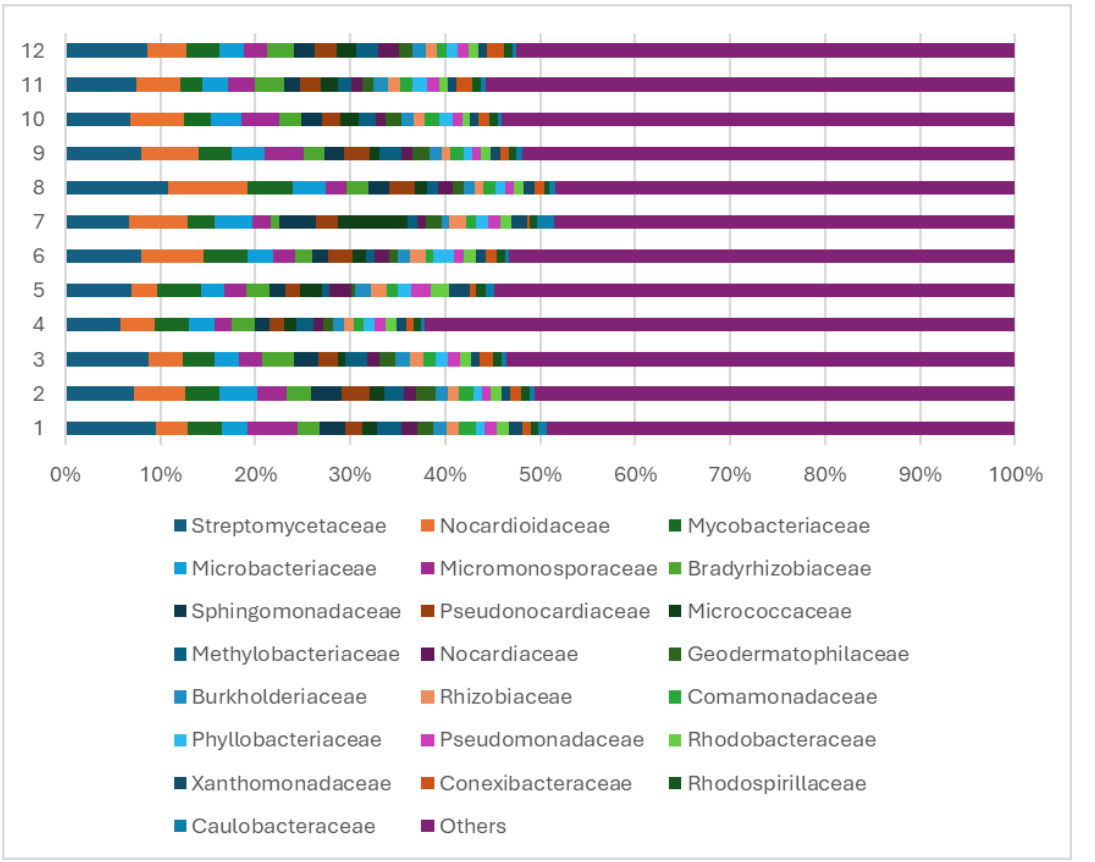

Streptomycetaceae was consistently the most abundant, with a relative abundance of 10.84% in sample 8; Nocardioidaceae also reached high levels in the same sample. Mycobacteriaceae remained stable (3–4.7%), while Microbacteriaceae and Pseudonocardiaceae were steady contributors, especially in samples 6–9. Micromonosporaceae were at variable levels, with a relatively low abundance in sample 4 (1.89%) and high levels in samples 9–10 (4.11%-3.89%).

Other moderately abundant families included Bradyrhizobiaceae, Sphingomonadaceae (notably high in sample 7, 3.86%), and Micrococcaceae (7.36%, in sample 7).

4.3.2 Soil physicochemical traits and metal content

The physico-chemical properties of the soil samples (**Table 4.2**) showed neutral to slightly alkaline pH (7.23–7.75) with minimal variation. Electrical conductivity varied widely, with sample 4 showing the highest value (16.73 dS/m), suggesting possible anthropogenic impact. Organic matter ranged from 2.14% to 9.75%, highest in sample 8, which also had the greatest phosphorus content (506 mg/kg).

Total carbon followed similar patterns to organic matter, peaking above 12% in samples 1, 3, and 8. Nitrogen levels were low to moderate (0.07%–0.61%).

Texture analysis indicated sandy dominance in samples 1–2 and 5–9, and higher clay content (≥ 51%) in samples 10–12 (**Figure 4.2**).

The elemental analysis of soil samples, summarized in **ANNEX B - Table B4.1**, revealed distinct patterns of metal and HMs distribution, likely indicative of anthropogenic influence. Pb showed strong variability, ranging from 8.51 mg/kg (sample 9) to 467.30 mg/kg (sample 11), with sample 8 also exhibiting a notable value (210.83 mg/kg), suggesting multiple contamination hotspots.

Zn reached particularly high concentrations in samples 3, 1, and 10 (6,340.72, 4,061.68, and 3,572.49 mg/kg respectively), well beyond typical background levels. Cu was mostly uniform but spiked in sample 11 (1,002.15 mg/kg). Cd remained generally low, although samples 2 and 12 exceeded 1 mg/kg. As was moderately elevated in samples 2 and 12.

Table 4.2 Physicochemical properties of the twelve soil samples; mean values. Parameters include pH, electrical conductivity (dS/m), organic matter (%), available phosphorus, moisture and dry matter content, total carbon and nitrogen (%), sulfur (%), and soil texture fractions (sand, clay, and silt %).

Sample	pH	EC (dS/m)	OM (%)	Available P	Moisture (%)	Dry Matter (%)	Tot. Carbon (%)	N (%)	S (%)	Sand (%)	Clay (%)	Silt (%)
1	7.60	1.40	5.88	306	20.52	79.48	12.80	0.46	0.02	60	10	30
2	7.62	0.58	3.79	118	13.17	86.83	8.27	0.12	0.92	63	12	25
3	7.40	1.30	3.68	228	23.17	76.83	12.27	0.35	0.05	32	35	33
4	7.47	16.73	4.30	296	5.48	94.52	9.22	0.30	1.21	46	18	36
5	7.42	4.13	5.12	462	9.77	90.23	10.20	0.21	0.06	55	15	30
6	7.23	4.08	3.62	212	9.51	90.49	5.68	0.16	0.01	35	20	45
7	7.62	5.96	2.14	73	17.93	82.07	10.61	0.07	0.01	53	10	37
8	7.43	2.84	9.75	506	16.08	83.92	12.31	0.61	0.08	53	11	36
9	7.57	1.26	4.97	668	11.97	88.03	9.81	0.27	0.06	50	10	40
10	7.66	1.00	2.26	131	21.34	78.66	6.06	0.17	0.04	39	51	10
11	7.68	0.90	2.43	71	20.55	79.45	4.32	0.07	0.03	30	53	17
12	7.75	0.55	4.32	136	20.46	79.54	5.34	0.32	0.01	20	51	29

Figure 4.2 A) USDA soil texture triangle; B) classification of the twelve samples (green number) based on particle size distribution (sand, silt, and clay percentages).

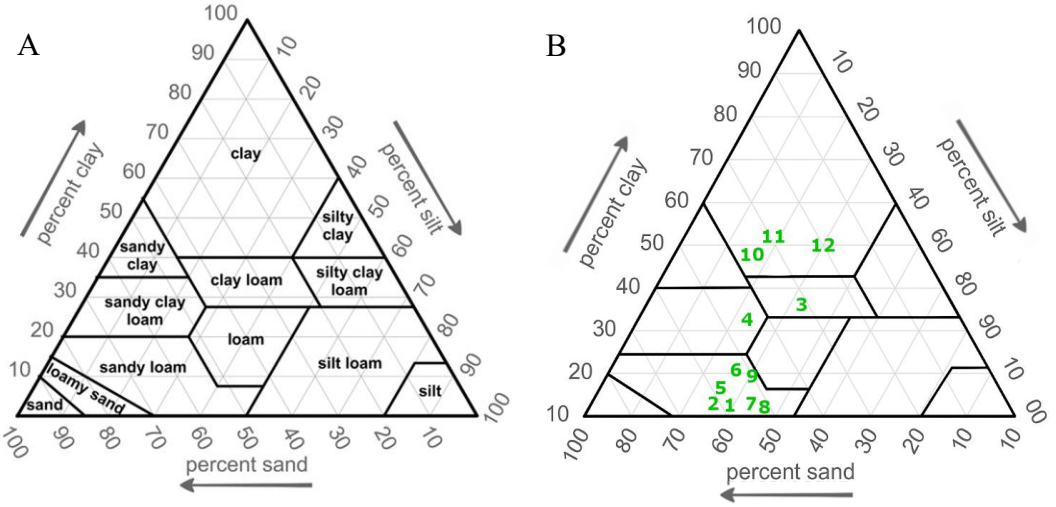

4.3.3 Ecological risk indices and contamination patterns

The heatmap in **Figure 4.3** presents the spatial distribution of HMs contamination according to Igeo, which quantifies anthropogenic enrichment relative to natural background levels, with contamination classes ranging from 0 (uncontaminated) to 6 (extremely contaminated).

As, Cr, and Ni generally fall within the lower classes (0–1), suggesting negligible contamination. In contrast, Cd reaches moderate to strong contamination in samples 2 and 12, indicating site-specific inputs. Cu shows pronounced heterogeneity, with Sample 11 reaching Class 5 (Igeo = 4.38), marking it as a potential hotspot. Pb follows a similar trend, with Sample 11 classified as heavily contaminated (Class 4–5). Zn stands out with extreme values in Sample 2 (Igeo = 6.10, Class 6) and Sample 9 (Igeo = 5.27, Class 5), confirming severe enrichment. These patterns highlight both localized and widespread anthropogenic influences on soil metal content.

Figure 4.3 Heatmap of Igeo (Geoaccumulation Index) values for selected HMs (As, Cd, Cr, Cu, Ni, Pb, Zn) across 12 soil samples, showing contamination classes from Class 0 (uncontaminated) to Class 6 (extremely contaminated) based on standardized thresholds.

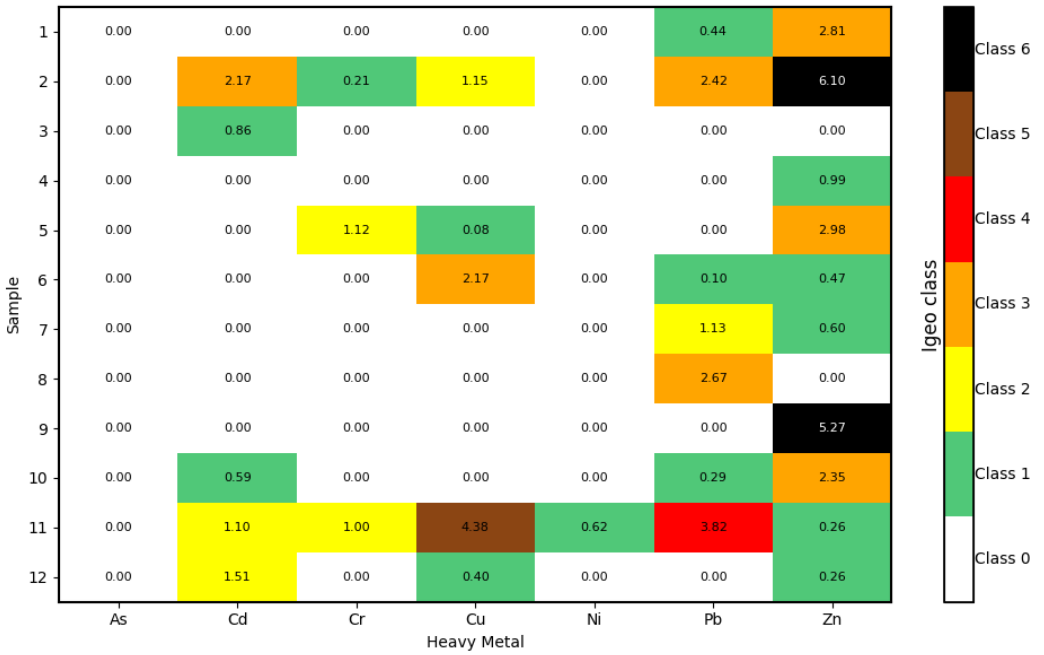

The IPERI (**Table B4.2**) and SPERI (**Table B4.3**) values were used to assess metal-specific and cumulative ecological risk. In the case of IPERI, Cd consistently exhibited the highest individual risk values, peaking in sample 2 (202.37) and sample 11 (96.45), indicating severe contamination potential. Additional high-risk values were observed for Cu and Pb in sample 11 (156.59 and 105.72 respectively), further establishing this

sample as a major pollution hotspot. Zn, although generally moderate across most samples, reached a maximum of 390.96 in the same site, reflecting a complex multi-metal stress profile. The SPERI index, which rescales risk values between 0 and 1, allows for direct comparison across metals and samples.

In this normalized framework, sample 11 again emerges as the most impacted, with Cd, Cu, Ni, Pb, and Zn all reaching a SPERI value of 1.00, indicating maximum relative risk. Notably, sample 2 and sample 12 also exhibit elevated SPERI scores for Cd and As, underscoring localized areas of concern within the dataset.

4.3.4 Correlation analysis and index selection

To assess the correlation among all the factors, the Spearman's index was used (**Figure B4.1)**, which illustrates the correlation coefficients among soil physicochemical parameters, elemental composition, and the relative abundance of dominant bacterial families. Data reveal that soil texture exerts a significant influence on both geochemical properties and microbial community structure. Clay content correlates positively with several trace metals (e.g., Cr, iron (Fe), vanadium (Vd)). In contrast, sand content shows negative correlations with elements like As and Zn.

Organic matter, total carbon, and nitrogen are closely interrelated and positively associated with bacterial families typical of nutrient-rich soils, such as Bradyrhizobiaceae, Streptomycetaceae, and Pseudonocardiaceae. Electrical conductivity aligns with calcium and barium levels—suggesting a geogenic salt source—and with bacterial groups tolerant to moderate salinity, like Pseudomonadaceae and Micrococcaceae. Available phosphorus is positively correlated with potential phosphate-solubilizing taxa, particularly Micromonosporaceae and Mycobacteriaceae.

Some taxa, such as Geodermatophilaceae and Nocardiaceae, show positive associations with HMs like Pb, Cd, and Cr, indicating possible ecological tolerance.

Conversely, families like Methylobacteriaceae and Sphingomonadaceae display negative correlations, suggesting sensitivity to contamination.

Given the complexity of the full correlation matrix, direct ecological patterns were difficult to understand. Therefore, attention was narrowed to microbial families most directly correlated with the ecological risk indices IPERI and SPERI. The resulting correlation table (**Table 4.3**) highlights both positively and negatively associated taxa.

Table 4.3 Spearman's correlation coefficients between selected bacterial families and the IPERI and SPERI indices

	IPERI	**SPERI**
Streptomycetaceae	-0.036	-0.153
Nocardioidaceae	-0.128	-0.144
Mycobacteriaceae	-0.524	-0.472
Microbacteriaceae	-0.016	0.032
Micromonosporaceae	0.023	-0.089
Bradyrhizobiaceae	0.558	0.440
Sphingomonadaceae	0.099	0.086
Pseudonocardiaceae	0.153	0.137
Micrococcaceae	-0.143	-0.002
Methylobacteriaceae	0.178	0.003
Nocardiaceae	-0.191	-0.103
Geodermatophilaceae	0.271	0.103
Burkholderiaceae	0.290	0.270
Rhizobiaceae	-0.046	0.021
Comamonadaceae	0.281	0.183
Phyllobacteriaceae	0.055	0.034
Pseudomonadaceae	-0.100	0.059
Rhodobacteraceae	-0.469	-0.331
Xanthomonadaceae	-0.401	-0.202
Conexibacteraceae	0.639	0.481
Rhodospirillaceae	0.175	0.292
Caulobacteraceae	-0.249	-0.129

Notably, Conexibacteraceae and Bradyrhizobiaceae showed strong positive correlations with both indices, suggesting their abundance increases with contamination severity. In contrast, Mycobacteriaceae, Xanthomonadaceae, and

Rhodobacteraceae exhibited negative correlations, implying potential sensitivity to polluted conditions.

Based on these results, the ten families most strongly correlated—positively or negatively—with the IPERI and SPERI indices were selected as candidate bioindicators. For SPERI, these included: Bradyrhizobiaceae, Conexibacteraceae, Burkholderiaceae, Rhodospirillaceae, Pseudonocardiaceae, Sphingomonadaceae, Comamonadaceae, Geodermatophilaceae, Phyllobacteriaceae, and Methylobacteriaceae.

For the IPERI index, the most correlated families included Conexibacteraceae, Bradyrhizobiaceae, Burkholderiaceae, Comamonadaceae, Geodermatophilaceae, Pseudonocardiaceae, Sphingomonadaceae, Methylobacteriaceae, Phyllobacteriaceae, and Rhodospirillaceae. These families were then incorporated into a C&RT (Classification and Regression Tree) model with the goal of developing a predictive framework capable of estimating the ecological pollution status based on shifts in the soil microbial community.

4.3.5 Predictive modelling using classification trees (C&RT)

Each classification/regression tree (C&RT) diagram visually represents a set of binary decisions (De'ath & Fabricius, 2000) that recursively gives a partition of the dataset. In this work, based on microbial family abundance, aiming to predict the pollution state expressed by either the IPERI or SPERI index. The root node at the top of each tree contains the full sample set and splits based on a threshold value for the relative abundance of a specific bacterial family. This split generates two branches, each forming a new internal node or terminal leaf. At each node, on its top, the splitting criterion is determined by the variable (a specific bacterial family) whose abundance best reduces intra-group variability. Two key statistics are displayed in each node: mu, the mean value of the index within that node, and var, the variance of that value. While mu reflects the expected pollution state for samples within that node, var indicates the

internal consistency of the prediction; lower variance implies higher predictive reliability.

The classification/regression tree model (C&RT) constructed on the IPERI index (**Figure B4.2**) reveals a branching structure that, while capturing variations in microbial abundance across the dataset, suffers from limited robustness.

The model splits first on the abundance of Conexibacteraceae, separating samples with lower values (≤ 1.15) from those with higher values. The latter group (N=4) immediately forms a terminal node with a markedly elevated mean IPERI value (mu = 263.00) but also exhibits very high internal variability (variance = 7690.62), indicating poor prediction precision. Although the model identifies microbial families associated with different pollution states, it lacks the ability to produce homogeneous, low-variance terminal nodes—reflected in large intra-group variability, particularly among the upper branches. This dispersion suggests that the model may be affected by an overfitting noise or influenced by high values in the unscaled IPERI data.

Overall, the IPERI-based C&RT tree does not provide strong predictive confidence due to the instability and high internal variance of its partitions.

Due to the elevated intra-node variance and the limited robustness of the IPERI-based C&RT, because of the influence of unscaled and high values, the normalized SPERI index was subsequently tested as an alternative predictor, with the aim of improving model stability, reducing dispersion, and enhancing the biological interpretability of node partitions.

To assess whether the normalized SPERI index retains the ecological risk patterns captured by IPERI while enhancing interpretability, a scatter plot analysis was performed. The resulting plot (**Figure B4.3**), in line with previous findings (Zerizghi et al., 2022), revealed a strong positive linear relationship ($R^2 = 0.896$). Despite being a normalized index, SPERI preserves the original contamination gradient and relative sample rankings established by IPERI, while minimizing dispersion and enhancing comparability.

This strong correlation confirmed the suitability of SPERI not only as a normalized risk descriptor but also as a reliable proxy for predictive modeling, prompting its implementation in a refined C&RT framework.

Compared to IPERI, the SPERI tree not only reduces noise but also avoids the influence of high levels of HMs by virtue of the normalized scale. In contrast to the IPERI-based model, the decision tree built on the SPERI index demonstrates a markedly more robust and reliable predictive structure. The first split occurs on the abundance of Mycobacteriaceae, effectively separating a single high-value outlier (Node 2, mu = 0.668) from the rest of the samples (Node 3, N = 11). This early partitioning reduces overall variance significantly. Subsequent branches—particularly those involving Xanthomonadaceae and Rhodospirillaceae—progressively segment the remaining samples into increasingly homogeneous groups. Each terminal node exhibits very low within-node variance (e.g., Var = 0.000172 and 0.000881), underscoring the model's stability and discriminative power.

This structure allows the user to input microbial abundance data and, by sequentially applying the decision thresholds, predict the contamination state. The SPERI decision tree (**Figure 4.4**) must be interpreted by following a top-down logic, where each internal node represents a binary decision rule based on the relative abundance of a specific bacterial family.

The root node begins with Mycobacteriaceae: if the abundance is ≤ 2.60, the sample is likely to have a higher SPERI value (at least 0.67, Node 2), whereas values > 2.60 lead to further refinement but generally are related to lower SPERIs and thus to less contaminated soils. In this context, a further classification can be done through the other families; in fact, the subsequent split on Xanthomonadaceae and then on Rhodospirillaceae further stratifies samples into narrow, well-defined ranges of SPERI scores, each with minimal internal variance.

Figure 4.4 Decision classification/regression tree model (C&RT) based on the SPERI index. Values on the branches represent the abundance of microbial families, while the box contain mean values (mu) and variance (var) of SPERI.

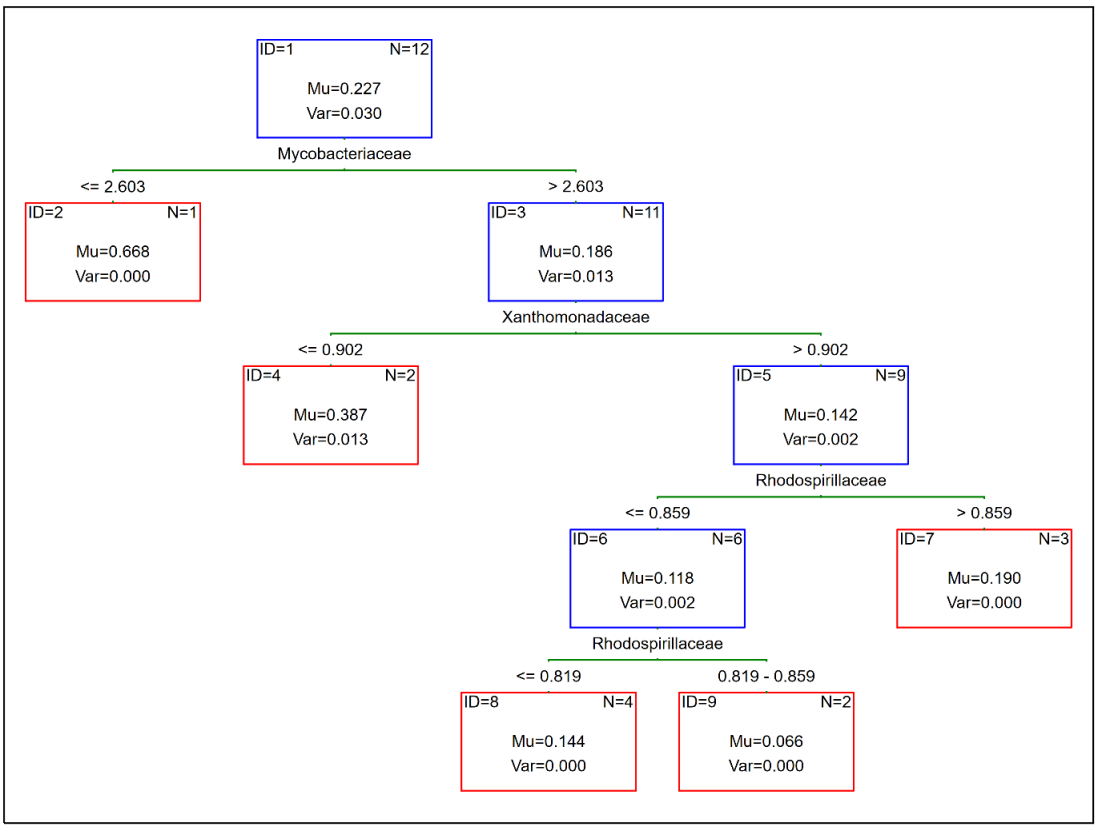

In particular, a lower abundance of Xanthomonadaceae (0.90) indicates soil with medium contamination levels (SPERI of 0.39), while less contaminated soils have a higher abundance of Xanthomonadaceae (SPERI at 0.14). Finally, a further refinement is possible through Rhodospirillaceae. In conclusion, low-contaminated or uncontaminated soils are characterized by high abundance of Mycobacteriaceae and Xanthomonadaceae and lower levels of Rhodospirillaceae.

4.4 Discussion

The results of this study offer a comprehensive assessment of the ecological impacts of HMs contamination on soil microbial communities in a Mediterranean agricultural region subject to heterogeneous anthropogenic pressure. Both culture-based and metagenomic analyses revealed a generally high microbial richness across the sampled soils, supported by α-diversity indices and the relative abundance of dominant bacterial families such as Streptomycetaceae, Nocardioidaceae, and Mycobacteriaceae. However, distinct compositional shifts were observed among sampling sites, reflecting variations in contamination levels, soil texture, salinity, and organic matter content.

The potentially toxic elements (PTEs) were selected based on three main criteria: (i) their regulatory relevance, as they are listed among the contaminants regulated by Italian legislation (Official Gazette of the Italian Republic, 2006) and explicitly mentioned in the recent European Soil Monitoring and Resilience Law proposal as priority substances for the identification of contaminated sites; (ii) their well-documented ecotoxicological effects on soil organisms and terrestrial ecosystems, as widely reported in the scientific literature (Hakanson, 1980, Li et al., 2025; Zerizghi et al., 2022); and (iii) the availability of harmonized geochemical background values, provided by the GEMAS project (Cicchella et al., 2015), which allows robust and comparable application of synthetic ecological risk indices. These PTEs also represent the most frequently reported inorganic contaminants in both agricultural and urban soils across Italy, making them particularly relevant for national and European risk assessments. Given their environmental and regulatory relevance, the analysis of these PTEs using synthetic indices provides an integrated understanding of both contamination levels and their potential ecological consequences.

Among the three synthetic indices applied to quantify contamination Igeo, IPERI, and SPERI, the latter demonstrated superior interpretability, effectively reducing the influence of high values and providing a more balanced view of ecological risk. This

was particularly evident in samples 2 and 11, where high concentrations of Zn and Cd significantly affected IPERI, while SPERI yielded ecologically interpretable risk classifications. These findings are in line with Zhang et al. (2023), who highlighted that unnormalized risk indices may inflate the influence of extreme values, supporting the adoption of normalization strategies such as those used in SPERI. Similarly, Ferreira et al. (2022) highlighted that unnormalized indices such as Igeo and IPERI can overemphasize the contribution of highly concentrated compounds. In contrast, SPERI's formulation enhances comparability and supports more proportionate ecological interpretations across heterogeneous environmental matrices.

Correlations between microbial taxa and contamination gradients revealed consistent trends. Families such as Bradyrhizobiaceae and Conexibacteraceae were positively associated with SPERI and IPERI, suggesting their potential tolerance or adaptive advantage under HMs stress. These results are in line with other studies in which both families are involved in HMs resistance mechanisms (Bao et al., 2024; Gao et al., 2021; Salmi & Boulila, 2021). In contrast, Mycobacteriaceae and Rhodobacteraceae were consistently depleted in highly contaminated samples, supporting their role as sensitive bioindicators. These families belong to the phyla Actinobacteria and Proteobacteria, respectively, both of which are commonly regarded as taxonomically and functionally versatile microbial groups in soil ecosystems. Interestingly, although Mycobacteriaceae are generally recognized for their metabolic flexibility and high resistance to environmental stressors, their marked decline in this study may reflect the crossing of a critical ecological threshold beyond which even resilient taxa are adversely affected. This observation aligns with findings from recent metagenomic studies showing that long-term or cumulative HMsal exposure can destabilize microbial community structures (Qi et al., 2022) and eliminate key generalist taxa, including Actinobacteria and Proteobacteria, under elevated ecological risk levels (Gao et al., 2021; Li et al., 2022; Zheng et al., 2025).

Importantly, many of the bacterial families observed in contaminated soils were also present in less impacted samples, albeit at different relative abundances. This supports the idea that microbial responses to contamination are not binary (presence/absence) but rather occur as compositional rebalancing across ecological gradients. Such shifts, even in the absence of biodiversity loss, can alter ecosystem functionality. These insights reinforce the need to combine diversity metrics with structural and functional analyses to capture the full ecological consequences of contamination (Campillo-Cora et al., 2025; Lu et al., 2022).

Another relevant finding relates to the consistent dominance of Streptomycetaceae across all samples, regardless of contamination levels. Given their known capabilities in decomposing organic matter and producing secondary metabolites, members of this family may contribute to ecosystem stability and functional compensation under stress. Their abundance may reflect structural resilience in the face of pollution, as proposed by Pu et al. (2025) in studies on metal-impacted soils.

The Classification and Regression Tree (C&RT) model built on SPERI values confirmed the predictive potential of microbial data, with a stable structure and informative splits based on Mycobacteriaceae, Xanthomonadaceae, and Rhodospirillaceae. Notably, no single microbial taxon was sufficient to classify ecological risk levels with high reliability; rather, it was the combination of multiple taxa, in specific hierarchical arrangements, that allowed for robust risk discrimination. These findings are in line with previous studies highlighting the advantages of multivariate, model-based approaches for environmental microbiology and risk classification. Xu et al (2022) and Wijaya et al. (2023) demonstrated that microbial indicators, when evaluated via decision tree or learning models, offered high-resolution classification of contamination status, outperforming single-taxon indicators. Similarly, Cipullo et al. (2019) emphasized that complex environmental signals require multidimensional interpretation through non-linear machine learning methods to support accurate ecological risk prediction.

Several site-specific patterns further enriched the interpretation of our findings. Sample 12 exhibited a reduction in CFU counts across all cultured taxa, suggesting a collapse in microbial viability potentially linked to cumulative or chronic contamination stress. Comparable cases of microbial suppression under Zn and Cu pressure have been documented by Song et al. (2018), who showed significant biomass C and ATP declines in soils exposed to single and combined metal stressors. In contrast, samples 1 and 8—despite moderate HMs levels—displayed high organic matter content and relatively rich microbial assemblages. This may reflect the protective role of organic matter in buffering metal bioavailability and sustaining microbial viability. Recent studies have demonstrated that dissolved organic matter (DOM), particularly from compost and waste sources, can reduce metal toxicity by complexation, while simultaneously supporting microbial diversity and enzymatic activity under HMs stress (Yang et al., 2024; Zeng et al., 2024; zhang et al., 2024).

Soil physicochemical properties also played a non-negligible role. Clay-rich soils appeared to harbor higher microbial abundances than sandy ones, even when contamination levels were similar. This finding supports earlier work by Naylor et al. (2022) and Bhaduri et al. (2022), who emphasized the buffering and stabilizing effects of finer soil textures through improved retention of water and nutrients and lower metal mobility.

In addition, sample 4 exhibited high electrical conductivity and an enrichment in halotolerant taxa such as Halomonadaceae and Nocardioidaceae, suggesting co-selection driven by salinity and HMs stress. These patterns align with recent findings by several authors (Diba et al., 2021; Orji et al., 2021; Sodhi et al., 2022), who described the presence of halotolerant and metal-resistant bacterial consortia in hypersaline, metal-contaminated environments. Their work emphasizes the ecological relevance of co-adaptive traits under multiple stressors in marginal and salt-affected soils.

Finally, the observation that α-diversity indices remained high even in some contaminated soils warrants attention. This finding suggests that biodiversity alone may not be a sufficient indicator of ecological integrity, as functional shifts in the microbial community may occur without significant changes in richness. This reinforces the value of integrating taxonomic, functional, and ecological dimensions when assessing soil health in contaminated environments.

In conclusion, this study presents an integrative framework for ecological risk assessment in contaminated soils, combining traditional chemical indices with culture-based and metagenomic microbial analyses. By applying synthetic risk metrics (Igeo, IPERI, and SPERI) and constructing classification models based on microbial community data, the work illustrates that normalized indices such as SPERI offer enhanced ecological interpretability and robustness against data skewness. Furthermore, compositional shifts in key microbial families, such as the decline of Mycobacteriaceae and Rhodobacteraceae and the persistence of Streptomycetaceae, provide functional insights into ecosystem resilience and degradation.

The consistent patterns uncovered by C&RT models reinforce the potential of microbial indicators as predictive tools for environmental monitoring. However, the predictive power arises not from individual taxa, but from their collective interactions and hierarchical configurations. The findings underscore the importance of incorporating microbial community structure and soil physicochemical traits into ecological risk frameworks, moving beyond mere biodiversity counts to encompass compositional and functional shifts.

Despite the robustness of these findings, this study has some limitations that warrant consideration. The relatively limited sample size and geographic scope constrain the generalizability of the results, while the taxonomic resolution, restricted to the family level, ensures statistical stability but may obscure finer ecological signals. Moreover, although SPERI demonstrated enhanced interpretability over traditional indices, the assignment of toxicological weights remains semi-empirical and would benefit from

local calibration. Future research should expand the spatial and temporal scope of sampling, adding functional gene profiling techniques, and refining risk indices through site-specific toxicological parameters. The integration of such approaches based on a more complex machine learning and high-throughput microbial data offers strong potential for the development of next-generation, biologically informed tools for ecological risk assessment.

References

Bao, Z., Wang, C., Cao, J., Zhang, T., Guo, Y., Sato, Y., Nishizawa, T., & Ohta, H. (2024). *Tardiphaga alba* sp. Nov., a heavy metal-tolerant bacterium isolated from garden soil. *International Journal of Systematic and Evolutionary Microbiology*, *74*(1). https://doi.org/10.1099/ijsem.0.006238

Bhaduri, D., Sihi, D., Bhowmik, A., Verma, B. C., Munda, S., & Dari, B. (2022). A review on effective soil health bio-indicators for ecosystem restoration and sustainability. *Frontiers in Microbiology*, *13*. https://doi.org/10.3389/fmicb.2022.938481

Brevik, E. C., Slaughter, L., Singh, B. R., Steffan, J. J., Collier, D., Barnhart, P., & Pereira, P. (2020). Soil and human health: Current status and future needs. *Air, Soil and Water Research*, *13*. https://doi.org/10.1177/1178622120934441

Campillo-Cora, C., Rodríguez-Seijo, A., Pérez-Rodríguez, P., Fernández-Calviño, D., & Santás-Miguel, V. (2025). Effect of heavy metal pollution on soil microorganisms: Influence of soil physicochemical properties. A systematic review. *European Journal of Soil Biology*, *124*, 103706. https://doi.org/10.1016/j.ejsobi.2024.103706

Cao, Y., Wang, R., Liu, Y., Li, Y., Jia, L., Yang, Q., Zeng, X., Li, X., Wang, Q., Wang, R., & Riaz, L. (2023). Improved calculations of heavy metal toxicity coefficients for evaluating potential ecological risk in sediments based on seven major Chinese water systems. *Toxics*, *11*(8), 650. https://doi.org/10.3390/toxics11080650

Cicchella, D., Giaccio, L., Dinelli, E., Albanese, S., Lima, A., Zuzolo, D., Valera, P., & De Vivo, B. (2015). GEMAS: Spatial distribution of chemical elements in agricultural and grazing land soil of Italy. *Journal of Geochemical Exploration*, *154*, 129–142. https://doi.org/10.1016/j.gexplo.2014.11.009

Cipullo, S., Snapir, B., Prpich, G., Campo, P., & Coulon, F. (2019). Prediction of bioavailability and toxicity of complex chemical mixtures through machine learning models. *Chemosphere*, *215*, 388–395. https://doi.org/10.1016/j.chemosphere.2018.10.056

De'ath, G., & Fabricius, K. E. (2000). Classification and regression trees: A powerful yet simple technique for ecological data analysis. *Ecology*, *81*(11), 3178–3192. https://doi.org/10.1890/0012-9658(2000)081%5B3178:CARTAP%5D2.0.CO;2

Diba, H., Cohan, R. A., Salimian, M., Mirjani, R., Soleimani, M., & Khodabakhsh, F. (2021). Isolation and characterization of halophilic bacteria with the ability of heavy metal bioremediation and nanoparticle synthesis from Khara salt lake in Iran. *Archives of Microbiology*, *203*(7), 3893–3903. https://doi.org/10.1007/s00203-021-02380-w

Faé, G. S., Montes, F., Bazilevskaya, E., Añó, R. M., & Kemanian, A. R. (2019). Making soil particle size analysis by laser diffraction compatible with standard soil texture determination methods. *Soil Science Society of America Journal*, *83*(4), 1244–1252. https://doi.org/10.2136/sssaj2018.10.0385

Ferreira, S. L. C., Da Silva, J. B., Dos Santos, I. F., De Oliveira, O. M. C., Cerda, V., & Queiroz, A. F. S. (2022). Use of pollution indices and ecological risk in the assessment of contamination from chemical elements in soils and sediments – Practical aspects. *Trends in Environmental Analytical Chemistry*, *35*, e00169. https://doi.org/10.1016/j.teac.2022.e00169

Gao, T., Li, H., He, Y., Shen, Y., Li, G., Li, X., Chen, Y., Liu, Y., Li, C., Ji, J., Xu, J., & Chang, G. (2021). The variations of bacterial community structures in tailing soils suffering from heavy metal contaminations. *Water, Air, & Soil Pollution*, *232*(9). https://doi.org/10.1007/s11270-021-05338-2

Gatta, G., Gagliardi, A., Disciglio, G., Lonigro, A., Francavilla, M., Tarantino, E., & Giuliani, M. (2018). Irrigation with treated municipal wastewater on artichoke crop: Assessment of soil and yield heavy metal content and human risk. *Water*, *10*(3), 255. https://doi.org/10.3390/w10030255

Grados, L., Pérot, M., Barbezier, N., Delayre-Orthez, C., Bach, V., Fumery, M., Anton, P. M., & Gay-Quéheillard, J. (2022). How advanced are we on the consequences of oral exposure to food contaminants on the occurrence of chronic non communicable diseases? *Chemosphere*, *303*, 135260. https://doi.org/10.1016/j.chemosphere.2022.135260

Grattacaso, M., Canali, G., Vannini, A., Protano, G., Nannoni, F., De Lucia, V., Lella, L. A. D., Biagiotti, S., & Loppi, S. (2025). Health and ecological risk from potentially toxic elements in soils and extra virgin olive oils from Valdichiana Senese, Tuscany (Italy). *Journal of Plant Nutrition and Soil Science*, *188*(2), 241–250. https://doi.org/10.1002/jpln.202400312

Hakanson, L. (1980). An ecological risk index for aquatic pollution control. A sedimentological approach. *Water Research*, *14*(8), 975–1001. https://doi.org/10.1016/0043-1354(80)90143-8

Hama Aziz, K. H., Mustafa, F. S., Omer, K. M., Hama, S., Hamarawf, R. F., & Rahman, K. O. (2023). Heavy metal pollution in the aquatic environment: Efficient and low-cost removal approaches to eliminate their toxicity: a review. *RSC Advances*, *13*(26), 17595–17610. https://doi.org/10.1039/d3ra00723e

Hammer, Ø., Harper, D., & Ryan, P. (2001). PAST: Paleontological statistics software package for education and data analysis. *Palaeontologia Electronica, 4*, 1–9.

Khatun, J., Intekhab, A., & Dhak, D. (2022). Effect of uncontrolled fertilization and heavy metal toxicity associated with arsenic (As), lead (Pb) and cadmium (Cd), and possible remediation. *Toxicology*, *477*, 153274. https://doi.org/10.1016/j.tox.2022.153274

Li, D., Chen, J., Zhang, X., Shi, W., & Li, J. (2022). Structural and functional characteristics of soil microbial communities in response to different ecological risk levels of heavy metals. *Frontiers in Microbiology*, *13*. https://doi.org/10.3389/fmicb.2022.1072389

Li, J., Li, X., Tai, X.-S., Tuo, X.-Y., Zhou, F.-Y., Rong, Y.-J., & Zang, F. (2025). Machine learning-assisted source identification and probabilistic ecological-health risk assessment of heavy metal(loid)s in urban park soils. *Scientific Reports*, *15*(1), 17451. https://doi.org/10.1038/s41598-025-02307-1

Li, Y., Yu, Y., Ding, S., Dai, W., Shi, R., Cui, G., & Li, X. (2025). Application of machine learning in soil heavy metals pollution assessment in the southeastern Tibetan plateau. *Scientific Reports*, *15*(1), 13579. https://doi.org/10.1038/s41598-025-97006-2

Link, D. D., Walter, P. J., & Kingston, H. M. (1998). Development and validation of the new EPA microwave-assisted leach method 3051A. *Environmental Science & Technology*, *32*(22), 3628–3632. https://doi.org/10.1021/es980559n

Lu, L., Chen, C., Ke, T., Wang, M., Sima, M., & Huang, S. (2022). Long-term metal pollution shifts microbial functional profiles of nitrification and denitrification in agricultural soils. *Science of The Total Environment*, *830*, 154732. https://doi.org/10.1016/j.scitotenv.2022.154732

Ma, F., Wang, C., Zhang, Y., Chen, J., Xie, R., & Sun, Z. (2022). Development of microbial indicators in ecological systems. *International Journal of Environmental Research and Public Health*, *19*(21), 13888. https://doi.org/10.3390/ijerph192113888

Marvelli, E. (2025). *Foggia, 618 thousand tons of illegal waste*. https://www.gat.report/28593/foggia-618-thousand-tons-of-illegal-waste/

Mavakala, B. K., Sivalingam, P., Laffite, A., Mulaji, C. K., Giuliani, G., Mpiana, P. T., & Poté, J. (2022). Evaluation of heavy metal content and potential ecological risks in soil samples from

wild solid waste dumpsites in developing country under tropical conditions. *Environmental Challenges*, *7*, 100461. https://doi.org/10.1016/j.envc.2022.100461

Munir, N., Jahangeer, M., Bouyahya, A., El Omari, N., Ghchime, R., Balahbib, A., Aboulaghras, S., Mahmood, Z., Akram, M., Ali Shah, S. M., Mikolaychik, I. N., Derkho, M., Rebezov, M., Venkidasamy, B., Thiruvengadam, M., & Shariati, M. A. (2021). Heavy metal contamination of natural foods is a serious health issue: A review. *Sustainability*, *14*(1), 161. https://doi.org/10.3390/su14010161

Naylor, D., McClure, R., & Jansson, J. (2022). Trends in microbial community composition and function by soil depth. *Microorganisms*, *10*(3), 540. https://doi.org/10.3390/microorganisms10030540

Nyiramigisha, P., Komariah, & Sajidan. (2021). Harmful impacts of heavy metal contamination in the soil and crops grown around dumpsites. *Reviews in Agricultural Science*, *9*(0), 271–282. https://doi.org/10.7831/ras.9.0_271

Official Gazette of the Italian Republic, Ministerial decree 13th September 1999 (1999).

Official Gazette of the Italian Republic, Legislative decree n. 152, 3rd April 2006 (2006).

Olsen, S. R., Cole, C. V., Watanabe, F. S., & Dean, L. A. (1954). Estimation of available phosphorus in soils by extraction with sodium bicarbonate. *Circular n.939*, 1–19.

Orji, O. U., Awoke, J. N., Aja, P. M., Aloke, C., Obasi, O. D., Alum, E. U., Udu-Ibiam, O. E., & Oka, G. O. (2021). Halotolerant and metalotolerant bacteria strains with heavy metals biorestoration possibilities isolated from Uburu Salt Lake, Southeastern, Nigeria. *Heliyon*, *7*(7), e07512. https://doi.org/10.1016/j.heliyon.2021.e07512

Patel, N., Chauhan, D., Shahane, S., Rai, D., Ali Khan, Md. Z., Mishra, U., & Chaudhary, V. K. (2021). Contamination and health impact of heavy metals. In *Environmental Chemistry for a Sustainable World* (pp. 259–280). Springer International Publishing. https://doi.org/10.1007/978-3-030-52421-0_10

Proposal for a Directive of the European Parliament and of the Council on Soil Monitoring and Resilience (Soil Monitoring Law) - General Approach (T_11). https://eur-lex.europa.eu/legal-content/EN/TXT/?uri=consil:ST_11299_2024_INIT

Pu, C., Huang, Z., Jiang, X., Zhu, J., Lin, L., Zhang, X., Xia, H., Liang, D., Wang, J., & Lv, X. (2025). Intercropping grapevine with *Solanum nigrum* enhances their cadmium tolerance through changing rhizosphere soil microbial diversity. *Frontiers in Microbiology*, *16*. https://doi.org/10.3389/fmicb.2025.1537123

Qi, R., Xue, N., Wang, S., Zhou, X., Zhao, L., Song, W., & Yang, Y. (2022). Heavy metal(loid)s shape the soil bacterial community and functional genes of desert grassland in a gold mining area in

the semi-arid region. *Environmental Research*, *214*, 113749. https://doi.org/10.1016/j.envres.2022.113749

Rashid, A., Schutte, B. J., Ulery, A., Deyholos, M. K., Sanogo, S., Lehnhoff, E. A., & Beck, L. (2023). Heavy metal contamination in agricultural soil: Environmental pollutants affecting crop health. *Agronomy*, *13*(6), 1521. https://doi.org/10.3390/agronomy13061521

Rattner, B. A., Bean, T. G., Beasley, V. R., Berny, P., Eisenreich, K. M., Elliott, J. E., Eng, M. L., Fuchsman, P. C., King, M. D., Mateo, R., Meyer, C. B., O'Brien, J. M., & Salice, C. J. (2024). Wildlife ecological risk assessment in the 21st century: Promising technologies to assess toxicological effects. *Integrated Environmental Assessment and Management*, *20*(3), 725–748. https://doi.org/10.1002/ieam.4806

Salmi, A., & Boulila, F. (2021). Heavy metals multi-tolerant *Bradyrhizobium* isolated from mercury mining region in Algeria. *Journal of Environmental Management*, *289*, 112547. https://doi.org/10.1016/j.jenvman.2021.112547

Shea, D., & Thorsen, W. (2012). Ecological Risk Assessment. In *Progress in Molecular Biology and Translational Science* (Vol. 112, pp. 323–348). Elsevier. https://doi.org/10.1016/b978-0-12-415813-9.00012-x

Sodhi, K. K., Mishra, L. C., Singh, C. K., & Kumar, M. (2022). Perspective on the heavy metal pollution and recent remediation strategies. *Current Research in Microbial Sciences*, *3*, 100166. https://doi.org/10.1016/j.crmicr.2022.100166

Song, J., Shen, Q., Wang, L., Qiu, G., Shi, J., Xu, J., Brookes, P. C., & Liu, X. (2018). Effects of Cd, Cu, Zn and their combined action on microbial biomass and bacterial community structure. *Environmental Pollution*, *243*, 510–518. https://doi.org/10.1016/j.envpol.2018.09.011

Sun, C., Wu, P., Wang, G., & Kong, X. (2022). Heavy metal pollution decreases the stability of microbial co-occurrence networks in the rhizosphere of native plants. *Frontiers in Environmental Science*, *10*. https://doi.org/10.3389/fenvs.2022.979922

Tiabou, A. F., Tanyi, T. A. M., Yiika, L. P., & Ayuk, M. M. A. (2024). Spatial distribution, ecological and ecotoxicity evaluation of heavy metals in agricultural soils along Lala-Manjo Highway, Cameroon Volcanic Line. *Discover Soil*, *1*(1). https://doi.org/10.1007/s44378-024-00010-7

Visca, A., Di Gregorio, L., Costanzo, M., Clagnan, E., Nolfi, L., Bernini, R., Orgiazzi, A., Jones, A., Vitali, F., Mocali, S., & Bevivino, A. (2025). Microbial bioindicators for monitoring the impact of emerging contaminants on soil health in the European framework. *Sustainability*, *17*(3), 1093. https://doi.org/10.3390/su17031093

Walkley, A. (1947). A critical examination of a rapid method for determining organic carbon in soils—Effect of variations in digestion conditions and of inorganic soil constituents. *Soil Science*, *63*(4), 251.

Wang, F., Wang, F., Yang, H., Yu, J., & Ni, R. (2023). Ecological risk assessment based on soil adsorption capacity for heavy metals in Taihu basin, China. *Environmental Pollution*, *316*, 120608. https://doi.org/10.1016/j.envpol.2022.120608

Wang, Z., Deng, G., Hu, C., Hou, X., Zhang, X., Fan, Z., Zhao, Y., & Peng, M. (2025). Microbial diversity and community assembly in heavy metal-contaminated soils: Insights from selenium-impacted mining areas. *Frontiers in Microbiology*, *16*. https://doi.org/10.3389/fmicb.2025.1561678

Wijaya, J., Byeon, H., Jung, W., Park, J., & Oh, S. (2023). Machine learning modeling using microbiome data reveal microbial indicator for oil-contaminated groundwater. *Journal of Water Process Engineering*, *53*, 103610. https://doi.org/10.1016/j.jwpe.2023.103610

Wilhelm, R. C., Amsili, J. P., Kurtz, K. S. M., Van Es, H. M., & Buckley, D. H. (2023). Ecological insights into soil health according to the genomic traits and environment-wide associations of bacteria in agricultural soils. *ISME Communications*, *3*(1). https://doi.org/10.1038/s43705-023-00236-6

Xu, N., Kang, J., Ye, Y., Zhang, Q., Ke, M., Wang, Y., Zhang, Z., Lu, T., Peijnenburg, W. J. G. M., Josep Penuelas, Bao, G., & Qian, H. (2022). Machine learning predicts ecological risks of nanoparticles to soil microbial communities. *Environmental Pollution*, *307*, 119528. https://doi.org/10.1016/j.envpol.2022.119528

Xu, X., Xu, Z., Liang, L., Han, J., Wu, G., Lu, Q., Liu, L., Li, P., Han, Q., Wang, L., Zhang, S., Hu, Y., Jiang, Y., Yang, J., Qiu, G., & Wu, P. (2024). Risk hotspots and influencing factors identification of heavy metal(loid)s in agricultural soils using spatial bivariate analysis and random forest. *Science of The Total Environment*, *954*, 176359. https://doi.org/10.1016/j.scitotenv.2024.176359

Yang, C., Zeng, Z., Wang, Y., He, G., Hu, Y., Gao, D., Dai, Y., Li, Q., & Zhang, H. (2023). Ecological risk assessment and identification of the distinct microbial groups in heavy metal-polluted river sediments. *Environmental Geochemistry and Health*, *45*(5), 1311–1329. https://doi.org/10.1007/s10653-022-01343-4

Yang, W., Zhu, Y., Jiang, Y., Zhang, J., Wang, W., Jin, Y., Liu, X., & Qu, J. (2024). Dissolve organic matter of mature chicken compost contributes to the protection of microorganisms from the stress of heavy metals. *Journal of Environmental Chemical Engineering*, *12*(5), 113590. https://doi.org/10.1016/j.jece.2024.113590

Zeng, K., Huang, X., Dai, C., He, C., Chen, H., Guo, J., & Xin, G. (2024). Bacterial community regulation of soil organic matter molecular structure in heavy metal-rich mangrove sediments. *Journal of Hazardous Materials*, *465*, 133086. https://doi.org/10.1016/j.jhazmat.2023.133086

Zerizghi, T., Guo, Q., Tian, L., Wei, R., & Zhao, C. (2022). An integrated approach to quantify ecological and human health risks of soil heavy metal contamination around coal mining area. *Science of The Total Environment*, *814*, 152653. https://doi.org/10.1016/j.scitotenv.2021.152653

Zhang, H., Liu, W., Xiong, Y., Li, G., Cui, J., Zhao, C., & Zhang, L. (2024). Effects of dissolved organic matter on distribution characteristics of heavy metals and their interactions with microorganisms in soil under long-term exogenous effects. *Science of The Total Environment*, *947*, 174565. https://doi.org/10.1016/j.scitotenv.2024.174565

Zhang, J., Liu, Z., Tian, B., Li, J., Luo, J., Wang, X., Ai, S., & Wang, X. (2023). Assessment of soil heavy metal pollution in provinces of China based on different soil types: From normalization to soil quality criteria and ecological risk assessment. *Journal of Hazardous Materials*, *441*, 129891. https://doi.org/10.1016/j.jhazmat.2022.129891

Zhao, Z., Wang, Y., Kong, L., Zhao, L., Li, Y., He, T., Liu, S., Han, X., Gu, S., Wu, S., Zhang, J., Zhang, J., & Li, B. (2025). Response of soil microbial community composition and function to prolonged heavy metal exposure. *Environmental Monitoring and Assessment*, *197*(8). https://doi.org/10.1007/s10661-025-14228-7

Zheng, M., Qi, X., Liu, Z., Wang, Y., Ren, Y., Li, Y., Zhang, Y., Chai, B., & Jia, T. (2025). Microbial taxonomic diversity and functional genes mirror soil ecosystem multifunctionality in nonferrous metal mining areas. *Journal of Hazardous Materials*, *492*, 138149. https://doi.org/10.1016/j.jhazmat.2025.138149

5. A preliminary investigation on heavy metals tolerance on *Pseudomonas* isolates: is there an effect of isolation site?[3]

Alessandro De Santis, Antonio Bevilacqua*, Angela Racioppo, Barbara Speranza, Maria Rosaria Corbo, Clelia Altieri and Milena Sinigaglia

Department of Agriculture, Food, Natural Resources and Engineering, University of Foggia, Foggia, ITALY

Abstract

In this preliminary study, one hundred presumptive *Pseudomonas* isolates recovered from 15 impacted sites from anthropogenic activity in the Foggia district (Italy) were screened for key adaptive and functional traits important for environmental applications. The isolates were phenotypically characterized for their ability to grow under pH (5.0–8.0) and temperature (15–37 °C) combined conditions, to produce proteolytic enzymes, pigments, exopolysaccharides, and to tolerate SDS. Moreover, the resistance to six environmentally relevant heavy metals (Cd, Co, Cu, Ni, Zn, As) was qualitatively assessed. The results highlighted a wide inter-strain variability, with distinct clusters of isolates showing unique combinations of stress tolerance, enzymatic potential, and resistance profiles. PERMANOVA analysis revealed significant effects of both the isolation site and metal type, as well as their interaction, on the observed resistance patterns. A subset of isolates showed co-tolerance to elevated temperature and heavy metals, suggesting possible cross-resistance mechanisms worthy of further molecular investigation. The findings offer an initial yet insightful overview of the adaptive diversity of soil-derived *Pseudomonas*, laying the groundwork for the rational selection of strains for bioaugmentation in contaminated soils.

---

[3] This chapter was published on Agriculture (De Santis, A., Bevilacqua, A., Racioppo, A., Speranza, B., Corbo, M. R., Altieri, C., & Sinigaglia, M. (2025). A Preliminary Investigation into Heavy Metal Tolerance in *Pseudomonas* Isolates: Does the Isolation Site Have an Effect? *Agriculture*, *15*(15), 1692. https://doi.org/10.3390/agriculture15151692)

5.1 Introduction

Soil ecosystems represent one of the most diverse and functionally essential components of the terrestrial biosphere, sustaining a vast array of microbial life that mediates critical biogeochemical processes (Srivastava et al., 2023). Among soil microorganisms, bacteria of the *Pseudomonas* genus have garnered significant attention due to their exceptional metabolic versatility, ecological plasticity, and potential applications in agro-environmental management and bioremediation (Chauhan et al., 2023). However, increasing anthropogenic pressures, such as contamination by petroleum hydrocarbons, heavy metals (HMs), and phytochemical residues are altering soil functions and imposing substantial stress on resident microbial communities (Yang et al., 2022). These disturbances not only compromise nutrient cycling and soil fertility but also affect microbial diversity and activity at both the structural and functional levels. In this context, understanding the ecological roles and adaptive mechanisms of *Pseudomonas* spp. in contaminated soils is critical for developing effective microbial-based remediation strategies aligned with sustainable environmental management goals (Yin et al., 2024).

Species of the *Pseudomonas* genus are characterized by their broad catabolic potential, rapid growth rates, high motility, and the ability to synthesize a wide array of secondary metabolites, including biosurfactants, siderophores, and degradative enzymes. These features confer a selective advantage in nutrient-limited or chemically stressed environments and support their adaptation to contaminated soils (Khoshru et al., 2025). In particular, strains belonging to *P. putida* and *P. aeruginosa* species have demonstrated the ability to degrade various environmental pollutants, including polycyclic aromatic hydrocarbons and chlorinated solvents, via specific enzymatic pathways (Medić & Karadžić, 2022; Vélez et al., 2021; Verasoundarapandian et al., 2021).

Although metal tolerance and bioremediation are mechanistically distinct processes, they are often interrelated. Many *Pseudomonas* strains that exhibit high levels of

resistance to HMs, through mechanisms such as efflux pumps (e.g., CzcCBA, CopA), sequestration by metallothioneins or polyphosphates, and binding via exopolysaccharides, also possess enhanced capabilities for biosorption and enzymatic detoxification (Igiri et al., 2018; Alotaibi et al., 2021; Mathivanan et al., 2021; Joshi et al., 2023). These traits not only allow survival in toxic conditions but can also promote active biotransformation of contaminants.

Moreover, the ability of *Pseudomonas* spp. to form biofilms and adapt to fluctuating pH, temperature, and oxygen levels enhances their resilience and persistence in contaminated soils, both in situ and under engineered remediation settings (Li et al., 2023). The growing research continues to elucidate the regulatory networks and stress response systems that underpin their environmental adaptability, reinforcing the relevance of *Pseudomonas* as a model genus in environmental microbiology and applied biotechnology.

The implementation of effective microbial remediation strategies requires the careful selection and characterization of bacterial strains exhibiting ecological fitness, high resistance at different stress condition and high degradation potential under site-specific environmental conditions (Nowak et al., 2021). Within the *Pseudomonas* genus, considerable inter-strain variability exists, highlighting the need for robust screening protocols to identify the most promising candidates (Doolotkeldieva et al., 2024). Traditional approaches include phenotypic assays based on growth kinetics, pollutant tolerance, and enzymatic activity, performed under simulated soil conditions or in the presence of contaminant analogs. The success of *Pseudomonas*-based bioremediation depends not only on intrinsic catabolic capacity, but also on the organism's ability to survive, persist, and interact with native microbiota and host plants in the targeted environment (Sun et al., 2024).

Abiotic factors such as pH, temperature, moisture content, and contaminant load significantly influence microbial survival, activity, and community structure, thereby affecting the efficiency of bioremediation processes. Although *Pseudomonas* spp., are

generally resilient, they exhibit variable physiological responses to these stressors. For example, suboptimal pH conditions may inhibit membrane transport systems and enzymatic activity, whereas nutrient imbalances, particularly carbon-to-nitrogen ratios, can shift metabolic pathways away from xenobiotic degradation (Song et al., 2021; Sun et al., 2024).

Pollutant bioavailability is often limited by adsorption to soil particles or entrapment in micropores, reducing microbial access and metabolic uptake. This challenge is often addressed using biosurfactant-producing strains of *Pseudomonas*, which enhance the solubility and dispersion of hydrophobic compounds. Similarly, the presence of HMs can exert selective pressure on microbial communities, favouring the proliferation of metal-resistant genotypes but simultaneously suppressing overall diversity and function. To mitigate such constraints, engineered approaches such as bioaugmentation and bioventing are frequently combined with microbial inoculation to optimize environmental conditions for target strain performance (Karishma et al., 2024).

Recent advances in microbial biotechnology and systems biology have led to the development of next generation remediation strategies that move beyond traditional single-strain applications. Increasingly, research is focusing on the design and deployment of naturally co-evolved microbial consortia, in which *Pseudomonas* spp. often serve as keystone degraders due to their complementary metabolic roles and ecological robustness (Qiao et al., 2024). These consortia can be tailored to site-specific contaminant profiles and environmental conditions, enhancing degradation efficiency and functional resilience (Kuppan et al., 2024). Furthermore, co-inoculation with arbuscular mycorrhizal fungi and plant growth-promoting rhizobacteria (PGPR) can synergistically improves plant health and pollutant uptake in phytoremediation systems (Sagar et al., 2021), with *Pseudomonas* acting as both a facilitator of degradation and a root colonizer (Li et al., 2023).

Despite the growing interest in microbial resistance to HMs, relatively few studies have investigated *Pseudomonas* isolates from unmanaged contaminated soils under real-world, multi-stressor conditions. In particular, limited attention has been given to how the history and typology of anthropogenic contamination may influence adaptive traits such as metal tolerance, acid–base resilience, and thermotolerance.

This study focuses on contaminated soils from the Foggia district (Apulia region, Southern Italy), a territory with many sites subjected to intense and long-standing anthropogenic pressures. The waste materials observed in these areas were largely composed of municipal solid waste (MSW), including plastics, packaging, household debris, etc., often mixed with construction rubble, obsolete electronics, and small-scale industrial discards. According to recent estimates by Legambiente (Marvelli, 2025), over 618,000 tons of such illegal waste have been deposited throughout the province of Foggia, particularly in marginal or unregulated zones. Complementary to this, the ARPA Puglia report 2022 (Agenzia Regionale per la Prevenzione e la Protezione dell'Ambiente - Siti potenzialmente contaminati, 2022) documents over 120 officially registered contaminated or potentially contaminated sites in the province of Foggia. These include former landfills, illegal dumping areas, and disused industrial zones. Environmental monitoring of these sites has revealed frequent exceedances of contamination thresholds for several key pollutants in surface soils, especially HMs (e.g., Pb, Zn, Cu, As, Sn), organic compounds, hydrocarbons (C>12), and, in some cases, PCBs and PAHs.

This complex contamination scenario, shaped by the coexistence of organic and inorganic pollutants, provides a realistic context for investigating the adaptive responses of indigenous soil bacteria. In particular, the persistence of HMs associated with decomposing waste and electronic residues is likely to exert selective pressure on microbial communities. The absence of remediation measures further reinforces the chronic nature of this environmental stressor and its potential impact on soil microbial ecology and functionality.

Therefore, this study aimed to explore the phenotypic and functional variability of *Pseudomonas* spp. isolates collected from contaminated areas in the Foggia district, focusing on their ability to tolerate HMs, pH fluctuation, and thermal stress. In addition, we investigated whether the site of origin, reflecting different types and intensities of anthropogenic disturbance, influenced the adaptive profiles of the isolates, with the broader goal of identifying potential ecological associations between environmental pressure and microbial resistance traits.

5.2 Materials and Methods

5.2.1 Isolation and preservation of Pseudomonas spp.

A total of 100 presumptive *Pseudomonas* spp. isolates were obtained in Spring 2023 from 15 contaminated soil samples collected from the topsoil layer (0–15 cm depth) across the Foggia district (Apulia region, Italy). GPS coordinates of each sample are reported in **Table 5.1**. The areas were chosen based on visible evidence of long-standing anthropogenic impact, particularly urban solid waste accumulation, and included roadside verges, abandoned peri-urban lots, and uncultivated rural zones.

Soil samples were collected under sterile conditions using clean spatulas and stored in sterile containers. Samples were transported to the laboratory under refrigerated conditions and processed within 24 hours to limit microbial community shifts during transport. Presumptive identification of the isolates as *Pseudomonas* spp. was based on selective cultivation on *Pseudomonas* Agar Base (PAB, Oxoid, Milan) supplemented with CFC (Cetrimide-Fusidin-Cephaloridine) (Oxoid), which inhibits

Table 5.1 Geographic coordinates and classification of the 15 soil sampling sites located in the Foggia district. All sites correspond to areas subject to long-term anthropogenic pressure. Coordinates were recorded using the Google Maps application during fieldwork

Site	Longitude (°E)	Latitude (°N)
A	15.585849	41.422099

B	15.597040	41.4334645
C	15.608232	41.44483
D	15.604090	41.466206
E	15.584307	41.477667
F	15.564805	41.4775115
G	15.545304	41.477356
H	15.528977	41.482316
I	15.510517	41.4781885
L	15.492058	41.474061
M	15.496651	41.452132
N	15.505415	41.433294
O	15.508348	41.413625
P	15.535685	41.421741
Q	15.560767	41.42192

the growth of Gram-positive bacteria and many other Gram-negative genera (Mead, 1985). Colonies exhibiting typical morphology and pigmentation were further subcultured and tested for oxidase activity. Although molecular confirmation (e.g., 16S rRNA gene sequencing) was not performed in this study, it is planned for future work. The purified cultures were maintained on Nutrient Agar (Oxoid) slants at 4 °C for short-term storage and cryopreserved in Nutrient broth + 33% glycerol (J.T. Baker, Milan) at –20 °C for long-term use.

All isolates were subsequently subjected to a series of biochemical and functional assays, including tolerance tests to HMs (Cu, Zn, Pb), pH (acidic and alkaline), and temperature stress, in order to assess their ecological fitness under contaminated soil conditions. These assays aimed to identify phenotypic traits associated with environmental resilience and potential applicability in microbial-based bioremediation strategies.

5.2.2 Phenotyping

The ability of isolates to produce fluorescent pigments was assessed by streaking on Nutrient Agar (NA; Oxoid). Plates were incubated at 25 °C for 48–72 hours and examined under visible light and ultraviolet (UV) illumination at 365 nm using a Wood's lamp, as described by Dyer & Foy (2022). Pigment production was recorded qualitatively as presence or absence of fluorescence. To further evaluate the synthesis of blue pigments (e.g., pyocyanin), isolates were also streaked on Mascarpone Agar (prepared as per Chierici et al. (2016) and incubated at 25 °C for 24–48 hours. Blue pigment expression was recorded qualitatively, based on the presence or absence of visible pigmentation in the agar.

EPS production was evaluated by two Congo Red Agar (CRA) protocols. The first was the original method by Freeman et al. (1989), slightly modified by using NA supplemented with 5% (w/V) sucrose as carbon source. The second followed the protocol by Maalej et al. (2015), which uses 1% (w/V) glucose in NA. In both cases Congo Red was added at a final concentration of 0.8 g/L after autoclaving.

Plates were incubated at 25 °C for 72 hours, and EPS production was assessed qualitatively, based on colony morphology, dye absorption, and mucoid consistency. Colonies were classified as positive when they appeared black, shiny, and viscous, and as negative when they are red, dry, and flat.

Protease activity was assessed using Skim Milk Agar (SMA) prepared according to the method of Pailin et al. (2001), with modifications. A 10% (w/v) skim milk powder solution was reconstituted in distilled water and autoclaved at 121 °C for 5 minutes. After cooling, it was added to sterile Nutrient Agar (Oxoid) to obtain final skim milk concentrations of 5% and 10% (v/v).

Each *Pseudomonas* isolate was spot-inoculated with 10 µL of a 24-hour culture onto both SMA formulations and incubated at 25 °C for 48 hours. Proteolytic activity was assessed qualitatively by the presence or absence of clear halos surrounding colonies,

indicating casein hydrolysis. Negative control plates (uninoculated) were used to exclude spontaneous clearing.

Resistance to sodium dodecyl sulfate (SDS) was evaluated following the protocol described by Furmanczyk et al. (2017). The test medium was M9 minimal agar. After autoclaving, the medium was cooled to 50 °C and supplemented with cold filtrated SDS at a final concentration of 2% (w/v).

Each *Pseudomonas* isolate was spot-inoculated (20 µL) and incubated at 25 °C for 48 hours. Growth was assessed qualitatively, based on the presence or absence of visible halo.

5.2.3 Antibacterial activity

The antagonistic potential of *Pseudomonas* isolates was evaluated using the method of Fernández-Fernández et al. (2022) modified as follows. The test was conducted against *Bacillus subtilis* DSM 10, obtained from the bacterial collection of the University of Foggia.

A fresh overnight culture of *B. subtilis* was streaked onto NA plate (9 cm diameter) and incubated at 37°C for a few hours (no more than 4 h). After incubation, each *Pseudomonas* isolate was spot-inoculated (20 µL) in the middle of plates and incubated at 25 °C for 48 hours under aerobic conditions. Antibacterial activity was evaluated qualitatively, based on the presence or absence of visible inhibition halos surrounding the *Pseudomonas* spot. Isolates were classified as positive (inhibition zone present) or negative (no inhibition). Each assay was performed in duplicate, and control plates without *Pseudomonas* inoculation were included (negative control).

5.2.4 Growth as a function of pH, temperature and HMs presence

To assess the physiological adaptability of the *Pseudomonas* isolates to environmental stress, each isolate was tested for its ability to grow on solid media under varying pH and temperature conditions, applying an internal protocol.

Bacterial suspensions were prepared from overnight cultures grown in Nutrient broth, and 10 µL aliquots were streaked onto Nutrient Agar plates adjusted to pH 5.0, 6.0, and 8.0 using sterile HCl or NaOH, as appropriate. The pH of each batch of medium was confirmed using a calibrated pH meter (Hanna Instruments, Woonsocket, USA). Following inoculation, plates were incubated under aerobic conditions at three distinct temperatures: 15 °C, 25 °C, and 37 °C. Growth was recorded after 48 and 72 hours and 1 week of incubation by visual inspection, with colony development indicating tolerance/growth (coded by "1") and absence of growth (coded by "0") to the specific environmental condition.

The resistance of *Pseudomonas* isolates to selected HMs was assessed onto solid Nutrient Agar supplemented with individual metal salts (Yasmin et al., 2022). The following compounds were used as metal sources: Cadmium chloride 2.5-hydrate ($CdCl_2 \cdot 2.5H_2O$), Copper(II) chloride dihydrate ($CuCl_2 \cdot 2H_2O$), Nickel(II) chloride hexahydrate ($NiCl_2 \cdot 6H_2O$), Zinc sulfate heptahydrate ($ZnSO_4 \cdot 7H_2O$), Sodium arsenite ($NaAsO_2$), Cobalt(II) chloride hexahydrate ($CoCl_2 \cdot 6H_2O$). HMs are from Sigma Aldrich (Missouri, USA).

Sterile stock solutions of each metal salt were added to the autoclaved molten Nutrient Agar to obtain final concentrations of 200 mg/L. Subsequently, plate was streak inoculated with overnight culture and incubated at 25 °C for 48 hours under aerobic conditions. Bacterial growth was visually assessed and categorized as no growth (0) or growth (1). The HMs concentration was chosen as a standardized high threshold to qualitatively assess the tolerance potential under strong selective pressure. While environmental concentrations may vary significantly among metals, this level was adopted to facilitate statistical comparative screening across isolates, and it is consistent with previous studies on phenotypic resistance profiling of soil bacteria (Renu et al., 2021; Firincă et al., 2023).

5.2.5 Statistics

Data were preliminary converted in a binary code (1, growth/enzymatic activity present; 0, no growth/no activity) and used to build frequency histograms for each assay (that is number of isolates showing growth in the tested condition), and preliminary treated through a Chi-Square test to point out possible differences.

The growth in presence of HMs was further analyzed and categorized as a function of isolation site and heavy metal (that is number of positive strains for each site) and analyzed through PERMANOVA, using the site and the HMs as categorical predictors (independent variables) and the number of positive strains for each condition as dependent variable. A graphical representation of this categorization was done through a heatmap, showing the number of strains able to growth in the presence of a specific heavy metal for each site.

Finally, correlations among the different assayed parameters (growth at difference pH and temperature, growth in presence of heavy metal) were assessed through Spearman coefficients. Statistical analyses were done through PAST software, ver. 5.2.2. (https://www.nhm.uio.no/english/research/resources/past/).

5.3 Results and Discussion

A total of 100 presumptive *Pseudomonas* isolates obtained from contaminated soils were evaluated for multiple functional traits related to bioremediation potential (**Figure 5.1**). The strains were subjected to various metabolic and environmental stress conditions to assess their ability to survive and function under harsh environments, typically encountered during soil bioremediation. The characterization includes the evaluation of some metabolic traits, connected to protein metabolism, resistance to SDS, pigment production and antimicrobial activity towards bacilli. In the second phase growth as a function of pH, temperature or heavy metal presence was assessed as a step prodromal to a future isolation of biological tools for bioremediation.

5.3.1 Phenotypical and technological characterization of presumptive Pseudomonas spp.

The isolates were evaluated for their ability to utilize different carbon sources, including complex and unconventional substrates, such as dairy proteins. Proteolytic activity was assessed on Skim Milk Agar, an uncommon protein substrate for soil bacteria, but an interesting matrix for lab experiments to assess the proteolytic potential of bacteria. Casein degradation was observed in 65% of isolates at a 5% milk concentration, and in 58% at a 10% concentration, suggesting a substantial proportion of strains possess enzymatic machinery capable of protein hydrolysis under nutrient-limited conditions. *Pseudomonas* generally has a complex proteolytic system, as also suggested by several authors for foodborne bacteria (Longhi et al., 2022; Narvhus et al., 2021); however, to best of authors' knowledge this aspect has not been fully explored in soil bacteria. Nevertheless, the presence of this enzymatic activity is indirect evidence of the catabolic potential of the studied isolates.

An important trait of pseudomonads is pigment production; however, it was detected in only 4% of isolates. This characteristic is typically associated with specific niches of *P. aeruginosa* and *P. fluorescens* (Carrascosa et al., 2021), is often produced in response to stress conditions (Honselmann Genannt Humme et al., 2024), or is a tool to protect bacteria from oxidative stress and UV radiation (Samrot et al., 2017). In addition, pigment production is probably linked to iron acquisition, virulence, competition with other microorganisms, and quorum sensing (Abdelaziz et al., 2023; El-Fouly et al., 2015). However, the low frequency of this trait, at least for the isolates studied in the present research, suggests the need of confirmatory experiments, also including the evaluation of the effects of environmental variable on pigment production.

Figure 5.1 Phenotypic characterization of soil-derived *Pseudomonas* isolates. Barplots indicate the percentage of strains positive for selected traits including extracellular protease activity (5% and 10% skim milk), EPS production (Freeman and Maalej methods), pigment production, SDS degradation, and antagonism against *B. subtilis* (relative frequency).

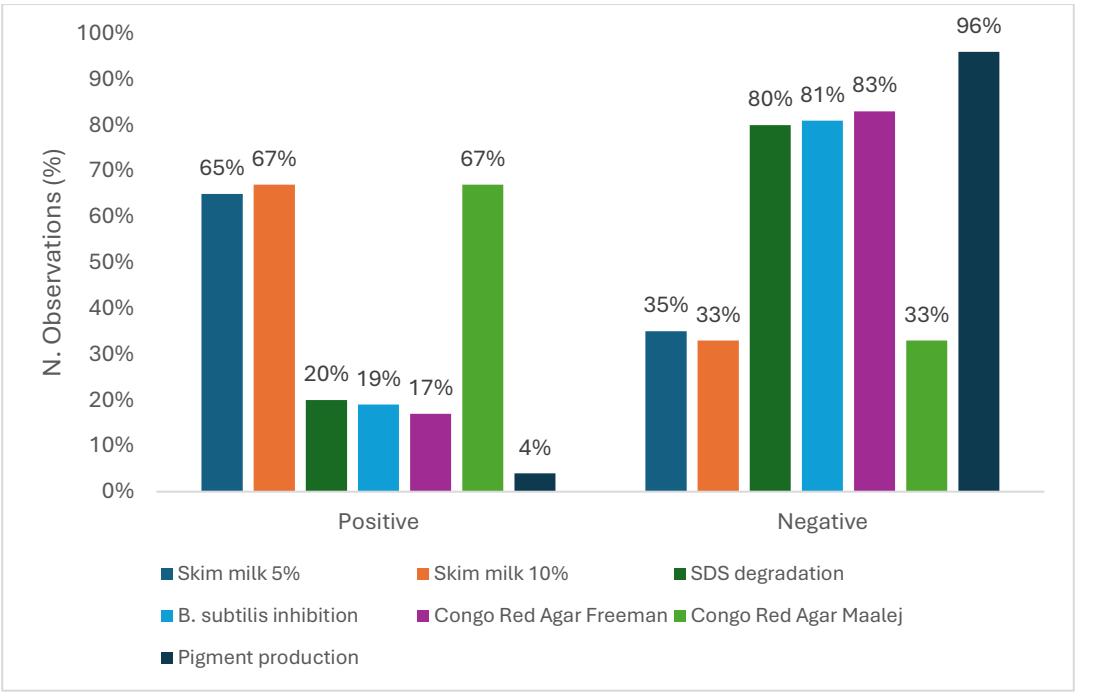

An important experiment, as least for the present research, was on the degradation of SDS (sodium dodecyl sulfate), which is a common soil pollutant due to its widespread use in detergents and industrial applications; this characteristic was detected in 20% of the isolates, highlighting a subset of strains with potential relevance for bioremediation of surfactant-contaminated environments because of their ability to use so harmful carbon source in harsh conditions (Panasia et al., 2019).

In a complex matrix, microorganisms, including bioremediation tools, should interact with a huge microbiota, thus expressing negative or positive interactions. Aerobic spore-forming bacteria represent an important part of bacterial microbiota of soil. Therefore, the antagonistic activity was tested by evaluating the inhibition of *B. subtilis* growth, as representative of soil spore-forming bacteria. This bioactivity, indicative of

antimicrobial compounds production or competitive traits important for survival in low-nutrients conditions (Bernabé-Pérez et al., 2024), was observed in 19% of the isolates. Such antagonistic potential is commonly reported in *Pseudomonas* spp., as confirmed by Lyng et al. (2024), reflecting the frequent competitive interactions between *Bacillus* and *Pseudomonas* genera (Lyng & Kovács, 2023).

Exopolysaccharide (EPS) production was assessed using two established protocols. The method described by Freeman et al. (1989) yielded positive results in 17% of the strains, while the modified protocol by Maalej et al. (2015) detected EPS production in 33% of the isolates. These findings suggest a moderate prevalence of EPS-producing phenotypes, which may enhance surface adhesion, biofilm formation, and resilience under fluctuating environmental conditions (Zanna et al., 2022). In addition, EPS are involved in the interaction of rhizosphere bacteria with plants, along with nutrient delivery and availability (Costa et al., 2018). Therefore, the selection of EPS-producing microorganisms is an added value for a correct role of bacteria in soil, and for a potential use of wild microorganisms for a biological application.

5.3.2 Growth response under combined pH and temperature conditions

After analyzing the metabolic potential of soil isolates, the second step was on growth profile as a function of pH, temperature, and heavy metal presence. Growth over a wide range of conditions is a main requisite for technological robustness of the assayed microorganisms.

To assess the physiological resistance of the *Pseudomonas* isolates, a combinatorial analysis of pH and temperature effects on bacterial growth was conducted. Cultures were inoculated on Petri plates adjusted to three pH levels (5.0, 6.0, and 8.0) and incubated at three distinct temperatures (15 °C, 25 °C, and 37 °C). Observations were recorded at three points: 48 h, 72 h, and one week. The experiments, as for the assays in presence of HMs, were performed in a complex laboratory medium, that is Nutrient Agar. Although for ecophysiological assays minimal media should be used to avoid a

masking effect due to medium, preliminary experiments performed on the isolates tested in this study revealed that a minimal medium could exert an additive or synergistic effect with other stresses, thus masking effective resistance/sensitivity.

For each condition, the number of isolates exhibiting visible growth (presence of colonies) was quantified and expressed as the number of positive observations. The use of a solid medium, while exerting the benefit of a matrix similar to soil at least for its macrostructure, does not consent the "building" of a kinetic; therefore, results were reported at different time intervals, as it is well known that some factors (mainly pH and temperature) could exert a transient stress on bacteria.

After 48 h of incubation (**Figure 5.2**), the highest number of growth positive isolates was recorded at 25 °C, regardless of the pH condition. Specifically, at 25 °C, 100% of the isolates grew at pH 8.0, while slightly fewer grew at pH 6.0 (98%) and pH 5.0 (86%)., while slightly lower but still high values (~85–90%) were observed at 15 °C ($p<0.05$). In contrast, growth at 37 °C, was significantly reduced across all pH levels ($p<0.05$), particularly under acidic conditions (pH 5.0), where only 54% of isolates formed visible colonies. These results suggest that *Pseudomonas* isolates exhibit optimal metabolic activity in mesophilic and near-neutral environments, a characteristic widely observed in the genus. In fact, previous studies have demonstrated that moderate temperatures (20–30 °C) and pH values between 6.5 and 8.0 support robust aerobic growth and membrane functionality in several *Pseudomonas* species (Tribelli & López, 2022). The poor performance observed at 37 °C, especially under acidic stress, aligns with known sensitivity to thermophilic conditions of *Pseudomonas* strains, which generally prefer lower temperature and neutral pH.

Figure 5.2 Bar charts represent the number of isolates showing growth (presence of visible colonies) after 48h on Nutrient Agar adjusted to pH 5.0, 6.0, and 8.0, and incubated at 15 °C (blue), 25 °C (orange), or 37 °C (grey) (absolute frequency). For each pH, the symbol "*" indicates a significant difference (Chi-squared test, P<0.05).

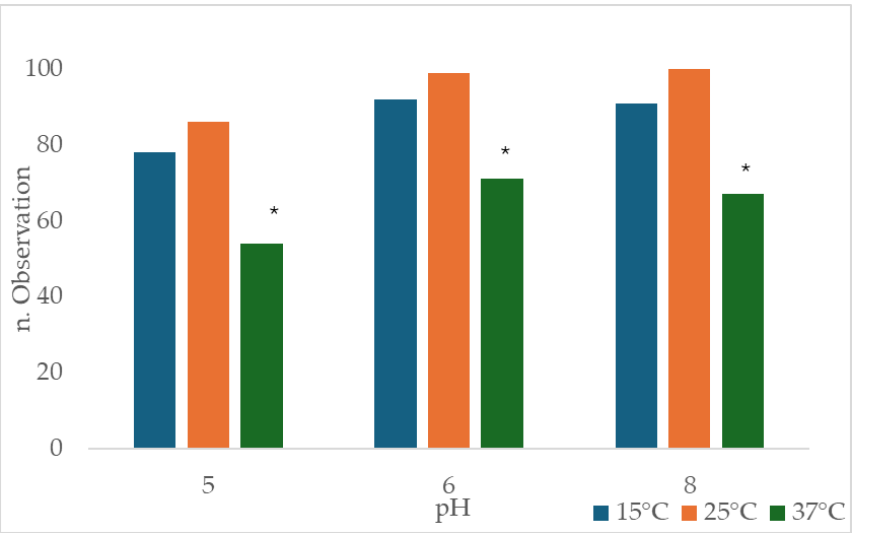

Figure 5.3 Bar charts represent the number of isolates showing growth (presence of visible colonies) after 72 hours on Nutrient Agar adjusted to pH 5.0, 6.0, and 8.0, and incubated at 15 °C (blue), 25 °C (orange), or 37 °C (green) (absolute frequency). For each pH, the symbol "*" indicates a significant difference (Chi-squared test, P<0.05).

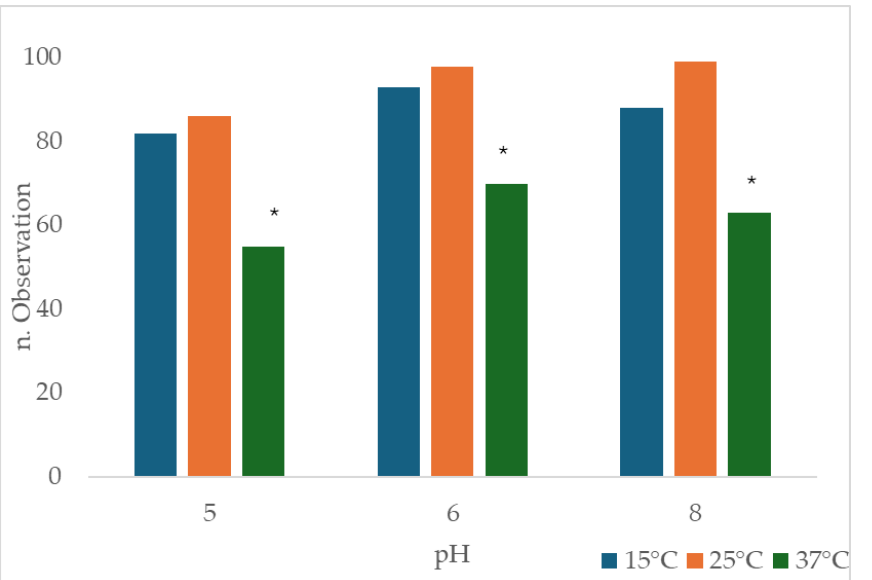

At 72 h (**Figure 5.3**), a general increase in growth positive observations were noted across most conditions, reflecting the ability of a larger fraction of the population to overcome initial environmental stress. The optimal performance remained at 25 °C and pH 6.0–8.0, where nearly all isolates exhibited visible growth. Notably, at 15 °C, the number of growth events increased significantly compared to 48 h ($p<0.05$).

Growth at 37 °C, while still suboptimal, improved modestly at pH 6.0 and 8.0 ($p<0.05$), indicating the potential presence of moderately thermotolerant phenotypes. Similar delayed-growth patterns at low temperature have been reported by Chahuan et al. (2023), who highlighted cold-induced metabolic adjustments as keys elements of *Pseudomonas* adaptability under suboptimal conditions.

After 1 week of incubation (**Figure 5.4**), growth was almost general at 15 °C and 25 °C across all pH conditions, with 100% of isolates growing at pH 6.0 and 8.0. The delayed growth observed at 15 °C confirms the presence of isolates capable of adapting to low temperatures over extended periods.

Figure 5.4 Bar charts represent the number of isolates showing growth (presence of visible colonies) after 1 week on Nutrient Agar adjusted to pH 5.0, 6.0, and 8.0, and incubated at 15 °C (blue), 25 °C (orange), or 37 °C (green) (absolute frequency).

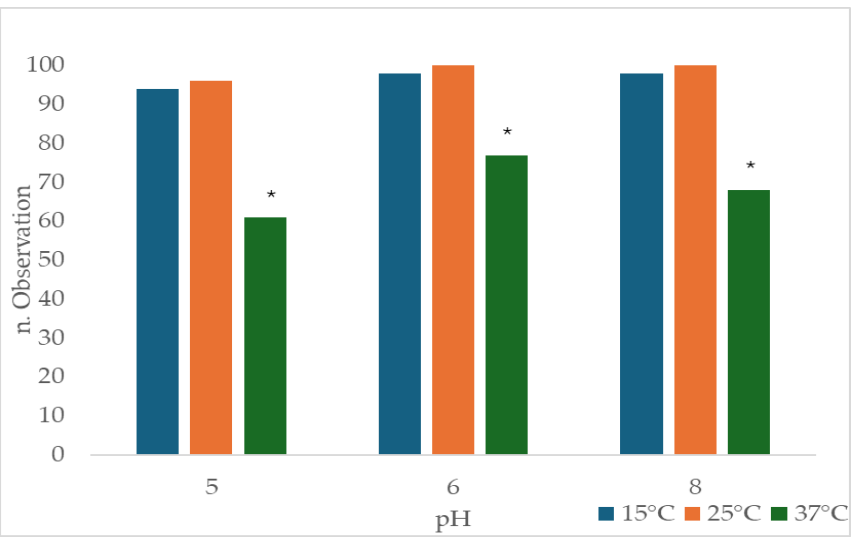

At 37 °C, although overall growth remained limited and significantly lower ($p<0.05$), a notable increase in positive observations were recorded compared to earlier time points, especially at pH 6.0 (77%) and pH 8.0 (67%) ($p<0.05$). The results suggest that *Pseudomonas* isolates exhibit significant ecological plasticity in response to combined abiotic stresses. Growth was robust in near neutral to slightly alkaline pH and at moderate temperatures, with delayed but substantial adaptation to colder environments and moderate resilience to thermal stress when pH was not acidic. The observed patterns are strongly supported by the current literature on *Pseudomonas* physiology and stress tolerance, which highlights the genus's capacity to modulate key metabolic and structural features across variable environmental conditions (Craig et al., 2021; Mozaheb et al., 2023).

5.3.3 Growth in presence of HMs

Technological robustness was also assessed against six environmentally relevant HMs: sodium arsenite, cobalt (II) chloride hexahydrate, zinc sulphate heptahydrate, nickel (II) chloride hexahydrate, copper (II) chloride dihydrate, and cadmium chloride dihydrate. The concentration of 200 mg/L, although not environmentally representative, was deliberately chosen as a high-threshold screening level to identify strongly resistant isolates. Similar concentrations have been used in previous qualitative tolerance studies (Firincă et al., 2023; Renu et al., 2021). The results were converted into a binary code, and used as input for a PERMANOVA analysis, with a kind of heavy metal and isolation site as categorical predictors. However, sodium arsenite was no further used, as more than 90% of strains were positive to the assay, and these results could mask or cause statistical artifact to the multivariate approaches. To perform this analysis, the dataset was preliminary categorized reporting for each site the number of positive strains for each heavy metal (that is the number of strains growing in the assayed conditions). Categorization was done through a heatmap showing the effective interaction site vs heavy metal tolerance (**Figure 5.5**); this

picture shows the actual values in terms of percentages of strains positive to the growth in presence of HMs for each site. This output revealed that most isolates from many sites showed a negative outcome (no growth in presence of heavy metal), with some exceptions. The heatmap visually summarizes the distribution of resistance traits across sites. A darker cell indicates a higher proportion of tolerant isolates at that site for a given metal. Mainly, isolates were tolerant (83 and 67%) if recovered from the sites C and N, while at least 50% of isolates from sites A, C and H were tolerant to Zn (respectively, 62.5, 50 and 67%). Another interesting result was that the isolates from C were also tolerant of Co (at least 50% of them).

Figure 5.5 Heatmap showing the frequency (%) of isolates tolerant to each heavy metal across the 15 sampling sites. Rows represent HMs (Cr, Ni, Co, Zn, Cu, Pb), and columns represent sampling sites (A–Q). The color scale indicates the percentage of tolerant isolates, with darker shades corresponding to higher frequencies. Data were derived from presence/absence growth tests at 200 mg/L.

	A	B	C	D	E	F	G	H	I	L	M	N	O	P	Q
Cd	0.0	0.0	83.3	37.5	22.2	20.0	0.0	22.2	0.0	0.0	0.0	66.7	25.0	0.0	0.0
Co	0.0	0.0	50.0	12.5	11.1	0.0	16.7	0.0	0.0	0.0	0.0	0.0	0.0	0.0	0.0
Cu	25.0	16.7	0.0	50.0	22.2	10.0	0.0	22.2	14.3	16.7	0.0	0.0	0.0	0.0	0.0
Ni	0.0	16.7	0.0	12.5	11.1	10.0	16.7	0.0	14.3	0.0	12.5	0.0	0.0	40.0	0.0
Zn	62.5	16.7	50.0	0.0	22.2	0.0	16.7	66.7	0.0	0.0	0.0	0.0	0.0	40.0	20.0

Then, PERMANOVA was run and the outputs are shown in **Table 5.1**; both predictors, as well as their interaction, were statistically significant.

Since the table provides no quantitative output, the results were also reported as decomposition of the statistical hypothesis, that is a "graphical portioning" of the effect of each predictor on the data set; in accordance with the results reported in the section 3.2, also for this test data were expressed as absolute frequencies. Regarding site influence (**Figure 5.6**), the mean recovery of tolerant isolates varied considerably: site C showed the highest tolerance rate (37%), followed by the sites A, D, E, and H (from 17 to 22%). Conversely, sites I, L, M, O, and Q showed the lowest tolerance (3-5%). This pattern may reflect site-specific environmental histories, such as prior exposure to industrial runoff or wastes discharge, which select for resistant genotypes. Previous studies have reported similar geospatial clustering of resistance traits in *Pseudomonas* spp., often correlated with localized anthropogenic impact (Liu et al., 2021) and heavy metal burden in soils (Rajeev et al., 2021; Shuaib et al., 2021; Zhang et al., 2022).

Table 5.1 Results of a two-way PERMANOVA performed on the dataset derived from microbiological profiles. The analysis tested the effects of sampling site, heavy metal type, and their interaction. Significant effects with $p < 0.05$. df, degrees of freedom; SS, sum of squares; MS, mean square; F, Fisher test.

Permutation N: 9999

Source	SS	df	MS	F	p
Sampling site	4.039	14	0.289	3.003	0.0007
Heavy metal	1.452	4	0.363	3.779	0.0059
Interaction	11.703	56	0.209	2.175	0.0002
Residual	40.828	425	0.096		
Total	58.022	499			

Figure 5.6 Decomposition of statistical hypothesis, by two-way PERMANOVA analysis, about the sampling sites, showing the distribution of samples across the 15 sampling sites (A–Q). Absolute frequency. Small letters indicate significant differences ($p<0.05$).

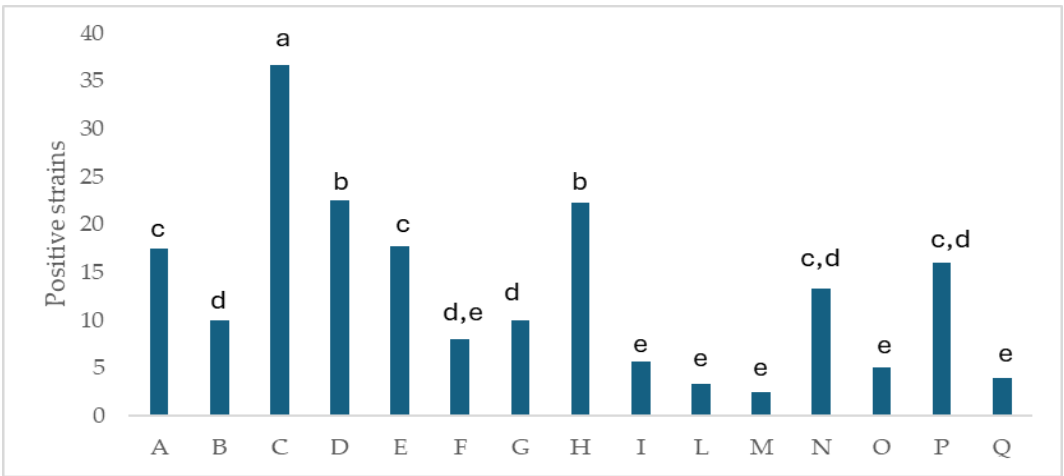

Figure 5.7 Decomposition of statistical hypothesis, by two-way PERMANOVA analysis, about the effect of HMs (Cd, Co, Cu, Ni, Zn) on microbial population. Absolute frequency. Small letters indicate significant differences ($p<0.05$).

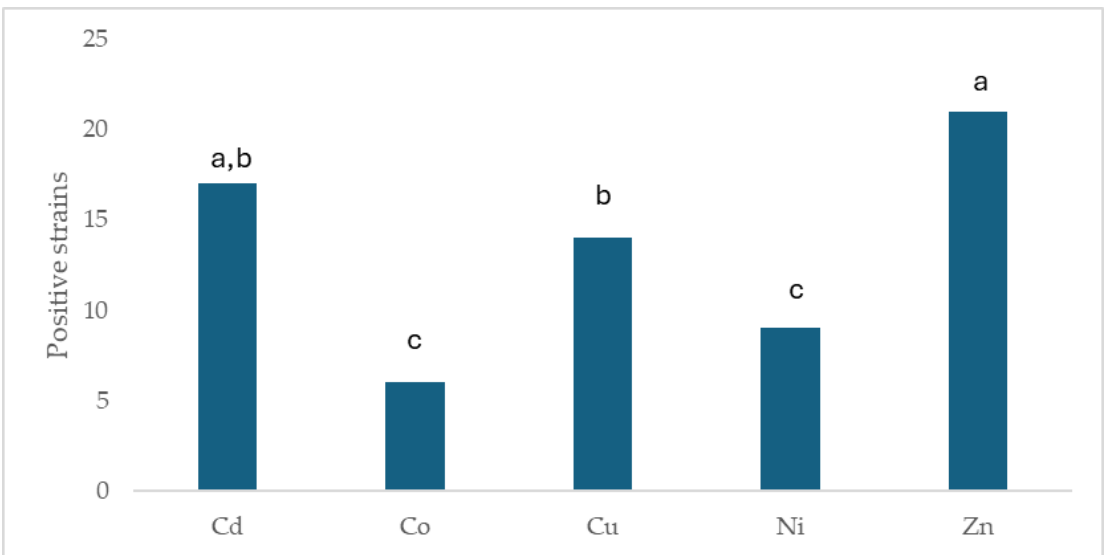

Concerning metal specific tolerance (**Figure 5.7**), positive outcomes were observed as follows: 21% for zinc, 17% for cadmium, 14% for copper, 9% for nickel, and 6% for cobalt. These differences likely reflect variations in metal toxicity and bioavailability. Zinc is an essential micronutrient and is often tolerated at moderate concentrations, whereas cadmium and cobalt are non-essential and highly toxic even at low concentrations (Bhojiya et al., 2022). The relatively high cadmium tolerance may suggest adaptive co-resistance mechanism, involving stress-response pathways, as also demonstrated in other studies (Abbas et al., 2014; Saha & Pal, 2023; Wu et al., 2022).

5.3.4 Correlation and multivariate analyses

The last step of this research employed multivariate approaches to address two main questions, that is the existence of possible correlations among some phenotypic properties and the growth in presence of HMs and the possibility of strain grouping into homogeneous classes. To address the first question, a multiple correlation through the Spearman coefficient was done. The output of this approach is a table showing a coefficient ranging from -1 (100% negative correlation) to +1 (100% positive correlation)

In **Figure 5.8** a blue circle highlights a significant positive correlation; the most interesting result was the partial positive correlation of growth in presence of cobalt (C8) with growth at 37°C (C5 and C6) (coefficient of 0.22-0.24) or the growth in presence of cobalt with cadmium (C7 and C8; coefficient at 0.22), while the use of SDS and casein (CC12 and C13) were negatively related to some growth conditions (respectively 25°C/pH 8-C4, and 37°C/pH 5, C5).

Although no direct causal relationship between cobalt resistance and thermotolerance has been reported in the literature to date, our finding suggests a potential link that deserves further investigation. This correlation may reflect the activation of shared cellular mechanisms involved in bacterial adaptation to environmental stress.

Figure 5.8 Correlation matrix among 13 experimental variables. The code from C1 to C13 include growth at different temperatures and pH levels: C1 = T15&pH5, C2 = T15&pH8, C3 = T25&pH5, C4 = T25&pH8, C5 = T37&pH5, and C6 = T37&pH8; tolerance to HMs: C7 = Cadmium, C8 = Cobalt, C9 = Copper, C10 = Nickel, and C11 = Zinc; uncommon carbon source: C12 = SDS and C13 = Skim Milk 10%. The correlation coefficients range from –1 to +1 and are color-coded from red (red circle=negative correlation) to blue (blue circle=positive correlation). Grey cells highlight significant correlations.

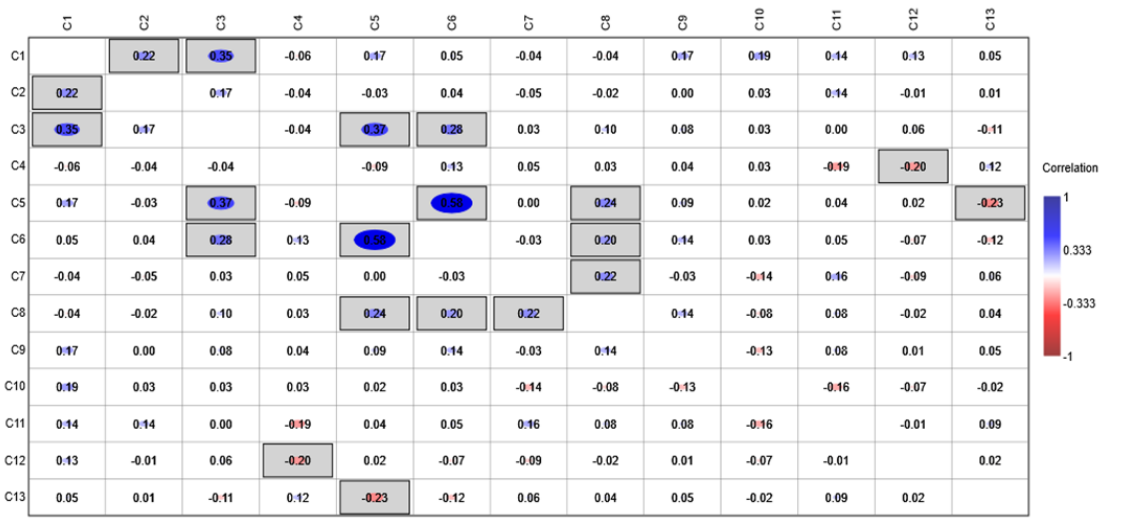

Recent studies have highlighted that several metal resistance systems, including efflux pumps (e.g., CzcCBA, CopA) and molecular chaperones such as GroEL and GroES, are upregulated under both heavy metal exposure (e.g., Co^{2+}, Cd^{2+}, Cu^{2+}) and elevated temperature. These findings support the existence of a cross-protective stress network that may underlie the observed phenotype (Oleńska et al., 2025; Wang et al., 2022).

The second question was on a possible isolate grouping, based on their response to phenotyping. The hierarchical clustering of isolates grouped the 100 microbial isolates into four phenotypical clusters (I-IV), reflecting different levels of environmental adaptability and stress tolerance. The hierarchical clustering was performed to group isolates based on phenotypic similarity. Clusters reflect shared resistance profiles rather than geographic origin. For a better readability, the four most important clusters are reported in **Table 5.2**, which shows the member of each cluster and the most important traits of the cluster itself.

Table 5.2 Isolates belonging to the four most relevant classes pointed out through Cluster Analysis.

Cluster I	Cluster I	Cluster III	Cluster IV
Mesophilic isolates	Moderately resistant isolates	Elevated thermotolerance and growth in the presence of HMs, high proteolytic potential, and variable resistance to SDS	Thermotolerant isolates but limited growth in presence of HMs
6, 8, 9, 14, 22, 30, 32, 34, 35, 37, 38, 41, 45, 47, 53, 61, 62, 64, 65, 66, 68, 72, 73, 74, 75, 76, 78, 79, 80, 81, 82, 83, 84, 87, 90, 95, 97, 98, 100	3, 11, 39, 42, 48, 50, 51, 69, 70, 89, 99	1, 15, 56, 57, 60, 93, 94, 96	10, 24, 33, 40, 67, 77, 91, 92

Cluster I, composed of 38 strains, is characterized by consistent growth under mesophilic conditions (15–25 °C across varying pH levels) but limited thermotolerance and minimal HMs and SDS resistance, with only partial proteolytic activity. Cluster II, comprising 11 strains, maintains robust growth under standard conditions and displays partial thermotolerance, with occasional tolerance to zinc or copper and moderate ability to utilize protein substrates, representing moderately resilient strains suited to mildly variable or contaminated habitats. In contrast, Cluster III, which includes 8 strains, exhibits a distinctly stress-tolerant profile, with consistent thermotolerance, elevated resistance to several HMs, occasional SDS tolerance, and high proteolytic potential, indicating a strong aptitude for biotechnological applications in harsh or polluted environments. Finally, Cluster IV, encompassing 9 isolates, grows reliably under standard environmental conditions with some

thermotolerance but limited chemical resistance and modest proteolytic capacity, depicting strains adapted to stable, non-selective niches. These findings confirm the presence of different adaptive strategies within *Pseudomonas* s populations, confirming the previous results, shaped by both environmental history and selective pressures related to temperature, pH, and metal contamination. In addition, isolates in Cluster III represent promising candidates for bioremediation applications.

5.4 Conclusions

This preliminary investigation explicates the phenotypic and functional variability of *Pseudomonas* spp. isolated from soils subjected to high anthropogenic pressure. The isolates demonstrated differential tolerance to abiotic stresses, particularly pH, temperature, and HMs exposure, underscoring their adaptive plasticity. Optimal growth was observed at 25 °C and neutral-to-slightly alkaline pH, whereas growth at 37 °C, especially under acidic conditions, was markedly reduced, indicating the general mesophilic nature of the tested strains. HMs tolerance varied by both compound and isolation site, with zinc and cadmium being the most tolerated, and cobalt and nickel exerting stronger inhibitory effects. PERMANOVA analysis confirmed the statistical significance of site- and metal-specific effects, suggesting local selective pressures as key drivers in shaping resistance phenotypes. The observed correlations between cobalt and cadmium resistance and thermotolerant growth traits may lead to new research line about the co-regulatory mechanisms that
warrant further molecular characterization. The phenotypic hierarchical clustering of isolates provided an additional layer of insight, revealing distinct subgroups with divergent stress response capacities. Collectively, the data support the hypothesis that *Pseudomonas* spp. from contaminated environments constitute a valuable reservoir of traits exploitable for bioremediation under variable environmental conditions.

References

Abbas, S. Z., Rafatullah, M., Ismail, N., & Lalung, J. (2014). Isolation, identification, and characterization of cadmium resistant *Pseudomonas* sp. M3 from industrial wastewater. *Journal of Waste Management*, *2014*, 1–6. https://doi.org/10.1155/2014/160398

Abdelaziz, A. A., Kamer, A. M. A., Al-Monofy, K. B., & Al-Madboly, L. A. (2023). *Pseudomonas aeruginosa*'s greenish-blue pigment pyocyanin: Its production and biological activities. *Microbial Cell Factories*, *22*(1). https://doi.org/10.1186/s12934-023-02122-1

Agenzia Regionale per la Prevenzione e la Protezione dell'Ambiente - Siti potenzialmente contaminati. (s.d.). Recuperato 16 luglio 2025, da https://www.arpa.puglia.it/pagina3239_siti-potenzialmente-contaminati.html

Alotaibi, B. S., Khan, M., & Shamim, S. (2021). Unraveling the underlying heavy metal detoxification mechanisms of *Bacillus* species. *Microorganisms*, *9*(8), 1628. https://doi.org/10.3390/microorganisms9081628

Bernabé-Pérez, E. A., Gaytán, P., Juárez-González, V. R., Hernández-García, I. J., Tapia-Pastrana, G., Quintero-Hernández, V., & Martínez-Martínez, L. L. (2024). Heterologous production of bacteriocin EMM1 from *Pseudomonas protegens* and its antimicrobial activity against multidrug-resistant clinical isolates. *International Journal of Peptide Research and Therapeutics*, *30*(6), 73. https://doi.org/10.1007/s10989-024-10649-z

Bhojiya, A. A., Joshi, H., Upadhyay, S. K., Srivastava, A. K., Pathak, V. V., Pandey, V. C., & Jain, D. (2022). Screening and optimization of zinc removal potential in *Pseudomonas aeruginosa*-HMR1 and its plant growth-promoting attributes. *Bulletin of Environmental Contamination and Toxicology*, *108*(3), 468–477. https://doi.org/10.1007/s00128-021-03232-5

Carrascosa, C., Martínez, R., Sanjuán, E., Millán, R., Del Rosario-Quintana, C., Acosta, F., García, A., & Jaber, J. R. (2021). Identification of the *Pseudomonas fluorescens* group as being responsible for blue pigment on fresh cheese. *Journal of Dairy Science*, *104*(6), 6548–6558. https://doi.org/10.3168/jds.2020-19517

Chauhan, M., Kimothi, A., Sharma, A., & Pandey, A. (2023). Cold adapted *Pseudomonas*: Ecology to biotechnology. *Frontiers in Microbiology*, *14*, 1218708. https://doi.org/10.3389/fmicb.2023.1218708

Chierici, M., Picozzi, C., La Spina, M. G., Orsi, C., Vigentini, I., Zambrini, V., & Foschino, R. (2016). Strain diversity of *Pseudomonas fluorescens* group with potential blue pigment phenotype isolated from dairy products. *Journal of Food Protection*, *79*(8), 1430–1435. https://doi.org/10.4315/0362-028X.JFP-15-589

Costa, O. Y. A., Raaijmakers, J. M., & Kuramae, E. E. (2018). Microbial extracellular polymeric substances: Ecological function and impact on soil aggregation. *Frontiers in Microbiology*, *9*. https://doi.org/10.3389/fmicb.2018.01636

Craig, K., Johnson, B. R., & Grunden, A. (2021). Leveraging *Pseudomonas* stress response mechanisms for industrial applications. *Frontiers in Microbiology*, *12*, 660134. https://doi.org/10.3389/fmicb.2021.660134

Doolotkeldieva, T., Bobusheva, S., & Konurbaeva, M. (2024). In vitro and in vivo screening of bacterial species from contaminated soil for heavy metal biotransformation activity. *Journal of Environmental Science and Health, Part B*, *59*(6), 315–332. https://doi.org/10.1080/03601234.2024.2343236

Dyer, J. M., & Foy, V. M. (2022). Revealing the unseen: A review of Wood's lamp in dermatology. *The Journal of Clinical and Aesthetic Dermatology*, *15*(6), 25–30.

El-Fouly, M. Z., Sharaf, A. M., Shahin, A. A. M., El-Bialy, H. A., & Omara, A. M. A. (2015). Biosynthesis of pyocyanin pigment by *Pseudomonas aeruginosa*. *Journal of Radiation Research and Applied Sciences*, *8*(1), 36–48. https://doi.org/10.1016/j.jrras.2014.10.007

Fernández-Fernández, R., Lozano, C., Eguizábal, P., Ruiz-Ripa, L., Martínez-Álvarez, S., Abdullahi, I. N., Zarazaga, M., & Torres, C. (2022). Bacteriocin-like inhibitory substances in *Staphylococci* of different origins and species with activity against relevant pathogens. *Frontiers in Microbiology*, *13*, 870510. https://doi.org/10.3389/fmicb.2022.870510

Firincă, C., Zamfir, L.-G., Constantin, M., Răut, I., Capră, L., Popa, D., Jinga, M.-L., Baroi, A. M., Fierăscu, R. C., Corneli, N. O., Postolache, C., Doni, M., Gurban, A.-M., Jecu, L., & Șesan, T. E. (2023). Microbial removal of heavy metals from contaminated environments using metal-resistant indigenous strains. *Journal of Xenobiotics*, *14*(1), 51–78. https://doi.org/10.3390/jox14010004

Freeman, D. J., Falkiner, F. R., & Keane, C. T. (1989). New method for detecting slime production by coagulase negative *Staphylococci*. *Journal of Clinical Pathology*, *42*(8), 872–874. https://doi.org/10.1136/jcp.42.8.872

Furmanczyk, E. M., Kaminski, M. A., Spolnik, G., Sojka, M., Danikiewicz, W., Dziembowski, A., Lipinski, L., & Sobczak, A. (2017). Isolation and characterization of *Pseudomonas* spp. Strains that efficiently decompose sodium dodecyl sulfate. *Frontiers in Microbiology*, *8*, 1872. https://doi.org/10.3389/fmicb.2017.01872

Honselmann Genannt Humme, J., Dubrowska, K., Grygorcewicz, B., Gliźniewicz, M., Paszkiewicz, O., Głowacka, A., Musik, D., Story, G., Rakoczy, R., & Augustyniak, A. (2024). Optimised stress

– intensification of pyocyanin production with zinc oxide nanoparticles. *Microbial Cell Factories*, *23*(1), 215. https://doi.org/10.1186/s12934-024-02486-y

Igiri, B. E., Okoduwa, S. I. R., Idoko, G. O., Akabuogu, E. P., Adeyi, A. O., & Ejiogu, I. K. (2018). Toxicity and bioremediation of heavy metals contaminated ecosystem from tannery wastewater: A review. *Journal of Toxicology*, *2018*, 1–16. https://doi.org/10.1155/2018/2568038

Joshi, S., Gangola, S., Bhandari, G., Bhandari, N. S., Nainwal, D., Rani, A., Malik, S., & Slama, P. (2023). Rhizospheric bacteria: The key to sustainable heavy metal detoxification strategies. *Frontiers in Microbiology*, *14*. https://doi.org/10.3389/fmicb.2023.1229828

Karishma, S., Saravanan, A., Deivayanai, V. C., Ajithkumar, U., Yaashikaa, P. R., & Vickram, A. S. (2024). Emerging strategies for enhancing microbial degradation of petroleum hydrocarbons: Prospects and challenges. *Bioresource Technology Reports*, *26*, 101866. https://doi.org/10.1016/j.biteb.2024.101866

Khoshru, B., Fallah Nosratabad, A., Mahjenabadi, V. A. J., Knežević, M., Hinojosa, A. C., Fadiji, A. E., Enagbonma, B. J., Qaderi, S., Patel, M., Baktash, E. M., Dawood, M. F. A., & Mitra, D. (2025). Multidimensional role of *Pseudomonas*: From biofertilizers to bioremediation and soil ecology to sustainable agriculture. *Journal of Plant Nutrition*, *48*(6), 1016–1042. https://doi.org/10.1080/01904167.2024.2416078

Kuppan, N., Padman, M., Mahadeva, M., Srinivasan, S., & Devarajan, R. (2024). A comprehensive review of sustainable bioremediation techniques: Eco friendly solutions for waste and pollution management. *Waste Management Bulletin*, *2*(3), 154–171. https://doi.org/10.1016/j.wmb.2024.07.005

Li, W., Li, W., Xing, L., & Guo, S. (2023). Effect of arbuscular mycorrhizal fungi (AMF) and plant growth-promoting rhizobacteria (PGPR) on microorganism of phenanthrene and pyrene contaminated soils. *International Journal of Phytoremediation*, *25*(2), 240–251. https://doi.org/10.1080/15226514.2022.2071832

Li, X., Gao, Y., Ning, X., & Li, Z. (2023). Research progress and hotspots on microbial remediation of heavy metal-contaminated soil: A systematic review and future perspectives. *Environmental Science and Pollution Research*, *30*(56), 118192–118212. https://doi.org/10.1007/s11356-023-30655-w

Liu, L., Wang, S., & Chen, J. (2021). Anthropogenic activities change the relationship between microbial community taxonomic composition and functional attributes. *Environmental Microbiology*, *23*(11), 6663–6675. https://doi.org/10.1111/1462-2920.15702

Longhi, R. D., Correia, S. D. S., Bruzaroski, S. R., Poli-Frederico, R. C., Fagnani, R., & Santana, E. H. W. D. (2022). *Pseudomonas fluorescens* and *Pseudomonas putida* from refrigerated raw milk: Genetic diversity and lipoproteolytic activity. *Journal of Dairy Research*, *89*(1), 86–89. https://doi.org/10.1017/S0022029922000048

Lyng, M., & Kovács, Á. T. (2023). Frenemies of the soil: *Bacillus* and *Pseudomonas* interspecies interactions. *Trends in Microbiology*, *31*(8), 845–857. https://doi.org/10.1016/j.tim.2023.02.003

Lyng, M., Þórisdóttir, B., Sveinsdóttir, S. H., Hansen, M. L., Jelsbak, L., Maróti, G., & Kovács, Á. T. (2024). Taxonomy of *Pseudomonas* spp. Determines interactions with *Bacillus subtilis*. *mSystems*, *9*(10), e00212-24. https://doi.org/10.1128/msystems.00212-24

Maalej, H., Hmidet, N., Boisset, C., Buon, L., Heyraud, A., & Nasri, M. (2015). Optimization of exopolysaccharide production from *Pseudomonas stutzeri* AS22 and examination of its metal-binding abilities. *Journal of Applied Microbiology*, *118*(2), 356–367. https://doi.org/10.1111/jam.12688

Marvelli, E. (2025). *Foggia, 618 thousand tons of illegal waste*. https://www.gat.report/28593/foggia-618-thousand-tons-of-illegal-waste/

Mathivanan, K., Chandirika, J. U., Vinothkanna, A., Yin, H., Liu, X., & Meng, D. (2021). Bacterial adaptive strategies to cope with metal toxicity in the contaminated environment – A review. *Ecotoxicology and Environmental Safety*, *226*, 112863. https://doi.org/10.1016/j.ecoenv.2021.112863

Mead, G. C. (1985). Enumeration of pseudomonads using cephaloridine-fucidin-cetrimide agar (CFC). *International Journal of Food Microbiology*, *2*(1–2), 21–26. https://doi.org/10.1016/0168-1605(85)90052-2

Medić, A. B., & Karadžić, I. M. (2022). *Pseudomonas* in environmental bioremediation of hydrocarbons and phenolic compounds- key catabolic degradation enzymes and new analytical platforms for comprehensive investigation. *World Journal of Microbiology and Biotechnology*, *38*(10), 165. https://doi.org/10.1007/s11274-022-03349-7

Mozaheb, N., Rasouli, P., Kaur, M., Van Der Smissen, P., Larrouy-Maumus, G., & Mingeot-Leclercq, M.-P. (2023). A mildly acidic environment alters *Pseudomonas aeruginosa* virulence and causes remodelling of the bacterial surface. *Microbiology Spectrum*, *11*(4), e04832-22. https://doi.org/10.1128/spectrum.04832-22

Narvhus, J. A., Nilsen Bækkelund, O., Tidemann, E. M., Østlie, H. M., & Abrahamsen, R. K. (2021). Isolates of *Pseudomonas* spp. From cold-stored raw milk show variation in proteolytic and

lipolytic properties. *International Dairy Journal*, *123*, 105049. https://doi.org/10.1016/j.idairyj.2021.105049

Nowak, A., Żur-Pińska, J., Piński, A., Pacek, G., & Mrozik, A. (2021). Adaptation of phenol-degrading *Pseudomonas putida* KB3 to suboptimal growth condition: A focus on degradative rate, membrane properties and expression of xylE and cfaB genes. *Ecotoxicology and Environmental Safety*, *221*, 112431. https://doi.org/10.1016/j.ecoenv.2021.112431

Oleńska, E., Małek, W., Swiecicka, I., Wójcik, M., Thijs, S., & Vangronsveld, J. (2025). Bacteria under metal stress—Molecular mechanisms of metal tolerance. *International Journal of Molecular Sciences*, *26*(12), 5716. https://doi.org/10.3390/ijms26125716

Pailin, T., Kang, D. H., Schmidt, K., & Fung, D. Y. C. (2001). Detection of extracellular bound proteinase in EPS-producing lactic acid bacteria cultures on skim milk agar. *Letters in Applied Microbiology*, *33*(1), 45–49. https://doi.org/10.1046/j.1472-765X.2001.00954.x

Panasia, G., Oetermann, S., Steinbüchel, A., & Philipp, B. (2019). Sulfate ester detergent degradation in *Pseudomonas aeruginosa* is subject to both positive and negative regulation. *Applied and Environmental Microbiology*, *85*(23), e01352-19. https://doi.org/10.1128/AEM.01352-19

Qiao, Y., Xu, W., Wei, J., Kong, L., Xue, J., Jiang, Q., Cheng, D., & Liu, Y. (2024). Novel agents consisting of *Pseudomonas zhaodongensis* and dimethylsulfoniopropionate (DMSP) enhancing bioremediation of oil-contaminated sediments at deep-sea condition. *Environmental Technology & Innovation*, *36*, 103744. https://doi.org/10.1016/j.eti.2024.103744

Rajeev, M., Sushmitha, T. J., Aravindraja, C., Toleti, S. R., & Pandian, S. K. (2021). Exploring the impacts of heavy metals on spatial variations of sediment-associated bacterial communities. *Ecotoxicology and Environmental Safety*, *209*, 111808. https://doi.org/10.1016/j.ecoenv.2020.111808

Renu, Sarim, K. M., Sahu, U., Bhoyar, M. S., Singh, D. P., Singh, U. B., Sahu, A., Gupta, A., Mandal, A., Thakur, J. K., & Manna, M. C. (2021). Augmentation of metal-tolerant bacteria elevates growth and reduces metal toxicity in spinach. *Bioremediation Journal*, *25*(2), 108–127. https://doi.org/10.1080/10889868.2020.1844133

Sagar, A., Rathore, P., Ramteke, P. W., Ramakrishna, W., Reddy, M. S., & Pecoraro, L. (2021). Plant growth promoting rhizobacteria, arbuscular mycorrhizal fungi and their synergistic interactions to counteract the negative effects of saline soil on agriculture: Key macromolecules and mechanisms. *Microorganisms*, *9*(7), 1491. https://doi.org/10.3390/microorganisms9071491

Saha, J., & Pal, A. (2023). Cadmium biosorption and plant growth promotion efficacy of a metalloresistant *Pseudomonas* sp. Unveils augmented growth with reduced metal

accumulation in *Brassica napus* L. *Vegetos*, *37*(6), 2311–2319. https://doi.org/10.1007/s42535-023-00724-z

Samrot, A. V., Rio, A. J., Kumar, S. S., & Samanvitha, S. K. (2017). Bioprospecting studies of pigmenting *Pseudomonas aeruginosa* SU-1, *Microvirga aerilata*</i> SU14 and *Bacillus megaterium* SU15 isolated from garden soil. *Biocatalysis and Agricultural Biotechnology*, *11*, 330–337. https://doi.org/10.1016/j.bcab.2017.08.003

Shuaib, M., Azam, N., Bahadur, S., Romman, M., Yu, Q., & Xuexiu, C. (2021). Variation and succession of microbial communities under the conditions of persistent heavy metal and their survival mechanism. *Microbial Pathogenesis*, *150*, 104713. https://doi.org/10.1016/j.micpath.2020.104713

Song, Y., Li, R., Chen, G., Yan, B., Zhong, L., Wang, Y., Li, Y., Li, J., & Zhang, Y. (2021). Bibliometric analysis of current status on bioremediation of petroleum contaminated soils during 2000–2019. *International Journal of Environmental Research and Public Health*, *18*(16), 8859. https://doi.org/10.3390/ijerph18168859

Srivastava, P., Sachan, K., Baskar, P., Saikanth, D. R. K., Lytand, W., Kumar, R. K. M. H., & Singh, B. V. (2023). Soil microbes expertly balancing nutrient demands and environmental preservation and ensuring the delicate stability of our ecosystems- A review. *International Journal of Plant & Soil Science*, *35*(18), 989–1000. https://doi.org/10.9734/ijpss/2023/v35i183363

Sun, W., Shahrajabian, M. H., & Soleymani, A. (2024). The Roles of Plant-Growth-Promoting Rhizobacteria (PGPR)-Based Biostimulants for Agricultural Production Systems. *Plants*, *13*(5), 613. https://doi.org/10.3390/plants13050613

Tribelli, P. M., & López, N. I. (2022). Insights into the temperature responses of *Pseudomonas* species in beneficial and pathogenic host interactions. *Applied Microbiology and Biotechnology*, *106*(23), 7699–7709. https://doi.org/10.1007/s00253-022-12243-z

Vélez, J. M. B., Martínez, J. G., Ospina, J. T., & Agudelo, S. O. (2021). Bioremediation potential of *Pseudomonas* genus isolates from residual water, capable of tolerating lead through mechanisms of exopolysaccharide production and biosorption. *Biotechnology Reports*, *32*, e00685. https://doi.org/10.1016/j.btre.2021.e00685

Verasoundarapandian, G., Wong, C.-Y., Shaharuddin, N. A., Gomez-Fuentes, C., Zulkharnain, A., & Ahmad, S. A. (2021). A review and bibliometric analysis on applications of microbial degradation of hydrocarbon contaminants in arctic marine environment at metagenomic and enzymatic levels. *International Journal of Environmental Research and Public Health*, *18*(4), 1671. https://doi.org/10.3390/ijerph18041671

Wang, J. L., Dragone, N. B., Avard, G., & Hynek, B. M. (2022). Microbial survival in an extreme martian analog ecosystem: Poás volcano, Costa Rica. *Frontiers in Astronomy and Space Sciences*, *9*. https://doi.org/10.3389/fspas.2022.817900

Wu, S., Zhou, Z., Zhu, L., Zhong, L., Dong, Y., Wang, G., & Shi, K. (2022). Cd immobilization mechanisms in a *Pseudomonas* strain and its application in soil Cd remediation. *Journal of Hazardous Materials*, *425*, 127919. https://doi.org/10.1016/j.jhazmat.2021.127919

Yang, G., Ryo, M., Roy, J., Lammel, D. R., Ballhausen, M.-B., Jing, X., Zhu, X., & Rillig, M. C. (2022). Multiple anthropogenic pressures eliminate the effects of soil microbial diversity on ecosystem functions in experimental microcosms. *Nature Communications*, *13*(1), 4260. https://doi.org/10.1038/s41467-022-31936-7

Yasmin, R., Zafar, M. S., Tahir, I. M., Asif, R., Asghar, S., & Raza, S. K. (2022). Biosorptive potential of *Pseudomonas* species RY12 toward zinc heavy metal in agriculture soil irrigated with contaminated wastewater. *Dose-Response*, *20*(3), 15593258221117352. https://doi.org/10.1177/15593258221117352

Yin, Q., He, K., Collins, G., De Vrieze, J., & Wu, G. (2024). Microbial strategies driving low concentration substrate degradation for sustainable remediation solutions. *Npj Clean Water*, *7*(1), 52. https://doi.org/10.1038/s41545-024-00348-z

Zanna, S., Mercier, D., Gardin, E., Allion-Maurer, A., & Marcus, P. (2022). EPS for bacterial anti-adhesive properties investigated on a model metal surface. *Colloids and Surfaces B: Biointerfaces*, *213*, 112413. https://doi.org/10.1016/j.colsurfb.2022.112413

Zhang, M., Zhang, T., Zhou, L., Lou, W., Zeng, W., Liu, T., Yin, H., Liu, H., Liu, X., Mathivanan, K., Praburaman, L., & Meng, D. (2022). Soil microbial community assembly model in response to heavy metal pollution. *Environmental Research*, *213*, 113576. https://doi.org/10.1016/j.envres.2022.113576

6. Phenotypic and functional characterization of soil *Pseudomonas* strains reveals multi-metal tolerance and bioremediation potential[4]

Alessandro De Santis[1], Antonio Bevilacqua[1], Sara Conceição[2], Marta Laranjo[2,3], Matteo Francavilla[1], Mauro Marone[1], Maria Rosaria Corbo[1], Milena Sinigaglia[1]

[1]Department of Agriculture, Food, Natural Resources and Engineering, University of Foggia, Foggia, ITALY

[2]MED-Mediterranean Institute for Agriculture, Environment and Development & CHANGE-Global Change and Sustainability Institute, IIFA-Institute for Advanced Studies and Research, Universidade de Évora, Pólo da Mitra, Évora, Portugal

[3]Departamento de Medicina Veterinária, Escola de Ciências e Tecnologia, Universidade de Évora, Pólo da Mitra, Évora, Portugal

Abstract

The increasing occurrence of illegal urban waste dumping represents a growing environmental concern due to the accumulation of heavy metals in soils and their long-term impact on soil health and microbial communities. This study investigated indigenous *Pseudomonas* isolates from twelve contaminated soils collected in Southern Italy, aiming to evaluate their adaptive responses to abiotic stress and their potential for bioremediation. A total of one hundred isolates were obtained and screened for growth under heavy metal stress conditions (Cu, Pb, Cr, Zn, As). Growth-based tolerance assays were used as a preliminary screening, and only isolates showing measurable removal capacity were further characterized using ICP–OES analysis. Selected strains exhibited broad tolerance across different single-metal exposures, with removal efficiencies exceeding 65 % for Cr, Zn, Cu, and As, and up to 90 % for

[4] This chapter was published on Frontiers in Microbiology (De Santis, A., Bevilacqua, A., Conceição, S., Laranjo, M., Francavilla, M., Marone, M., Corbo, M. R., & Sinigaglia, M. (2025). Phenotypic and functional characterization of soil Pseudomonas strains reveals multi-metal tolerance and bioremediation potential. Frontiers in Microbiology, 16, 1731818. https://doi.org/10.3389/fmicb.2025.1731818)

Pb. These isolates also demonstrated robust growth under osmotic and acidic stress, and maintained viability at low temperatures, suggesting a high level of ecological adaptability. Phylogenetic analysis based on 16S rRNA sequencing confirmed their affiliation within the *P. fluorescens* and *P. putida* groups, taxa known for their metabolic flexibility and stress resistance. The convergence of high removal efficiency, stress tolerance, and phylogenetic diversity indicates that these isolates represent strong candidates for bioaugmentation in metal-polluted soils. Future studies will focus on co-exposure experiments with mixed metals to evaluate synergistic and antagonistic effects and to validate their performance under complex contamination scenarios.

6.1 Introduction

Environmental pollution caused by the illegal dumping of urban waste has become a critical environmental concern worldwide. The uncontrolled deposition of household, industrial, and construction waste in unauthorized areas introduces persistent pollutants into the environment, particularly heavy metals (HMs) such as lead (Pb), cadmium (Cd), chromium (Cr), copper (Cu), and zinc (Zn) (Alengebawy et al., 2021; Mitra et al., 2022; Sazykin et al., 2023). Due to their non-biodegradable nature and high potential for bioaccumulation, HMs persist in soils and sediments, where they disrupt microbial communities, alter nutrient cycling, and impair soil fertility and ecosystem functioning (Pande et al., 2022; Popoola et al., 2024; Rashid et al., 2023). Their accumulation also represents a risk for human health through the contamination of crops and groundwater resources (Briffa et al., 2020; Perković et al., 2022; Rai et al., 2019).

Traditional physicochemical remediation techniques, such as soil excavation, chemical immobilization, and soil washing, can reduce metal concentrations but are often costly, invasive, and environmentally disruptive (Kumar et al., 2023). In contrast, bioremediation, based on the metabolic capabilities of microorganisms, offers a more

sustainable and eco-compatible alternative. Through processes such as biosorption, bioaccumulation, enzymatic reduction, and precipitation, microorganisms can detoxify or immobilize HMs while preserving soil functionality (Coelho et al., 2015; Singh et al., 2022).

Among the microbial taxa explored, the genus *Pseudomonas* is of particular interest due to its remarkable metabolic versatility, resistance to oxidative and osmotic stress, and its ability to produce extracellular polymeric substances (EPS) that enhance biofilm formation and metal sequestration (Qurbani et al., 2022; Roy et al., 2024). The presence of multiple efflux systems and metal-resistance operons (e.g., czc, cop, cad, ars) allows *Pseudomonas* spp. to survive and adapt in contaminated environments, making them strong candidates for biotechnological applications in soil restoration (Rahman & Singh, 2020). Recent studies have confirmed their high detoxification potential: for example, *Pseudomonas* isolates achieved up to 96 % Cr(VI) removal through bioflocculant-assisted biosorption (Monga et al., 2022), 76 % Cr(VI) reduction coupled with pyrene degradation via chrA and copZ genes (Su et al., 2022), and over 90 % Cd and Ni removal when immobilized on biochar (Manikandan & Nair, 2023). Additional reports demonstrated As(III) oxidation (Satyapal et al., 2024) and plasmid-encoded chromate reduction in *P. putida* (Sundarraj et al., 2023), reinforcing the role of this genus as a model system for heavy metal bioremediation.

In the past decade, genomic and metagenomic studies have expanded our understanding of *Pseudomonas* adaptability and the genetic basis of metal resistance (Khan et al., 2022). However, these approaches often remain predictive: they describe the genetic potential of microbial communities without validating their actual physiological performance under stress. Many studies isolate only a single highly resistant strain from environmental samples, overlooking other microorganisms that may contribute to detoxification through complementary mechanisms. This bias limits our understanding of how phenotypic diversity and ecological adaptation emerge within native microbial communities exposed to multiple contaminants. For this

reason, integrating metagenomic insights with classical culture-based screening is essential to link genotypes to functional traits. Controlled phenotypic assays enable the quantification of tolerance and removal efficiency, offering a direct measure of bioremediation potential.

Illegal dumping sites, chronically exposed to mixed waste streams, represent unique ecological niches where indigenous microorganisms are naturally selected for resilience to complex contamination. These environments constitute valuable reservoirs of strains capable of surviving extreme physicochemical stress and exhibiting relevant detoxification traits (Bora et al., 2025; Mishra et al., 2019; Sharma et al., 2022).

In this context, the present study aims to isolate and characterize indigenous *Pseudomonas* strains from soils affected by illegal urban waste dumping, combining phenotypic and molecular identification with the evaluation of their tolerance and removal capacities toward multiple HMs. This work seeks to (i) identify native isolates showing significant resistance and detoxification efficiency; (ii) elucidate physiological traits potentially linked to metal stress adaptation, such as EPS production; and (iii) provide a framework for the selection of promising strains for future bioaugmentation and bioremediation strategies.

6.2 Materials and Methods

6.2.1 Sampling context and characteristics

Soil samples were collected from twelve different sites surrounding the city of Foggia (Southern Italy), an area affected by long-standing illegal dumping activities. The sites were georeferenced using WGS84 coordinates (**Table C6.1**), with precise latitude and longitude recorded for each location. The selection was based on visual indicators of anthropogenic disturbance and the likelihood of harboring microbial populations exposed to metal stress. Samples were collected from the top 0-10 cm of the soil surface using sterile tools, transported to the laboratory under refrigerated conditions,

and processed within 24 hours. They exhibited neutral to slightly alkaline pH (7.2–7.8), EC 0.55–16.7 dS m^{-1}, organic matter 2.1-9.8 %, and available P 71-668 mg kg^{-1}. Total metal concentrations (mg kg^{-1}) were: Pb 45-467, Cd 0.1–1.8, Cr 15-109, Cu 13-1002, Ni 10-73, Zn 30-6341, As 3.3-11.1.

6.2.2 Isolation and maintenance of Pseudomonas spp.

Soil samples (1 g) were suspended in sterile physiological saline (0.9% NaCl) and serially diluted. Aliquots (100 µL) of appropriate dilutions were spread on Pseudomonas Agar Base (PAB) (Oxoid) supplemented with Cetrimide-Fucidin-Cephaloridine (C-F-C) (Oxoid), a selective supplement to inhibit non-*Pseudomonas* bacteria. Plates were incubated aerobically at 25 °C for 48 hours. Colonies with distinct *Pseudomonas*-like morphology (mucoid, convex, translucent to opaque, often pigmented) were subcultured on fresh PAB plates and purified through successive streaking.

A total of 100 bacterial isolates presumptively belonging to Pseudomonadaceae were recovered from contaminated soils, with strain identifiers assigned sequentially and mapped to specific sampling sites as follows: site 1 (IDs FG1–FG9), site 2 (FG10–FG19), site 3 (FG20–FG27), and so forth, up to site 12 (FG92–100), as described in **ANNEX C - Table C6.1**. To improve readability, the code used in figures will take into account just the number of the code. Purified isolates were maintained on Nutrient agar (Oxoid, Basingstoke, UK) slants at 4 °C for short-term use and preserved in glycerol stocks at –20 °C for long-term storage. These isolates were later subjected to morphological, biochemical, and functional screening to assess their ecological and bioremediative potential.

6.2.3 Morphological and biochemical characterization of Pseudomonas isolates

The morphology of the colonies that was observed on PAB was used for evaluation of pigment production, surface texture, elevation, edge definition, and opacity. Gram

staining was performed on fresh cultures, after 24h incubation at optimum temperature, to confirm Gram-negative cell structure and rod-shaped morphology. Furthermore, a series of key biochemical assays were conducted to assess the metabolic functionality of the isolates. Catalase activity was evaluated based on the formation of oxygen bubbles upon exposure to 3% hydrogen peroxide, indicating the presence of the catalase enzyme (Whittenbury, 1964). Oxidase activity (Steel, 1961) was determined using commercial oxidase reagent strips (Merck Millipore, Darmstadt, Germany), allowing for the detection of cytochrome c oxidase. The oxidative or fermentative metabolism of glucose was assessed through the oxidative/fermentative (O/F) test (Porres & Stanyon, 1974), performed in Hugh and Leifson's medium (Biolife, Milan, Italy). Finally, bacterial motility was investigated using a semi-solid agar medium (0.4% w/v) (Tittsler & Sandholzer, 1936), enabling the observation of active cellular movement through diffuse growth patterns within the medium.

6.2.4 Functional phenotypical characterization

6.2.4.1 Growth Index assessment under pH and temperature stress

Overnight cultures of each isolate were grown in nutrient broth (Oxoid, Basingstoke, UK) and subsequently inoculated at a concentration of 5–6 log CFU/mL into 5 mL of fresh nutrient broth. Prior to inoculation, the medium was adjusted to specific environmental conditions to evaluate the physiological adaptability of the strains. In particular, the pH of the broth was modified to 4.5, 5.5, 6.5 (used as the control), 7.5, and 8.5, using sterile 1 M HCl or 1 M NaOH prior to autoclaving and verified with a calibrated pH, while temperature conditions were set at 15 °C, 25 °C (control), and 37 °C.

Cultures were incubated under agitation (150 rpm) for 24 and 48 hours. The optical density at 600 nm (OD_{600}) was measured at both times using a UV-Vis spectrophotometer.

The Growth Index (GI) was calculated for each condition as described by Bevilacqua et al. (2009), using the following equation (**Eq. 6.1**):

$$GI = (Abs_{sample} / Abs_{control}) \times 100 \qquad \textbf{(Eq. 6.1)}$$

Where Abs_{sample} corresponds to the OD_{600} under stress conditions and $Abs_{control}$ is the OD_{600} under optimal conditions (pH 6.5 and 25 °C).

6.2.4.2 Drought tolerance simulation

Osmotic stress resistance was tested in nutrient broth supplemented with polyethylene glycol (PEG 6000) (Sigma-Aldrich, Darmstadt, Germany) at final concentrations of 0% (control), 5%, 10%, 15%, and 20%. Isolates were incubated for 48 hours at 25°C, and growth was assessed spectrophotometrically (OD_{600}). The drought resistance (DR) was determined by comparing the samples' OD_{600} against the control by the equation (**Eq. 6.2)**:

$$DR = (Abs_{sample} / Abs_{control}) \times 100 \qquad \textbf{(Eq. 6.2)}$$

Where Abs_{sample} corresponds to the OD_{600} under stress conditions and $Abs_{control}$ is the OD_{600} under optimal conditions (pH 6.5 and 25 °C).

6.2.5 Heavy metal resistance assays

6.2.5.1 Growth assay in liquid medium

Minimum Inhibitory Concentration (MIC) assays were performed as a preliminary qualitative screening to identify isolates capable of sustaining growth under increasing metal concentrations. This step was used to reduce the initial collection to the most resistant isolates, which were subsequently tested for quantitative removal capacity. The isolates were exposed to zinc sulfate ($ZnSO_4 \cdot 7H_2O$), lead nitrate ($Pb(NO_3)_2$),

potassium dichromate ($K_2Cr_2O_7$), copper sulfate ($CuSO_4 \cdot 5H_2O$), cadmium chloride ($CdCl_2 \cdot 2.5H_2O$) and sodium arsenite ($NaAsO_2$). All 100 isolates were initially inoculated into 10 mL of nutrient broth containing 100 mg/L, 200 mg/L or 300 mg/L of a heavy metal. Cultures were prepared from overnight metal-free precultures and standardized to an initial OD_{600} of approximately 0.05. Incubation was carried out at 28 °C with shaking at 150 rpm for 48 hours. At the end of the incubation period, bacterial growth was quantified by measuring optical density at 600 nm (OD_{600}). All assays included a zero-metal control prepared with the same medium without heavy metal supplementation. Data were modeled as Growth Index, using the zero-metal samples as references.

6.2.5.2 Removal assay in liquid medium

To evaluate the heavy metal removal potential of *Pseudomonas* isolates, strains that had shown the highest resistance in preliminary assays were selected. Test concentrations were 200 mg/L for Cr and Zn, and 300 mg/L for Cu, Pb, As. Cd removal was not assessed because no isolates survive to more than 100 mg/L.

Each isolate was inoculated at a concentration of 5-6 log CFU/mL into 5 mL of nutrient broth supplemented with specific concentrations of selected heavy metal salts, to evaluate their tolerance thresholds. Cultures were incubated in contaminated nutrient broth for 48 hours at 25 °C with shaking at 150 rpm. After incubation, samples were centrifuged at 5000 × g for 10 minutes to separate the biomass. The supernatant was collected and subjected to organic matter digestion to eliminate potential interference prior to metal quantification.

The residual metal concentrations in digested broth were determined by Inductively Coupled Plasma Optical Emission Spectroscopy (ICP-OES, Agilent 5800) following acid digestion according to ISO 14870:2001. Samples were mineralized in a microwave oven (MARS6-CEM) using a nitric acid–hydrogen peroxide-hydrofluoridric acid solution (20:7.5:2.5 volume ratio) in accordance with standard

protocols for trace metal analysis in biological matrices. Metals quantification was perfomed using a certified multi-standard (Periodic table mix1 for ICP, Supelco).
The removal efficiency (RE%) for each metal was calculated using the formula (**Eq. 6.3**):

$$RE\ (\%) = ((C_0 - C_x) / C_0) \times 100 \quad \textbf{(Eq. 6.3)}$$

Where: C_0 = initial metal concentration (mg/L), C_x = residual metal concentration after incubation (mg/L)
Uninoculated control samples containing only the metal-supplemented medium were included to account for abiotic losses.

6.2.6 Molecular identification of bacterial isolates

Genomic DNA was extracted from 24-hour cultures grown in nutrient broth using the E.Z.N.A.® Bacterial DNA Kit (Omega Bio-Tek, USA), according to the manufacturer's instructions and stored at −20 °C until use.
The 16S rRNA gene was amplified using the forward primer **Y1** (5′-TGGCTCAGAACGAACGCTGGCGGC-3′) (Young et al., 1991) and the reverse primer **Y3** (5′-TACCTTGTTACGACTTCACCCCAGTC-3′) (Laranjo et al., 2004). Each reaction was prepared in a final volume of 50 µL, consisting of: 34.25 µL nuclease-free water (NZYTech, Portugal), 5 µL 10× buffer (NZYTech), 2.5 µL $MgCl_2$ (50 mM) (NZYTech), 1 µL dNTP (10mM) mix (NZYTech), 3 µL of each primer 5 pmol/ µL, 0.25 µL Taq polymerase (5 U/µL) (NZYTech), 1 µL of DNA template (NZYTech).
Polymerase Chain Reaction (PCR) was carried out using a Bio-Rad MJ Mini thermal cycler, following a standardized amplification protocol. The cycling conditions included an initial denaturation at 95°C for 3 min, followed by 25 cycles (denaturation at 95°C for 30 s, annealing at 62°C for 30 s, extension at 72°C for 90 s) and a final

extension at 72°C for 10 min. PCR products were visualized by agarose gel electrophoresis. Each PCR product (1µL) was mixed with 2 µL of GelRed and 2µL Gel Loading Solution (GLS) (0.25% bromophenol blue, 30% glycerol) and then examined under UV transillumination. Amplicons showing a clear band of expected size, against an appropriate molecular weight marker (Ladder III), were purified using ExoCleanUp FAST (VWR, Denmark), according to the manufacturer instructions. Purified products were stored at −20 °C until Sanger sequencing. Raw chromatograms were trimmed, and consensus FASTA sequences were assembled and inspected in Bioedit (v. 7.7.1) (Laranjo et al., 2008). After quality filtering and trimming, a final alignment of approximately 1400 bp was obtained for each isolate. Chimera screening was performed using UCHIME (Edgar et al., 2011) implemented in VSEARCH (v. 2.30.0) with default parameters (Rognes et al., 2016). The 16S rRNA sequences obtained were compared with reference sequences retrieved from the NCBI GenBank database. Phylogenetic reconstruction was performed in MEGA v.12 (S. Kumar et al., 2024) using MUSCLE as aligning algorithm and the Maximum Likelihood (ML) method under Hasegawa–Kishino–Yano model with a proportion of invariable sites (HKY+I) (Hasegawa et al., 1985; Luo et al., 2010), selected as the best-fit model based on the lowest Bayesian Information Criterion (BIC) score. Gaps and missing data were handled with the partial deletion (95% site coverage) option. The robustness of the resulting topology was assessed by bootstrap analysis with 1000 replicates (Laranjo et al., 2012). *Escherichia coli* (accession number X80725.1) and *Aeromonas media* (accession number X60410.2) were included as outgroup sequences.

6.2.7 Statistics

All experiments were performed at least in duplicate. Preliminary assays, including minimum inhibitory concentration (MIC) screening and morphological characterization on PAB, were conducted in duplicate to verify reproducibility. Growth index measurements under temperature, pH, and osmotic stress, as well as

metal removal assays determined by ICP–OES, were performed in triplicate to allow statistical evaluation. Data from triplicate experiments were analyzed using STATISTICA software version 12 (StatSoft Inc., Tulsa, OK, USA). Significant differences between groups were assessed using paired t-tests for two-group comparisons or one-way analysis of variance (ANOVA) followed by Tukey's HSD post-hoc test. For duplicate datasets, only descriptive statistics (mean ± standard deviation) were performed. Differences were considered statistically significant at $P < 0.05$.

6.3 Results

6.3.1 Morphological and biochemical characterization of Pseudomonas isolates

A total of 100 presumptive *Pseudomonas* isolates, previously recovered from polluted soils, were screened for multiple functional traits related to bioremediation capacity. All isolates were confirmed as Gram-negative, consistent with the taxonomic characteristics of the genus. Biochemical profiling revealed a predominance of oxidase-positive (87%) and catalase-positive (94%) phenotypes, reflecting the presence of active respiratory enzyme systems. Moreover, the strains predominantly exhibited an oxidative metabolism when tested on O/F medium, in line with their aerobic lifestyle.

6.3.2 Growth index under temperature and pH stress conditions

Growth Index (GI) was evaluated under different abiotic stress conditions at 24 h and 48 h (**Figure 6.1**). Under acidic conditions (**panels A–B**), isolates exhibited variable tolerance: growth was markedly reduced at pH 4.5, while it remained stable between pH 5.5 and 8.5, indicating broad pH adaptability with limited acid resistance. Temperature stress (**panels C–D**) revealed that most isolates maintained substantial growth at 15°C but were strongly inhibited at 37°C, confirming adaptation to moderate rather than elevated temperatures. After 48 h, growth generally improved across all

tested conditions, suggesting that most isolates are psychrotolerant and capable of recovering under suboptimal environments. It is worth mentioning that GI approach differs from the normally used method of growth rate and growth kinetic evaluation; in fact, Gi is a "static" measure as it gives a growth performance in some sampling points (for this research 24 and 48 h), and is used by authors a screening tool to reduce the number of assays in the case of many isolates, as reported elsewhere (Corbo et al., 2017). To summarize the multivariate behaviour of the isolates across all tested conditions, a principal component analysis (PCA) was performed using GI values at 24 h. The PCA loading plot (**Figure 6.2A**) revealed that Factor 1, which explained 47.44% of the total variance, was primarily influenced by growth at pH 4.5 and 37 °C. Factor 2 (16.64% of variance) was mainly driven by growth at pH 5.5, 7.5, 8.5 and 15°C.

Figure 6.1 Growth Index (GI) of *Pseudomonas* isolates at 24 (A, C) and 48 (B, D) hours under different stress conditions. Boxplots represent responses to thermal (15 °C, 37 °C) and pH (4.5 to 8.5) treatments, 25°C and pH 6.5 used as control. Outliers indicate high-performing or stress-sensitive strains.

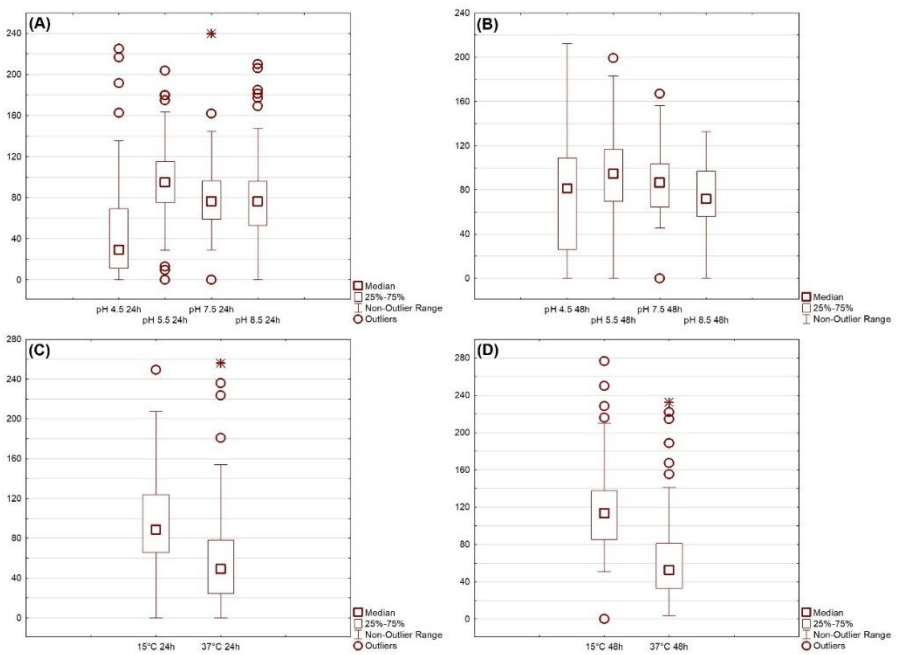

The PCA score plot (**Figure 6.2B**) showed that most isolates clustered near the origin, corresponding to neutral pH and temperature conditions. A few isolates (17, 28, 63, 79, 89) were positioned along the left-upper quadrant, indicating a tendency to better grow in pH 7.5-8.5 and 15°C conditions. The cluster formed by the isolates 45, 91 and 97 showed a better resistance to acid pH (4.5) and higher temperatures (37°C) meanwhile the cluster composed by the isolates 66 and 88 appeared at the far right of Factor 1, suggesting low resistance to both acid and thermal stress.

Figure 6.2. Principal Component Analysis (PCA) of growth responses of *Pseudomonas* isolates in liquid medium in different stress conditions, after 24 h of incubation. A loading plot indicating the contribution of each metal variable to the first two principal components. B score plot showing the distribution of isolates.

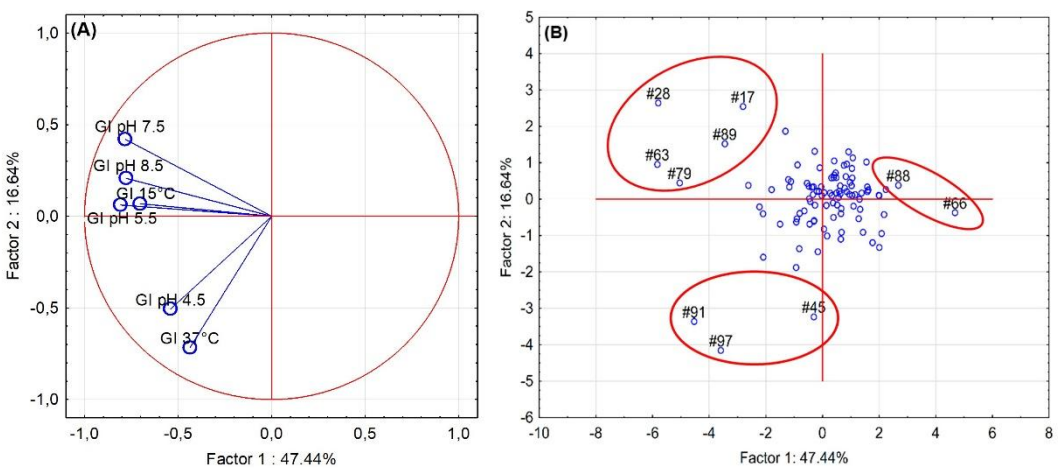

6.3.3 Osmotic stress tolerance under PEG conditions

The tolerance of *Pseudomonas* isolates to osmotic stress was evaluated in media supplemented with polyethylene glycol (PEG) at concentrations of 5 %, 10 %, 15 %, and 20 % (**Figure 6.3A–D**). Most isolates maintained normal growth at 5 % PEG (**Figure 6.3A**), showing little to no inhibition compared with control conditions. At 10 % PEG (**Figure 6.3B**), moderate inhibition appeared in several isolates, although the

majority still sustained positive growth indices, suggesting a general capacity to cope with mild osmotic pressure. When PEG concentration increased to 15 % (**Figure 6.3C**), growth performance markedly declined, with most isolates exhibiting negative GI values and only a limited number maintaining normal growth. At the highest concentration, 20 % PEG (**Figure 6.3D**), inhibition became widespread, and only a few isolates displayed measurable growth activity, confirming that severe osmotic stress significantly restricts proliferation.

Detailed isolate-specific responses and visual comparisons across PEG concentrations are provided in the Annex C (**Figure C6.1**). The heatmap representation allows quick identification of tolerant isolates such as FG36, FG54, FG91, and FG97, which consistently retained neutral or positive growth under high PEG levels, supporting their potential role as robust candidates for application in fluctuating or stress-prone soils.

Figure 6.3 Frequency distribution of bacterial growth responses under increasing concentrations of polyethylene glycol (PEG) as an osmotic stressor. Histograms represent the number of isolates showing specific growth deviations (Y-axis) under PEG concentrations of 5% (3A), 10% (3B), 15% (3C), and 20% (3D). The red curve indicates the fitted normal distribution for each dataset.

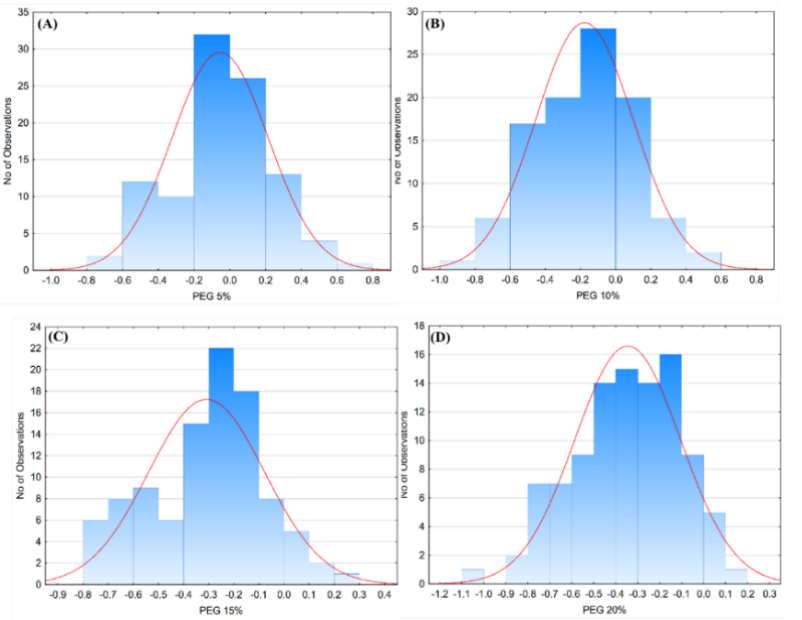

6.3.4 Growth performance in presence of HMs

The performance of resistance under HMs stress (Cu, As, Cr, Pb, Zn, 100mg/L per each) are resumed in the heatmap representation (**Figure 6.4**) after 48 h of incubation in liquid medium supplemented with HMs to highlight the different tolerance profiles. In **Figure 6.4A**, isolate FG31 displayed consistently good growth or biomass accumulation across Cu, As, Pb, and Zn evident in all corresponding heatmap rows. Isolate FG33 showed a similar trend, particularly under Cu and Pb exposure, while maintaining intermediate growth under Cr and As. Other isolates, such as FG29, stood out for their elevated growth under As stress, showing one of the highest GI values within the dataset. In contrast, isolates from FG17 to FG21 were characterized by low residual growth, under all HMs exposure. In the second group of isolates (from FG34 to FG66), shown in **Figure 6.4B**, heterogeneous growth patterns were observed across the five tested metals. Isolate FG50 displayed high GI values in all polluted conditions, suggesting consistent growth in these conditions. Isolates FG37 and FG40 maintained elevated OD levels in Cu, while their response to Zn was comparatively lower. Isolate FG43 showed strong growth in the presence of As, with reduced growth under other metals, indicating a selective response pattern. The remaining isolates in the group displayed mixed and variable behavior, with intermediate to low values more frequently observed under Cu and Pb. In the third group (from FG67 to FG100), represented in **Figure 6.4C**, isolate FG94 showed uniformly high growth across all metal conditions, with red intensities evident for Cu, As, Pb, Zn, and Cr. Isolates FG83 and FG89 exhibited elevated GI values particularly under As and Cu, respectively. Isolate FG79 demonstrated high growth in Cu and Cr, while showing moderate values for the remaining metals. Isolate FG74 had its highest growth under As, with lower responses for Zn and Cr. Isolate FG76 displayed poor growth under Zn exposure but maintained high GI levels in Cu and As conditions.

Figure 6.4 Heatmaps showing growth performance of *Pseudomonas* isolates after 48 h incubation in liquid medium supplemented with 100 mg/L of copper (Cu), arsenic (As), chromium (Cr), lead (Pb), and zinc (Zn). Growth was measured spectrophotometrically and expressed as Growth Index (GI). Values are color-coded from dark green (low GI) to dark red (high GI). A isolates from FG1 to FG33; B isolates from FG34 to FG66; C isolates from FG67 to FG100

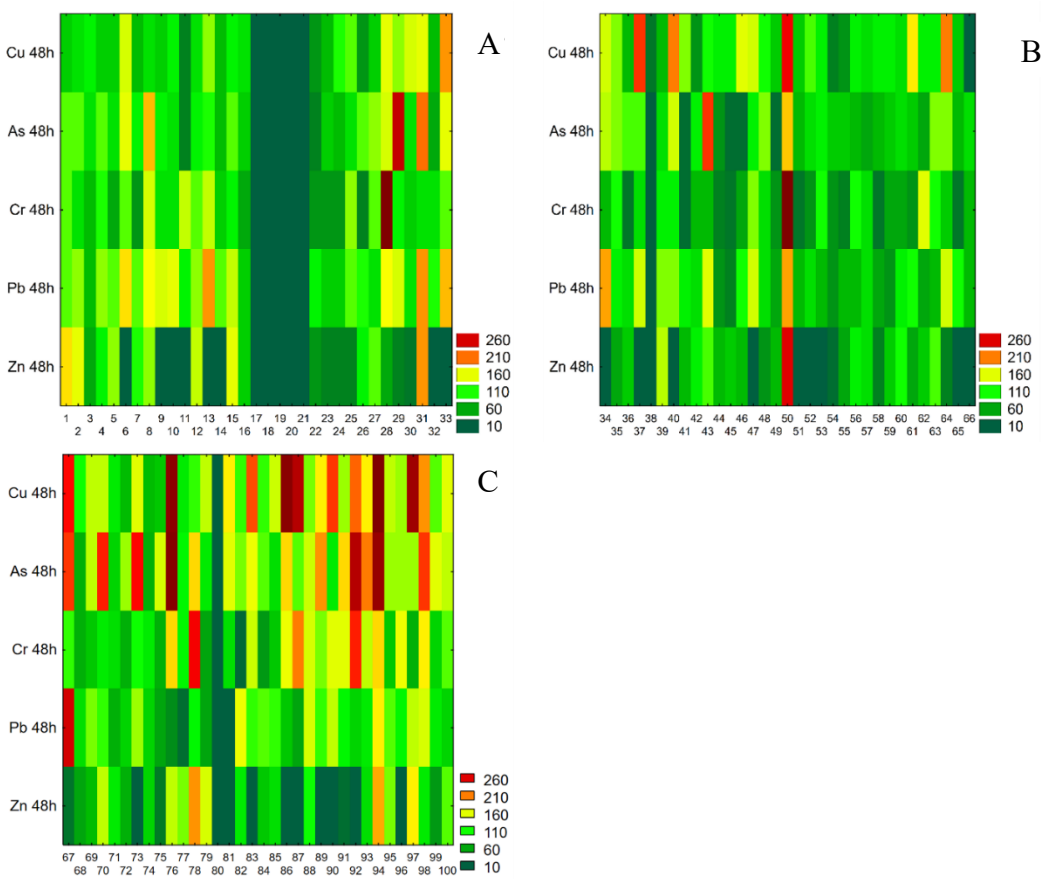

The isolates that exhibited a Growth Index (GI) >75% after incubation in liquid medium supplemented with 100 mg/L of HMs (Zn, Pb, Cr, As, Cu) were subsequently inoculated into medium containing 200 mg/L of the same HM. The same selection criterion (GI >75%) was then applied to identify candidates for further testing at 300 mg/L. Microorganisms not included in the subsequent tables (**Annex tables C6.2 and C6.3**) failed to reach the 75% GI threshold and were therefore excluded from the following steps.

At 200 mg/L (**Table C6.2**), several *Pseudomonas* isolates retained growth capacity above the 75% threshold in response to at least one metal. Among these, isolate FG1 displayed a broad tolerance profile, with GI values of 110.9% in Zn, 81.4% in Cr, 89.2% in As, and 139.7% in Cu, although Pb resulted in a lower GI (58.5%). Isolate FG5 exhibited consistent high growth across Zn (82.7%), Pb (84.8%), As (140.8%), and Cu (126.5%), while isolate 4 showed GI values above 100% in Zn (120.7%) and Pb (104.8%), but reduced growth in As (20.5%) and Cr (54.1%).

Isolate 7 stood out for its performance under Pb (141.4%), As (104.9%), and Cu (137.3%), despite lower growth under Zn and Cr. Other isolates (e.g. FG2 and FG15) exceeded the threshold in Cu (108.2% and 91.3%, respectively), with FG2 also performing in Pb (75.7%). These results suggest a subset of microorganisms with stable growth responses across metals, particularly As and Cu.

At 300 mg/L (**Table C6.3**), overall growth performance declined, yet several isolates retained GI values >75%. Isolate FG5 maintained elevated tolerance to As (108.4%) and moderate growth in Zn (72.0%), while isolate FG7 again showed high GI in Cu (126.5%) and sustained growth in As (85.2%). Strain FG4 exceeded the threshold only in Zn (81.7%).

Beyond these, additional isolates demonstrated specific resistance. Isolate FG28 retained high GI under Zn (89.1%), and FG32 responded well to Cu (91.4%). Isolate FG59 showed tolerance to As (90.9%), while FG94 and FG95 were among the few to remain above threshold in Pb (76.0% and 82.0%, respectively), with FG95 also achieving 98.0% in As.

6.3.5 Evaluation of heavy metal removal

Based on MIC screening, only isolates maintaining growth at or above 200 mg/L were retained for subsequent quantitative analyses. These selected strains were subjected to ICP–OES measurements to verify their metal-removal performance.

While the previously described GI evaluation focused on microbial growth in the presence of HMs, a confirmatory experiment was carried out to assess their actual metal removal capacity. Each isolate was inoculated in liquid medium supplemented with a single metal at defined concentrations: 200 mg/L for chromium and zinc, and 300 mg/L for copper, lead, and arsenic. Residual metal concentrations were quantified via ICP-OES and compared to initial values to estimate removal efficiency.

The results, summarized in **Table C6.4**, revealed marked variability among isolates in terms of residual concentration of HMs in supernatant, expressed as mg/L. For chromium, isolate FG43 showed the best performance (residual Cr: 56.3±0.14 mg/L), followed closely by isolate FG94 (57.3±0.05 mg/L). In the case of lead, isolate FG27 showed the highest removal (14.7±0.11 mg/L), followed by isolates FG76 (69.9±0.04 mg/L) and FG43 (30.0±0.08 mg/L). Zinc removal was most efficient in strain FG77 (42.1±0.12 mg/L), while for arsenic, isolates FG55 the lowest residual concentrations (0.22±0.08 mg/L). Copper removal was generally modest but isolates FG89 (81.7±0.11 mg/L) and FG94 (87.8±0.07 mg/L) performed better than others.

The HMs removal percentages were calculated relative to initial concentrations (**Table 6.1)**, and twenty-two best performing isolates were selected. There were three inclusion criteria, based on isolates performance I) removal of at least 3 HM; II) removal of at least two HM; III) >90% HM removal in at least one metal Several isolates showed broad removal capacity across different single-metal, making them promising candidates for bioremediation.

Among the top performers, isolate FG4 removed 68.5% of Cr, 75.3% of Zn, 66.4% of Cu, and 79.8% of As, indicating broad-spectrum activity. FG1 showed similar efficiency, particularly for Zn (76.3%), Cu (66.3%), Cr (69.5%), except for arsenic. FG15 was especially effective for As (80.2%), Cu (66.5%), and Zn (75.6%), while FG25 stood out for Pb (78.6%) and Cu (74.8%). Other notable isolates included FG76 (Pb>90%) and FG55 (As>95% 79.2%).

Table 6.1 Heavy metal removal, expressed as percentage, by selected *Pseudomonas* isolates in polluted liquid medium. Isolates performance thresholds are I) removal of at least 3 HM; II) removal of at least 2 HM; III) >90% HM removal in at least one metal.

Strain Code	Cr Removal (%)	Zn Removal (%)	Cu Removal (%)	As Removal (%)	Pb Removal (%)
FG1	69.31	76.28	66.33		
FG4	68.51	75.29	66.40	79.81	
FG12		74.99		79.54	
FG15		75.61	66.46	80.23	
FG25				74.71	78.65
FG43	71.88				90.01
FG48	67.28			79.45	
FG55				99.93	
FG57				79.77	89.02
FG61			67.27	79.49	
FG63	69.86		68.55	80.09	
FG73				80.08	82.75
FG76					93.45
FG77		78.96		80.28	
FG78		77.49		79.61	88.23
FG83				80.03	76.71
FG88	70.73			79.71	
FG90				80.59	82.10
FG92	68.02			80.93	80.21
FG94	71.41	68.63	70.73		
FG95		77.87			77.55
FG97		77.84	67.47	80.31	77.29

6.3.6 Genomic identification of potential bioremediating Pseudomonas spp.

The 16S rRNA gene sequences from 22 isolates identified as promising bioremediation candidates in vitro were deposited in GenBank; accession numbers are provided in **Table C6.5** BLAST alignment against the NCBI GenBank database revealed sequence identities ranging between 98.7% and 100% with reference strains belonging to the genus *Pseudomonas*, confirming genus-level assignment.

A phylogenetic tree was constructed using the Maximum Likelihood method with 1000 bootstrap replicates (**Figure 6.5**). The resulting topology resolved the isolates into several well-supported clades (bootstrap ≥92%), consistent with species-level classification.

Cluster I grouped isolates FG4, FG15 and FG25 with *Pseudomonas poae* (AB495132.1) and *Pseudomonas azotoformans* (OP164742.1), with sequence similarity >99%, suggesting their affiliation to the *P. fluorescens* group. FG1 and FG94 clustered tightly with *Pseudomonas reactans* (MK114600.1), sharing 99.1% similarity, while FG12 associated with *P. libanensis* (KP208622.1) at 99.2% identity. Isolates FG43 and FG76 formed a small sub-clade within this group, indicating a close phylogenetic relationship with *P. libanensis* (98.9% similarity) but potentially representing distinct haplotypes. Cluster II included FG88, FG78, FG55, FG77 and FG83, positioned within the *P. brenneri* complex (bootstrap 100, 99.0-99.3% similarity), while FG61, FG63, FG73, FG90 and FG57 grouped with *Pseudomonas proteolytica* (KU647672.1), showing 98.8-99.1% identity. FG48 was closely related to *P. alkylphenolica* (PQ781525.1), sharing 99.3% sequence identity. A distinct and robust clade (bootstrap ≥97%) included FG92, FG95 and FG97, which clustered with *Pseudomonas putida* reference strains (EU118779.1, PQ444060.1), with >99% sequence similarity, confirming their classification as *P. putida*.

Figure 6.5 Maximum Likelihood phylogenetic tree based on 16S rRNA gene sequences of 22 *Pseudomonas* isolates obtained from polluted soils in the Foggia area (Italy). Sequences were aligned with reference strains retrieved from NCBI GenBank, and evolutionary distances were computed using the Hasegawa, Kishino, and Yano model. Bootstrap values (1000 replicates) >90% are shown at the branch nodes. *Escherichia coli* (X80725.1) and *Aeromonas media* (X60410.2) were used as outgroups. Scale bar indicates 0.02 nucleotide substitutions per site.

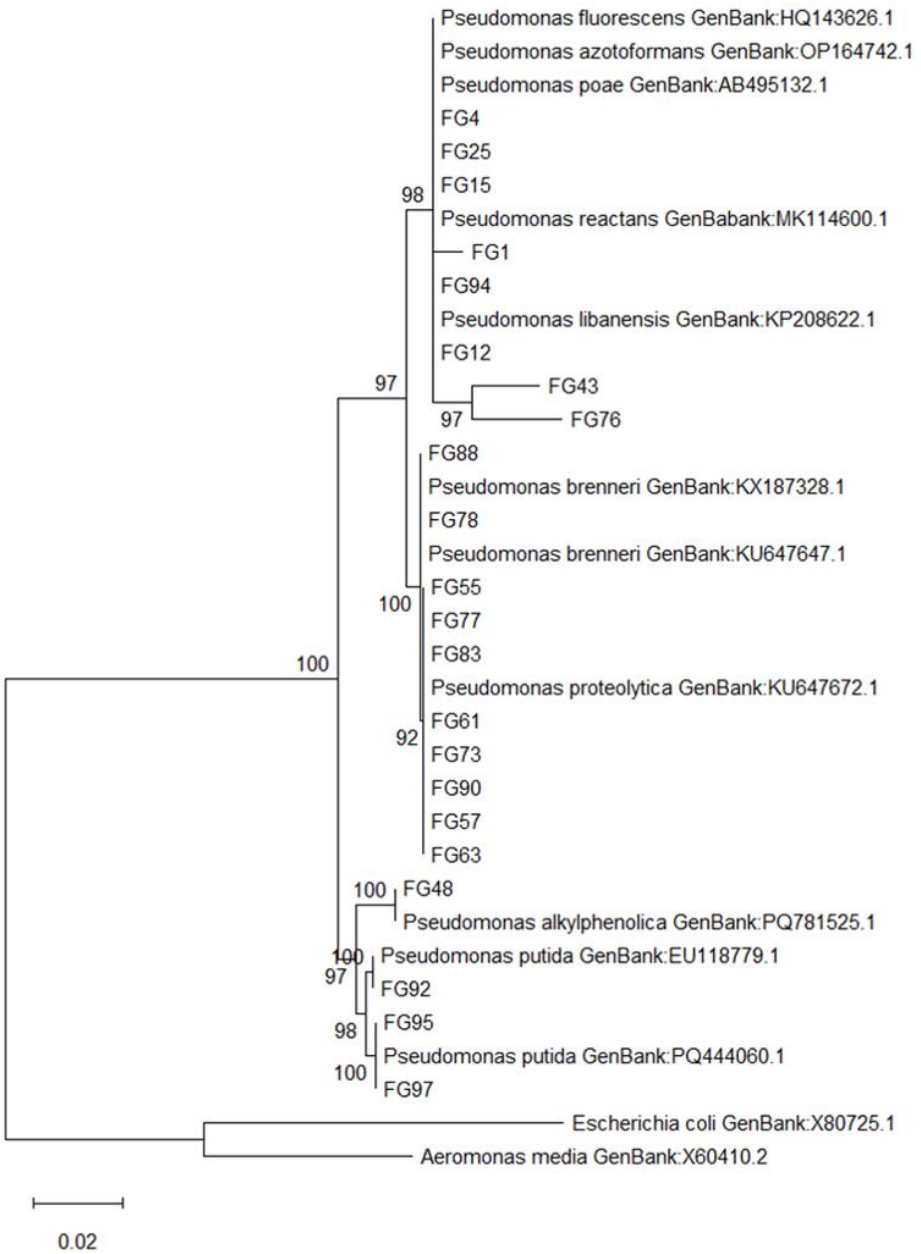

6.4 Discussion

This study provides a comprehensive phenotypic and genotypic characterization of *Pseudomonas* isolates from multi-metal contaminated soils, integrating growth performance under physico-chemical stresses, heavy metal tolerance, quantitative removal capacity, and phylogenetic structure. Microbial communities in polluted soils are continuously subjected to selective pressures such as metal toxicity, oxidative stress, nutrient imbalance, and co-contamination with organic pollutants, which act as evolutionary filters favoring microorganisms equipped with robust detoxification systems, efflux pumps, and regulatory networks for stress adaptation (Qi et al., 2022; Wang et al., 2023; Zou et al., 2024).These conditions may drive microevolutionary divergence within local balance between stress resistance and metabolic efficiency. *Pseudomonas* spp. is paradigmatic in this scenario, with large genomes, metabolic versatility (Silby et al., 2011), and complex regulons that allow them to survive and function under metal and redox stress (Gillieatt & Coleman, 2024). The isolates characterized here can therefore be interpreted not simply as survivors, but as functionally adapted members of the soil microbiota, actively contributing to natural attenuation and offering potential for bioaugmentation strategies.

Growth Index data confirmed that most isolates are psychrotolerant, sustaining growth at 15°C and thus ecologically suited for temperate soils, whereas growth was markedly reduced at 37°C, consistent with the thermal niche of psychrotolerant soil bacteria (Chauhan et al., 2023; Vollmer et al., 2023). Similar observations have been reported for *Pseudomonas* sp. B14-6, a cold-adapted isolate with optimal physiology at low temperatures (Kang et al., 2022), and for *P. fluorescens* strains showing morphological stress at 37°C (Kahli et al., 2022). This suggests that temperature acts as a stabilizing factor shaping metabolic specialization in these lineages. Psychrotolerance may confer an advantage under field conditions by ensuring enzymatic activity at low temperatures when metal solubility and mobility increase, thus sustaining bioremediation potential in cold or seasonal soils. A subset of strains maintained GI >

80 % at pH 4.5, suggesting acid-tolerant ecotypes; this aligns with the well-documented role of pH as a dominant driver of soil community composition, where acidification decreases α-diversity and selects for specialized acidophiles (Hu et al., 2024; Wang et al., 2022; Zhang, et al., 2024). PEG assays revealed heterogeneous osmotic tolerance, with some isolates retaining normal GI even under high osmotic pressure, an advantageous trait for bioaugmentation in arid or drought-prone soils (Bouremani et al., 2024). This aspect is particularly relevant given that many multi-contaminated soils are marginal or abandoned lands, frequently characterized by poor water retention and seasonal drought. Successful bioaugmentation in such environments requires strains capable of coping with osmotic stress and desiccation, as water scarcity can limit microbial activity and metal immobilization efficiency Under PEG-imposed stress, superior isolates likely activate sigma-factor (*AlgU*)-mediated regulons controlling membrane stability and stress response (Wang et al., 2024) and induce biosynthesis or uptake of compatible solutes (glycine betaine, proline, ectoine, trehalose) via pathways such as *betB* upregulation (Fan et al., 2024). EPS production and biofilm formation further protect cells by retaining water and buffering local water potential, thereby enhancing persistence under dry or osmotically challenging conditions (Chai et al., 2024; Karash & Yahr, 2022; Quan et al., 2022). It can therefore be hypothesized that osmotic tolerance indirectly contributes to metal resistance, since EPS matrices and compatible solutes also limit ionic toxicity and oxidative stress.

In parallel, heavy metal exposure imposes oxidative stress, and survival depends on activation of OxyR/SoxR regulons and antioxidant enzymes (catalase, peroxidase, superoxide dismutase), mechanisms recently documented in metal-resistant *Pseudomonas* (Da Cruz Nizer et al., 2021; Li et al., 2024; Méndez et al., 2022; Palma et al., 2005; Pang et al., 2023). MIC screening revealed tolerance up to 300 mg/L for Cu, Pb, and As, consistent with environmental *Pseudomonas* from mining soils (De Santis et al., 2025; Pramanik et al., 2021). Importantly, ICP-OES results confirmed

that tolerance translated into actual sequestration: FG4, FG15, FG76, and FG92 removed > 65 % of Cr, Zn, Cu, and As, and FG76 achieved > 90 % Pb removal, values that place our isolates among the most efficient bioremediators reported in the literature. Growth-based tolerance and metal-removal capacity were intentionally evaluated as distinct traits. MIC data served as preliminary screening to identify viable and resistant isolates, whereas ICP–OES assays provided quantitative evidence of detoxification potential. The absence of a strict linear correlation between MIC and removal efficiency confirms that tolerance and detoxification are governed by partially independent physiological pathways. Highly tolerant isolates likely rely on active efflux and intracellular detoxification, whereas moderately tolerant but high-removal strains depend on surface biosorption and EPS-mediated immobilization.

Comparable efficiencies have been documented for *Pseudomonas* spp. in a variety of systems: for instance, *Pseudomonas stutzeri* LBR achieved significant Pb removal in field soils through bioaugmentation, leading to a measurable decrease in exchangeable Pb fractions and reduced ecological risk indices after treatment (Ridene et al., 2023). In another study, *Pseudomonas alcaliphila* NEWG-2 removed up to 96.6 % of Cr(VI) at 200 mg/L using alginate-immobilized cells, with FTIR and SEM–EDS analyses confirming biosorption via carboxyl, hydroxyl, and amide groups and partial bioreduction of Cr(VI) to less toxic Cr(III) (El-Naggar et al., 2020). Similarly, *Pseudomonas veronii* 2E displayed high Cu biosorption capacity (71.4 % in 24 h) and maintained performance in continuous packed-bed systems, with successful metal recovery via desorption and potential for process recycling (Busnelli & Vullo, 2022). Together, these studies support the view that the metal removal efficiencies achieved by our isolates are not only quantitatively significant but also mechanistically consistent with established biosorption and bioaccumulation processes observed in high-performance *Pseudomonas* strains. These outcomes are consistent with a composite mechanism involving EPS-mediated biosorption, intracellular bioaccumulation, and microbially induced carbonate precipitation (MICP). It can

therefore be hypothesized that FG76 and FG92, characterized by the highest Pb and Cu removals, exploit a combination of EPS-mediated sequestration and MICP processes to achieve rapid and stable immobilization, while FG4 and FG15 may rely more on intracellular accumulation mechanisms supported by membrane-bound reductases. Functional groups within EPS provide abundant cation-binding sites (Balíková et al., 2022), while MICP has been shown to lower Cd bioavailability and is increasingly recognized as a field-viable remediation strategy (Zhang et al., 2023). Beyond physiological mechanisms, genomic determinants such as *czc, cad, cop, ars,* and *mer* operons likely underpin the observed broad-spectrum tolerance, with cross-regulatory interactions (e.g., Czc-Cad systems in *P. putida* KT2440) enhancing multi-metal resilience (Liu et al., 2021; Sánchez-Corona et al., 2025). The phylogenetic reconstruction was performed with the sole aim of confirming the taxonomic affiliation of the isolates within the *Pseudomonas* genus. Given the high intra-specific variability typical of *Pseudomonas*, functional traits such as tolerance and detoxification efficiency are often strain-dependent and cannot be reliably inferred from phylogenetic proximity. The presence of multiple phylogenetic clades among our isolates indicates functional redundancy, a well-recognized stabilizing factor that buffers microbial ecosystem functions under disturbance (Chen et al., 2024; Khidr et al., 2025; Lanari et al., 2022; Yang et al., 2024). This redundancy suggests that metal-removal activity would likely persist even if individual strains were inhibited, consistent with evidence that multi-strain bacterial consortia outperform single isolates for multi-metal bioremediation and enhance system resilience (Khidr et al., 2025; Qattan, 2025). In this perspective, assembling consortia combining tolerant and high-removal isolates could maximize efficiency while minimizing ecological risk, a hypothesis that warrants mesocosm validation. Overall, the convergence of anthropogenic-stress adaptation, psychrotolerance, osmotic and oxidative stress resilience, high MICs with quantitatively verified removals, EPS/MICP-driven immobilization, genomic determinants of resistance, and clade-level redundancy

positions FG4, FG15, FG76, and FG92 as excellent candidates for pilot-scale bioaugmentation. Although the tested isolates demonstrated broad tolerance across individual HMs, these results do not prove a true multi-metal tolerance under simultaneous exposure. The experiments were performed under single-metal conditions to ensure reproducibility and to disentangle individual metal effects. However, in natural environments, metals often co-occur and may interact additively, antagonistically, or synergistically, influencing both toxicity and detoxification dynamics. Future work will therefore test binary and ternary metal combinations at environmentally relevant ratios to determine whether tolerance and removal capacities are maintained or modified under mixed-metal stress. Such experiments will provide a more realistic evaluation of the ecological performance and biotechnological applicability of the selected strains. Future research should include mechanistic validation (EPS, siderophore, osmolyte, and antioxidant assays; metal speciation), genome-wide screening for resistance loci and ARGs (Sánchez-Corona et al., 2025), design of complementary consortia, mesocosm trials to assess persistence and competitiveness, and immobilization on carriers such as biochar or alginate to maximize survival and operational reusability (Hu et al., 2025; Jhariya et al., 2025).

This study provides an integrated assessment of the adaptive, physiological, and phylogenetic traits of *Pseudomonas* isolates recovered from multi-metal contaminated soils. The combined use of phenotypic screening, metal tolerance assays, and molecular identification enabled the characterization of strains exhibiting diverse stress-response profiles and significant detoxification potential. The results underline the ecological plasticity of *Pseudomonas*, a genus widely recognized for its metabolic versatility, environmental resilience, and ability to persist in complex and contaminated matrices.

The findings support the view that native *Pseudomonas* populations represent an important biological resource for environmentally friendly soil restoration strategies. Their ability to tolerate and remove different metals suggests a promising role in the

implementation of bioaugmentation and biostabilization processes aimed at reducing metal mobility and bioavailability. In this perspective, understanding the interplay between tolerance mechanisms, metal-binding structures, and phylogenetic background may facilitate the rational selection of efficient strains and the design of tailored microbial consortia.

Future research should focus on genome-level mapping of resistance operons and co-localized ARGs, detailed metabolite assays (EPS, siderophores, osmolytes, antioxidants), pilot-scale mesocosm trials to assess persistence and competitiveness, and immobilization of selected isolates on carriers such as biochar or alginate to enhance survival, reusability, and operational stability.

References

Alengebawy, A., Abdelkhalek, S. T., Qureshi, S. R., & Wang, M.-Q. (2021). Heavy metals and pesticides toxicity in agricultural soil and plants: Ecological risks and human health implications. *Toxics*, *9*(3), 42. https://doi.org/10.3390/toxics9030042

Balíková, K., Vojtková, H., Duborská, E., Kim, H., Matúš, P., & Urík, M. (2022). Role of exopolysaccharides of *Pseudomonas* in heavy metal removal and other remediation strategies. *Polymers*, *14*(20), 4253. https://doi.org/10.3390/polym14204253

Bevilacqua, A., Corbo, M. R., & Sinigaglia, M. (2009). Selection of yeasts as starter cultures for table olives: A step-by-step procedure. *Frontiers in Microbiology*, *3*. https://doi.org/10.3389/fmicb.2012.00194

Bora, B., Kauser, H., & Geed, S. R. (2025). Bioremediation strategies for xenobiotic degradation in petroleum-impacted industrial ecosystems: Practical challenges and future directions. *Journal of Water Process Engineering*, *70*, 106877. https://doi.org/10.1016/j.jwpe.2024.106877

Bouremani, N., Cherif-Silini, H., Silini, A., Rabhi, N. E. H., Bouket, A. C., & Belbahri, L. (2024). Osmotolerant plant growth promoting bacteria mitigate adverse effects of drought stress on wheat growth. *AIMS Microbiology*, *10*(3), 507–541. https://doi.org/10.3934/microbiol.2024025

Briffa, J., Sinagra, E., & Blundell, R. (2020). Heavy metal pollution in the environment and their toxicological effects on humans. *Heliyon*, *6*(9), e04691. https://doi.org/10.1016/j.heliyon.2020.e04691

Busnelli, M. P., & Vullo, D. L. (2022). Copper removal mediated by *Pseudomonas veronii* 2E in batch and continuous reactors. *Journal of Sustainable Development of Energy, Water and Environment Systems*, *10*(1), 1–16. https://doi.org/10.13044/j.sdewes.d8.0351

Chai, L., Zaburdaev, V., & Kolter, R. (2024). How bacteria actively use passive physics to make biofilms. *Proceedings of the National Academy of Sciences*, *121*(40), e2403842121. https://doi.org/10.1073/pnas.2403842121

Chauhan, M., Kimothi, A., Sharma, A., & Pandey, A. (2023). Cold adapted *Pseudomonas*: Ecology to biotechnology. *Frontiers in Microbiology*, *14*, 1218708. https://doi.org/10.3389/fmicb.2023.1218708

Chen, H., Lei, L., Li, Z., Zhou, H., Cheng, H., Chen, Z., Wang, Y., & Wang, Y. (2024). Redundancy and resilience of microbial community under aniline stress during wastewater treatment. *Science of The Total Environment*, *951*, 175822. https://doi.org/10.1016/j.scitotenv.2024.175822

Coelho, L. M., Rezende, H. C., Coelho, L. M., De Sousa, P. A. R., Melo, D. F. O., & Coelho, N. M. M. (2015). Bioremediation of polluted waters using microorganisms. In N. Shiomi (A c. Di), *Advances in Bioremediation of Wastewater and Polluted Soil*. InTech. https://doi.org/10.5772/60770

Corbo, M. R., Bevilacqua, A., Speranza, B., Gallo, M., Campaniello, D., & Sinigaglia, M. (2017). Selection of wild lactic acid bacteria for sausages: Design of a selection protocol combining statistic tools, technological and functional properties. *LWT - Food Science and Technology*, *81*, 144–152. https://doi.org/10.1016/j.lwt.2017.03.051

Da Cruz Nizer, W. S., Inkovskiy, V., Versey, Z., Strempel, N., Cassol, E., & Overhage, J. (2021). Oxidative stress response in *Pseudomonas aeruginosa*. *Pathogens*, *10*(9), 1187. https://doi.org/10.3390/pathogens10091187

De Santis, A., Bevilacqua, A., Racioppo, A., Speranza, B., Corbo, M. R., Altieri, C., & Sinigaglia, M. (2025). A preliminary investigation into heavy metal tolerance in *Pseudomonas* isolates: Does the isolation site have an effect? *Agriculture*, *15*(15), 1692. https://doi.org/10.3390/agriculture15151692

Edgar, R. C., Haas, B. J., Clemente, J. C., Quince, C., & Knight, R. (2011). UCHIME improves sensitivity and speed of chimera detection. *Bioinformatics*, *27*(16), 2194–2200. https://doi.org/10.1093/bioinformatics/btr381

El-Naggar, N. E.-A., El-khateeb, A. Y., Ghoniem, A. A., El-Hersh, M. S., & Saber, W. I. A. (2020). Innovative low-cost biosorption process of Cr6+ by *Pseudomonas alcaliphila* NEWG-2. *Scientific Reports*, *10*(1), 14043. https://doi.org/10.1038/s41598-020-70473-5

Fan, M., Tan, S., Wang, W., & Zhang, X. (2024). Improvement in salt tolerance ability of *Pseudomonas putida* KT2440. *Biology*, *13*(6), 404. https://doi.org/10.3390/biology13060404

Gillieatt, B. F., & Coleman, N. V. (2024). Unravelling the mechanisms of antibiotic and heavy metal resistance co-selection in environmental bacteria. *FEMS Microbiology Reviews*, *48*(4), fuae017. https://doi.org/10.1093/femsre/fuae017

Hasegawa, M., Kishino, H., & Yano, T. (1985). Dating of the human-ape splitting by a molecular clock of mitochondrial DNA. *Journal of Molecular Evolution*, *22*(2), 160–174. https://doi.org/10.1007/BF02101694

Hu, Y., Wang, C., & Wang, Y. (2025). Biochar-immobilized *Pseudomonas aeruginosa* enhances copper remediation and growth of chinese milk vetch (*Astragalus sinicus*). *Microorganisms*, *13*(8), 1793. https://doi.org/10.3390/microorganisms13081793

Hu, Z., Delgado-Baquerizo, M., Fanin, N., Chen, X., Zhou, Y., Du, G., Hu, F., Jiang, L., Hu, S., & Liu, M. (2024). Nutrient-induced acidification modulates soil biodiversity-function relationships. *Nature Communications*, *15*(1), 2858. https://doi.org/10.1038/s41467-024-47323-3

International Organization for Standardization. ISO 14870:2001. (2001). *Soil Quality-Extraction of Trace Elements by Buffered DTPA Solution*.

Jhariya, U., Chien, M.-F., Umetsu, M., & Kamitakahara, M. (2025). New insights into immobilized bacterial systems for removal of heavy metals from wastewater. *International Journal of Environmental Science and Technology*, *22*(9), 8319–8334. https://doi.org/10.1007/s13762-025-06369-6

Kahli, H., Béven, L., Grauby-Heywang, C., Debez, N., Gammoudi, I., Moroté, F., Sbartai, H., & Cohen-Bouhacina, T. (2022). Impact of growth conditions on *Pseudomonas fluorescens* morphology characterized by atomic force microscopy. *International Journal of Molecular Sciences*, *23*(17), 9579. https://doi.org/10.3390/ijms23179579

Kang, M., Choi, T.-R., Ahn, S., Heo, H. Y., Kim, H., Lee, H. S., Lee, Y. K., Joo, H.-S., Yune, P. S., Kim, W., & Yang, Y.-H. (2022). Arctic psychrotolerant *Pseudomonas* sp. B14-6 exhibits temperature-dependent susceptibility to aminoglycosides. *Antibiotics*, *11*(8), 1019. https://doi.org/10.3390/antibiotics11081019

Karash, S., & Yahr, T. L. (2022). Genome-wide identification of *Pseudomonas aeruginosa* genes important for desiccation tolerance on inanimate surfaces. *mSystems*, *7*(3), e00114-22. https://doi.org/10.1128/msystems.00114-22

Khan, D., Kabiraj, A., Roy, R. K., Let, M., Majhi, K., & Bandopadhyay, R. (2022). Bioremediation of heavy metals by metagenomic approaches. In V. Kumar & I. S. Thakur (A c. Di), *Omics*

Insights in Environmental Bioremediation (pp. 393–413). Springer Nature Singapore. https://doi.org/10.1007/978-981-19-4320-1_17

Khidr, R., Qurbani, K., Muhammed, V., Salim, S., Abdulla, S., & Wsw, H. (2025). Synergistic effects of indigenous bacterial consortia on heavy metal tolerance and reduction. *Environmental Geochemistry and Health*, *47*(3), 79. https://doi.org/10.1007/s10653-025-02392-1

Kumar, S., Stecher, G., Suleski, M., Sanderford, M., Sharma, S., & Tamura, K. (2024). MEGA12: Molecular Evolutionary Genetic Analysis version 12 for adaptive and green computing. *Molecular Biology and Evolution*, *41*(12), msae263. https://doi.org/10.1093/molbev/msae263

Kumar, V., Rout, C., Singh, J., Saharan, Y., Goyat, R., Umar, A., Akbar, S., & Baskoutas, S. (2023). A review on the clean-up technologies for heavy metal ions contaminated soil samples. *Heliyon*, *9*(5), e15472. https://doi.org/10.1016/j.heliyon.2023.e15472

Lanari, M., Horta, P. A., & Da Silva Copertino, M. (2022). Functional redundancy and stability in a subtidal macroalgal community in the Southwestern Atlantic coast. *Marine Environmental Research*, *173*, 105519. https://doi.org/10.1016/j.marenvres.2021.105519

Laranjo, M., Alexandre, A., Rivas, R., VelÃ¡zquez, E., Young, J. P. W., & Oliveira, S. (2008). Chickpea rhizobia symbiosis genes are highly conserved across multiple *Mesorhizobium* species: Mesorhizobia symbiosis genes are conserved. *FEMS Microbiology Ecology*, *66*(2), 391–400. https://doi.org/10.1111/j.1574-6941.2008.00584.x

Laranjo, M., Machado, J., Young, J. P. W., & Oliveira, S. (2004). High diversity of chickpea *Mesorhizobium* species isolated in a Portuguese agricultural region. *FEMS Microbiology Ecology*, *48*(1), 101–107. https://doi.org/10.1016/j.femsec.2003.12.015

Laranjo, M., Young, J. P. W., & Oliveira, S. (2012). Multilocus sequence analysis reveals multiple symbiovars within *Mesorhizobium* species. *Systematic and Applied Microbiology*, *35*(6), 359–367. https://doi.org/10.1016/j.syapm.2012.06.002

Li, C., Wei, Z., He, X., He, H., Liu, Y., Zuo, Y., Xiao, H., Wang, Y., Shen, X., & Zhu, L. (2024). OxyR-regulated T6SS functions in coordination with siderophore to resist oxidative stress. *Microbiology Spectrum*, *12*(2), e03231-23. https://doi.org/10.1128/spectrum.03231-23

Liu, H., Zhang, Y., Wang, Y., Xie, X., & Shi, Q. (2021). The connection between CzC and CAD systems involved in cadmium resistance in *Pseudomonas putida*. *International Journal of Molecular Sciences*, *22*(18), 9697. https://doi.org/10.3390/ijms22189697

Luo, A., Qiao, H., Zhang, Y., Shi, W., Ho, S. Y., Xu, W., Zhang, A., & Zhu, C. (2010). Performance of criteria for selecting evolutionary models in phylogenetics: A comprehensive study based on simulated datasets. *BMC Evolutionary Biology*, *10*(1), 242. https://doi.org/10.1186/1471-2148-10-242

Manikandan, S. K., & Nair, V. (2023). Developing a biocatalyst showcasing the synergistic effect of rice husk biochar and bacterial cells for the removal of heavy metals. *New Journal of Chemistry*, *47*(46), 21199–21213. https://doi.org/10.1039/D3NJ02889E

Méndez, V., Rodríguez-Castro, L., Durán, R. E., Padrón, G., & Seeger, M. (2022). The OxyR and SoxR transcriptional regulators are involved in a broad oxidative stress response in *Paraburkholderia xenovorans* LB400. *Biological Research*, *55*(1), 7. https://doi.org/10.1186/s40659-022-00373-7

Mishra, A., Saxena, A., & Singh, S. P. (2019). Isolation and characterization of microbial strains from refinery effluent to screen their bioremediation potential. *Journal of Pure and Applied Microbiology*, *13*(4), 2325–2332. https://doi.org/10.22207/JPAM.13.4.48

Mitra, S., Chakraborty, A. J., Tareq, A. M., Emran, T. B., Nainu, F., Khusro, A., Idris, A. M., Khandaker, M. U., Osman, H., Alhumaydhi, F. A., & Simal-Gandara, J. (2022). Impact of heavy metals on the environment and human health: Novel therapeutic insights to counter the toxicity. *Journal of King Saud University - Science*, *34*(3), 101865. https://doi.org/10.1016/j.jksus.2022.101865

Monga, A., Fulke, A. B., Gaud, A., Sharma, A., Ram, A., & Dasgupta, D. (2022). Isolation and identification of novel chromium tolerant bacterial strains from a heavy metal polluted urban creek: An assessment of bioremediation efficiency and flocculant production. *Thalassas: An International Journal of Marine Sciences*, *38*(2), 1233–1244. https://doi.org/10.1007/s41208-022-00458-w

Palma, M., Zurita, J., Ferreras, J. A., Worgall, S., Larone, D. H., Shi, L., Campagne, F., & Quadri, L. E. N. (2005). *Pseudomonas aeruginosa* SoxR does not conform to the archetypal paradigm for SoxR-dependent regulation of the bacterial oxidative stress adaptive response. *Infection and Immunity*, *73*(5), 2958–2966. https://doi.org/10.1128/IAI.73.5.2958-2966.2005

Pande, V., Pandey, S. C., Sati, D., Bhatt, P., & Samant, M. (2022). Microbial interventions in bioremediation of heavy metal contaminants in agroecosystem. *Frontiers in Microbiology*, *13*, 824084. https://doi.org/10.3389/fmicb.2022.824084

Pang, X., Chen, C., Sun, J., Zhan, H., Xiao, Y., Cai, J., Yu, X., Liu, Y., Long, L., & Yang, G. (2023). Effects of complex pollution by microplastics and heavy metals on soil physicochemical properties and microbial communities under alternate wetting and drying conditions. *Journal of Hazardous Materials*, *458*, 131989. https://doi.org/10.1016/j.jhazmat.2023.131989

Perković, S., Paul, C., Vasić, F., & Helming, K. (2022). Human health and soil health risks from heavy metals, micro(nano)plastics, and antibiotic resistant bacteria in agricultural soils. *Agronomy*, *12*(12), 2945. https://doi.org/10.3390/agronomy12122945

Popoola, O. J., Ogundele, O. D., Ladapo, E. A., & Senbore, S. (2024). The impact of heavy metal contamination in soils on soil microbial communities and its potential health risks for humans. In S. A. Aransiola, H. I. Atta, & N. R. Maddela (A c. Di), *Soil Microbiome in Green Technology Sustainability* (pp. 351–375). Springer Nature Switzerland. https://doi.org/10.1007/978-3-031-71844-1_15

Porres, J. M., & Stanyon, R. E. (1974). One-tube Oxidation-Fermentation Test. *American Journal of Clinical Pathology*, *61*(3), 368–374. https://doi.org/10.1093/ajcp/61.3.368

Pramanik, K., Mandal, S., Banerjee, S., Ghosh, A., Maiti, T. K., & Mandal, N. C. (2021). Unraveling the heavy metal resistance and biocontrol potential of *Pseudomonas* sp. K32 strain facilitating rice seedling growth under Cd stress. *Chemosphere*, *274*, 129819. https://doi.org/10.1016/j.chemosphere.2021.129819

Qattan, S. Y. A. (2025). Harnessing bacterial consortia for effective bioremediation: Targeted removal of heavy metals, hydrocarbons, and persistent pollutants. *Environmental Sciences Europe*, *37*(1), 85. https://doi.org/10.1186/s12302-025-01103-y

Qi, Q., Hu, C., Lin, J., Wang, X., Tang, C., Dai, Z., & Xu, J. (2022). Contamination with multiple heavy metals decreases microbial diversity and favors generalists as the keystones in microbial occurrence networks. *Environmental Pollution*, *306*, 119406. https://doi.org/10.1016/j.envpol.2022.119406

Quan, K., Hou, J., Zhang, Z., Ren, Y., Peterson, B. W., Flemming, H.-C., Mayer, C., Busscher, H. J., & Van Der Mei, H. C. (2022). Water in bacterial biofilms: Pores and channels, storage and transport functions. *Critical Reviews in Microbiology*, *48*(3), 283–302. https://doi.org/10.1080/1040841X.2021.1962802

Qurbani, K., Khdir, K., Sidiq, A., Hamzah, H., Hussein, S., Hamad, Z., Abdulla, R., Abdulla, B., & Azizi, Z. (2022). *Aeromonas sobria* as a potential candidate for bioremediation of heavy metal from contaminated environments. *Scientific Reports*, *12*(1), 21235. https://doi.org/10.1038/s41598-022-25781-3

Rahman, Z., & Singh, V. P. (2020). Bioremediation of toxic heavy metals (THMs) contaminated sites: Concepts, applications and challenges. *Environmental Science and Pollution Research*, *27*(22), 27563–27581. https://doi.org/10.1007/s11356-020-08903-0

Rai, P. K., Lee, S. S., Zhang, M., Tsang, Y. F., & Kim, K.-H. (2019). Heavy metals in food crops: Health risks, fate, mechanisms, and management. *Environment International*, *125*, 365–385. https://doi.org/10.1016/j.envint.2019.01.067

Rashid, A., Schutte, B. J., Ulery, A., Deyholos, M. K., Sanogo, S., Lehnhoff, E. A., & Beck, L. (2023). Heavy metal contamination in agricultural soil: Environmental pollutants affecting crop health. *Agronomy*, *13*(6), 1521. https://doi.org/10.3390/agronomy13061521

Ridene, S., Werfelli, N., Mansouri, A., Landoulsi, A., & Abbes, C. (2023). Bioremediation potential of consortium *Pseudomonas stutzeri* LBR and *Cupriavidus metallidurans* LBJ in soil polluted by lead. *PLOS ONE*, *18*(6), e0284120. https://doi.org/10.1371/journal.pone.0284120

Rognes, T., Flouri, T., Nichols, B., Quince, C., & Mahé, F. (2016). VSEARCH: A versatile open source tool for metagenomics. *PeerJ*, *4*, e2584. https://doi.org/10.7717/peerj.2584

Roy, R., Samanta, S., Pandit, S., Naaz, T., Banerjee, S., Rawat, J. M., Chaubey, K. K., & Saha, R. P. (2024). An overview of bacteria-mediated heavy metal bioremediation strategies. *Applied Biochemistry and Biotechnology*, *196*(3), 1712–1751. https://doi.org/10.1007/s12010-023-04614-7

Sánchez-Corona, C. G., Gonzalez-Avila, L. U., Hernández-Cortez, C., Rojas-Vargas, J., Castro-Escarpulli, G., & Castelán-Sánchez, H. G. (2025). Impact of heavy metal and resistance genes on antimicrobial resistance: Ecological and public health implications. *Genes*, *16*(6), 625. https://doi.org/10.3390/genes16060625

Satyapal, G. K., Haque, R., & Kumar, N. (2024). Gamma irradiation in modulating arsenic bioremediation potential of *Pseudomonas* sp. AK1 and AK9. *International Journal of Radiation Biology*, *100*(6), 934–939. https://doi.org/10.1080/09553002.2024.2345137

Sazykin, I., Khmelevtsova, L., Azhogina, T., & Sazykina, M. (2023). Heavy metals influence on the bacterial community of soils: A review. *Agriculture*, *13*(3), 653. https://doi.org/10.3390/agriculture13030653

Sharma, P., Bano, A., Singh, S. P., Dubey, N. K., Chandra, R., & Iqbal, H. M. N. (2022). Recent advancements in microbial-assisted remediation strategies for toxic contaminants. *Cleaner Chemical Engineering*, *2*, 100020. https://doi.org/10.1016/j.clce.2022.100020

Silby, M. W., Winstanley, C., Godfrey, S. A. C., Levy, S. B., & Jackson, R. W. (2011). *Pseudomonas* genomes: Diverse and adaptable. *FEMS Microbiology Reviews*, *35*(4), 652–680. https://doi.org/10.1111/j.1574-6976.2011.00269.x

Singh, P., Singh, R. K., Zhou, Y., Wang, J., Jiang, Y., Shen, N., Wang, Y., Yang, L., & Jiang, M. (2022). Unlocking the strength of plant growth promoting *Pseudomonas* in improving crop productivity in normal and challenging environments: A review. *Journal of Plant Interactions*, *17*(1), 220–238. https://doi.org/10.1080/17429145.2022.2029963

Steel, K. J. (1961). The oxidase reaction as a taxonomic tool. *Journal of General Microbiology*, *25*(2), 297–306. https://doi.org/10.1099/00221287-25-2-297

Su, Y., Sun, S., Liu, Q., Zhao, C., Li, L., Chen, S., Chen, H., Wang, Y., & Tang, F. (2022). Characterization of the simultaneous degradation of pyrene and removal of Cr(VI) by a bacteria consortium YH. *Science of The Total Environment*, *853*, 158388. https://doi.org/10.1016/j.scitotenv.2022.158388

Sundarraj, S., Sudarmani, D. N. P., Samuel, P., & Sevarkodiyone, S. P. (2023). Bioremediation of hexavalent chromium by transformation of *Escherichia coli* DH5α with chromate reductase (ChrR) genes of *Pseudomonas putida* isolated from tannery effluent. *Journal of Applied Microbiology*, *134*(1), lxac019. https://doi.org/10.1093/jambio/lxac019

Tittsler, R. P., & Sandholzer, L. A. (1936). The use of semi-solid agar for the detection of bacterial motility. *Journal of Bacteriology*, *31*(6), 575–580. https://doi.org/10.1128/jb.31.6.575-580.1936

Vollmer, T., Knabbe, C., & Dreier, J. (2023). Dual-temperature microbiological control of cellular products: A potential impact for bacterial screening of platelet concentrates? *Microorganisms*, *11*(9), 2350. https://doi.org/10.3390/microorganisms11092350

Wang, J., Wang, Y., Lu, S., Lou, H., Wang, X., & Wang, W. (2024). AlgU mediates hyperosmotic tolerance in *Pseudomonas protegens* SN15-2 by regulating membrane stability, ROS scavenging, and osmolyte synthesis. *Applied and Environmental Microbiology*, *90*(8), e00596-24. https://doi.org/10.1128/aem.00596-24

Wang, T., Cao, X., Chen, M., Lou, Y., Wang, H., Yang, Q., Pan, H., & Zhuge, Y. (2022). Effects of soil acidification on bacterial and fungal communities in the Jiaodong peninsula, northern China. *Agronomy*, *12*(4), 927. https://doi.org/10.3390/agronomy12040927

Wang, X., Dai, Z., Zhao, H., Hu, L., Dahlgren, R. A., & Xu, J. (2023). Heavy metal effects on multitrophic level microbial communities and insights for ecological restoration of an abandoned electroplating factory site. *Environmental Pollution*, *327*, 121548. https://doi.org/10.1016/j.envpol.2023.121548

Whittenbury, R. (1964). Hydrogen peroxide formation and catalase activity in the lactic acid bacteria. *Journal of General Microbiology*, *35*(1), 13–26. https://doi.org/10.1099/00221287-35-1-13

Yang, X., Huang, X., Cheng, Z., Li, S., Mahjoob, H. A., Xu, J., & He, Y. (2024). Response of soil general and specific functions following loss of microbial diversity: A review. *Soil Security*, *15*, 100151. https://doi.org/10.1016/j.soisec.2024.100151

Young, J. P., Downer, H. L., & Eardly, B. D. (1991). Phylogeny of the phototrophic *Rhizobium* strain BTAi1 by polymerase chain reaction-based sequencing of a 16S rRNA gene segment. *Journal of Bacteriology*, *173*(7), 2271–2277. https://doi.org/10.1128/jb.173.7.2271-2277.1991

Zhang, H., Jiang, N., Zhang, S., Zhu, X., Wang, H., Xiu, W., Zhao, J., Liu, H., Zhang, H., & Yang, D. (2024). Soil bacterial community composition is altered more by soil nutrient availability than pH following long-term nutrient addition in a temperate steppe. *Frontiers in Microbiology*, *15*, 1455891. https://doi.org/10.3389/fmicb.2024.1455891

Zhang, W., Zhang, H., Xu, R., Qin, H., Liu, H., & Zhao, K. (2023). Heavy metal bioremediation using microbially induced carbonate precipitation: Key factors and enhancement strategies. *Frontiers in Microbiology*, *14*, 1116970. https://doi.org/10.3389/fmicb.2023.1116970

Zou, M., Zhang, Q., Li, F., Chen, L., Qiu, Y., Yin, Q., & Zhou, S. (2024). Impacts of multiple environmental factors on soil bacterial community assembly in heavy metal polluted paddy fields. *Scientific Reports*, *14*(1), 14696. https://doi.org/10.1038/s41598-024-65678-x

PART III

7. General conclusion

The research presented in this doctoral thesis develops a comprehensive and unified interpretation of how illegal waste dumping affects soil systems and how these degraded environments can be understood, assessed and restored through an integrated scientific approach. Throughout the work, the different strands of investigation converge toward the same objective: to capture the complexity of contaminated soils by examining their chemical burdens, their ecological transformations along with potential for recovery through native microbial resources. This perspective moves beyond traditional compartmentalized analyses and embraces a vision of soil as a dynamic ecological system whose health depends on the interaction between contaminants and the living communities that inhabit it. The thesis, therefore, considers soil not as a passive element, and in most cases, victim of pollution but as an active and evolving environment whose transformations can be measured, interpreted and incorporated into effective remediation strategies.

The starting point of the research lies in recognizing the limitations of existing approaches that address contamination solely through chemical parameters. The soils of the peri-urban area of Foggia illustrate how illegal waste dumping produces contamination patterns that are both persistent and structurally complex. Concentrations of metals such as lead, chromium, copper and zinc reveal long-term accumulation, but this chemical information alone does not describe the full extent of degradation. The biological analyses conducted in this work show that contamination reshapes soil microbiota, reducing diversity and altering community structure in ways that reflect both ecological stress and adaptive responses. Moreover, soil microbiota is not merely an indicator of contamination but an integral part of the system's functional integrity. Microbial communities, in fact, are sensitive markers of ecological transformation and that their responses carry information that cannot be captured through chemical measurements alone.

This recognition led to the development of the Soil Pollution and Ecological Risk Index, known as SPERI, which represents a core methodological contribution of the thesis. SPERI integrates chemical data, biodiversity indicators and shifts in microbial community composition into a single measure capable of depicting soil health more realistically. Through this index, the research demonstrates that ecological information is essential for evaluating the consequences of pollution and for classifying soil conditions in a way that reflects both contamination and ecological function. SPERI is not an abstract construct but a practical tool that supports decision-making processes by providing a unified view of soil degradation. It serves as a bridge between scientific understanding and environmental management, aligning research with the needs of institutions responsible for remediation activities. The index is flexible enough to be applied across different contexts and solid enough to form the basis for future refinement and expansion.

While SPERI provides an integrative framework for assessment, the thesis also investigates the potential for recovery embedded within the contaminated soils themselves. The selection and characterization of *Pseudomonas* strains from the study area reveal that prolonged exposure to contamination pressures can select for microorganisms with valuable adaptive traits. These strains tolerate elevated concentrations of HMs and maintain metabolic activity under multiple stresses, suggesting the existence of mechanisms such as biosorption, intracellular accumulation and redox-based transformations. Their functional performance shows that even heavily impacted environments can host microbial populations capable of contributing to detoxification processes. The research therefore suggests that contamination does not simply degrade the soil but reshapes it in ways that can be transformed into opportunities for remediation. The strains isolated during this study represent practical resources for the design of bioremediation strategies that rely on locally adapted organisms rather than external or engineered solutions. This biological dimension of recovery adds depth to the overall framework and aligns with

contemporary approaches to nature-based solutions and circular use of biological resources.

The most significant contribution of this thesis, however, is not found in any individual component but in the holistic perspective it establishes. The research demonstrates that chemical assessment, ecological interpretation and microbial biotechnology can be combined into a unified framework capable of addressing the complexity of illegal waste dumping. This integrated approach aligns with the strategic objectives of the PNRR, which emphasize sustainability, resilience, local valorization and the restoration of ecosystem functions. By combining contaminant profiling, ecological diagnostics and adaptive microbial resources, the thesis offers a model that can support both scientific inquiry and policy development. It shows that soil restoration is most effective when it considers the interconnected nature of degradation processes and the interplay between pollutants and biological systems.

The broader significance of this work lies in its ability to reposition contaminated soils within a narrative of transformation rather than irreversible decline. The findings show that polluted soils retain ecological potential and adaptive capacity. Microbial communities respond to stress not only through loss but also through reorganization and functional specialization. These responses are valuable because they can guide the development of remediation techniques grounded in local environmental conditions. The thesis therefore contributes to a more mature understanding of ecological resilience and demonstrates that even degraded soils can become active participants in their own recovery. From an operational standpoint, the tools and evidence generated in this thesis provide a concrete basis for future decision-making in waste-related soil management. The SPERI index can support environmental agencies in prioritizing interventions, while the characterization of indigenous *Pseudomonas* isolates opens the way to field-scale pilot applications grounded in locally adapted bioresources. Future developments should include the validation of SPERI across broader territorial contexts, the integration of microbial datasets into digital monitoring platforms, and

the scaling-up of bio-based remediation strategies. These actions will be essential to translate the scientific contributions of this work into practical, circular, and territorially relevant solutions. In practical terms, this means that illegal waste dumping, while symptomatic of critical failures in waste governance, can be reconceptualized as the starting point of bio-based, waste-to-resource trajectories in which the very ecological alterations induced by waste become leverage for soil regeneration. This perspective is essential for designing interventions that are realistic, sustainable and grounded in the ecological realities of contaminated environments.

Beyond the scientific contributions, the thesis also encourages a shift in how contaminated sites are conceptualized and managed. It highlights the need to integrate ecological understanding into regulatory frameworks, monitoring protocols and remediation policies. It shows that chemical concentrations, while essential, do not capture the full spectrum of degradation, and that neglecting biological indicators risks underestimating the true extent of soil impairment. The unified model presented here supports a transition toward more comprehensive evaluation tools and more adaptive remediation strategies capable of responding to the changing conditions of soil ecosystems.

Looking ahead, the thesis opens several directions for future research and application. The SPERI index, while already functional, can be refined further by incorporating additional ecological indicators such as functional gene profiles, measures of enzymatic activity and assessments of microbial network stability. These integrations could increase the sensitivity of the index and enhance its ability to detect early signs of ecological deterioration or recovery. Expanding SPERI to include temporal monitoring would allow researchers and policymakers to track the evolution of contaminated soils over time and to evaluate the effectiveness of remediation actions. The index could also be adapted to different environments such as agricultural soils, post-industrial sites or areas affected by diffuse pollution, broadening its applicability across various territorial challenges.

From a biotechnological perspective, the strains identified in this thesis represent the foundation for further research aimed at clarifying the genetic and molecular bases of their adaptive traits. Whole-genome sequencing could reveal the pathways involved in metal resistance and provide insight into the mechanisms that allow these microorganisms to thrive under high levels of contamination. Such knowledge would not only deepen the scientific understanding of microbial adaptation but also improve the development of targeted bioremediation strategies that maximize efficiency while minimizing ecological disruption. The strains could also be tested under soil-based conditions that better reflect environmental realities, allowing researchers to evaluate their performance outside controlled laboratory settings.

Another promising direction concerns the integration of microbiological and modelling approaches for predicting the behaviour of contaminated soils. Linking ecological and chemical data with statistical or machine learning models could facilitate the identification of patterns that are not easily observable through traditional analyses. Predictive modelling could support early-warning systems, optimize sampling strategies and guide resource allocation for remediation efforts. This computational dimension would complement the ecological and biotechnological components already established in the thesis and strengthen the overall framework for soil restoration.

Finally, the outcomes of this research suggest a broader need for collaboration between scientific institutions, environmental agencies and policymakers. The integrated model developed in this thesis can contribute to decision-making processes aimed at identifying priority areas, designing context-specific interventions and monitoring the progress of restoration programs. The approach aligns naturally with the objectives of sustainable land management and can support regional and national frameworks committed to environmental protection and ecological transition.

In conclusion, this thesis demonstrates that illegal waste dumping presents complex and multidimensional challenges, yet these challenges can be understood and

addressed through integrated scientific strategies. By combining chemical analyses, ecological interpretation and microbial biotechnology, the research provides a holistic framework capable of supporting the restoration of contaminated soils. It shows that degraded environments retain the capacity for resilience and adaptation and that these qualities can be transformed into resources for remediation.

Annexes

Annex A: Supplementary material for chapter 3

Table A3.1

PRISMA 2020 checklist summarizing compliance of the present systematic review with reporting standards

Section / Topic	Item #	Checklist Item (abridged)	Location in manuscript
TITLE	1	Identify the report as a systematic review.	Title page + Abstract
ABSTRACT	2	Provide a structured summary including background, objectives, data sources, eligibility criteria, results, and conclusions.	Abstract
INTRODUCTION	3	Describe the rationale for the review.	Section 3.1 (Introduction)
	4	State the objectives or research questions.	Section 3.1, final paragraph
METHODS	5	Specify inclusion and exclusion criteria.	Section 3.2.3 + Table A3.2
	6	Specify all information sources (databases, registers).	Section 3.2.2
	7	Present full search strategy for at least one database.	Section 3.2.2 + Table A3.2
	8	Describe the selection process.	Section 3.2.4
	9	Describe data-collection process.	Section 3.2.5
	10	Describe data items (variables extracted).	Section 3.2.5
	11	Describe methods used to assess risk of bias or study quality.	Section 3.2.6
	12	Specify effect-measures or summary measures used.	Section 3.2.8
	13	Describe synthesis methods and any subgroup or sensitivity analyses.	Section 3.2.8

	14	Describe how certainty or confidence in the evidence was assessed.	Section 3.2.6
RESULTS	16a	Describe results of search and selection (ideally with a flow diagram).	Section 3.2.4 + Figure 3.1
	16b	Cite reasons for exclusion at each stage.	Section 2.4 + Supp. Table S2
	17	Present characteristics of included studies.	Section 3.3.1 + Section 3.3.2
	18	Present results of individual studies.	Results section 3.3.1–3.3.4
	19	Present synthesis of results.	Results & Discussion
DISCUSSION	23	Summarize main findings, limitations, implications.	Section 3.3.4
	24	Discuss limitations of evidence and of the review process.	Section 3.4.5
	25	Provide a general interpretation in the context of other evidence.	Section 3.3.5

Table A3.2

Resume of research strings used per each platform and obtained results

Scientific platform	Research query	Results
Scopus	1. TITLE-ABS-KEY ("bioremediation" AND ("heavy metals" OR cadmium OR lead OR chromium OR nickel OR mercury OR arsenic OR copper OR zinc)) AND PUBYEAR > 2000	34.230
Scopus	2. TITLE-ABS-KEY ("microbiota" OR "bacteria" OR "microorganism*") AND TITLE-ABS-KEY ("heavy metals" OR cadmium OR lead OR chromium OR nickel OR mercury OR arsenic OR copper OR zinc) AND PUBYEAR > 2000	149.001
Scopus	3. TITLE-ABS-KEY (microbial OR bacteria OR microorganism* OR microbiota) AND TITLE-ABS-KEY ("bioremediation") AND TITLE-ABS-KEY ("heavy metals" OR cadmium OR lead OR chromium OR nickel OR mercury OR arsenic OR copper OR zinc) AND PUBYEAR > 2000 AND (LIMIT-TO (SUBJAREA , "ENVI") OR LIMIT-TO (SUBJAREA , "BIOC") OR LIMIT-TO (SUBJAREA , "IMMU") OR LIMIT-TO (SUBJAREA , "AGRI"))	11.547
Scopus	4. TITLE (microbial OR bacteria OR microorganism* OR microbiota) AND TITLE ("bioremediation") AND TITLE ("heavy metals" OR cadmium OR lead OR chromium OR nickel OR mercury OR arsenic OR copper OR zinc) AND NOT TITLE-ABS-KEY (aquaculture OR marine OR dye* OR textile* OR "organic pollutant*" OR "nanoparticle*" OR "rare earth*" OR "photocatalys*" OR "antibiotic*") AND PUBYEAR > 2020 AND (LIMIT-TO (SUBJAREA,"ENVI") OR LIMIT-TO (SUBJAREA,"BIOC") OR LIMIT-TO (SUBJAREA,"IMMU") OR LIMIT-TO (SUBJAREA,"AGRI"))	315
Scopus	5. TITLE-ABS-KEY (*Pseudomonas* OR *Bacillus* OR *Rhodococcus* OR *Acinetobacter* OR *Shewanella* OR *Geobacter*) AND TITLE-ABS-KEY (microbial OR bacteria OR microorganism* OR microbiota) AND TITLE-ABS-KEY ("bioremediation") AND TITLE-ABS-KEY ("heavy metals" OR cadmium OR lead OR chromium OR nickel OR mercury OR arsenic OR copper OR zinc) AND NOT TITLE-ABS-KEY (phytoremediation OR aquaculture OR dye* OR textile* OR "organic pollutant*" OR "nanoparticle*" OR "rare earth*" OR "photocatalys*" OR "antibiotic*") AND PUBYEAR > 2022 AND (LIMIT-TO (SUBJAREA , "ENVI") OR LIMIT-TO (SUBJAREA , "BIOC") OR LIMIT-TO (SUBJAREA , "IMMU") OR LIMIT-TO (SUBJAREA , "AGRI")) AND (LIMIT-TO (DOCTYPE , "ar") OR LIMIT-TO (DOCTYPE , "re")) AND (LIMIT-TO (PUBYEAR , 2022) OR LIMIT-TO (PUBYEAR , 2023) OR LIMIT-TO (PUBYEAR , 2024) OR LIMIT-TO (PUBYEAR , 2025))	825

Scopus	6. TITLE-ABS-KEY (*Pseudomonas* OR *Bacillus* OR *Rhodococcus* OR *Acinetobacter* OR *Shewanella* OR *Geobacter*) AND TITLE-ABS-KEY (microbial OR bacteria OR microorganism* OR microbiota) AND TITLE-ABS-KEY (soil OR dirt) AND TITLE-ABS-KEY ("bioremediation") AND TITLE-ABS-KEY ("heavy metal*" OR cadmium OR lead OR chromium OR nickel OR mercury OR arsenic OR copper OR zinc) AND TITLE-ABS-KEY (biosorption OR bioaccumulation OR biomineralization OR bioprecipitation OR "redox transformation") AND NOT TITLE-ABS-KEY (phytoremediation OR phytoremediation OR aquaculture OR dye* OR textile* OR "organic pollutant*" OR "nanoparticle*" OR "rare earth*" OR "photocatalys*" OR "antibiotic*") AND PUBYEAR > 2022 AND (LIMIT-TO (SUBJAREA,"ENVI") OR LIMIT-TO (SUBJAREA,"BIOC") OR LIMIT-TO (SUBJAREA,"IMMU") OR LIMIT-TO (SUBJAREA,"AGRI")) AND (LIMIT-TO (DOCTYPE,"ar") OR LIMIT-TO (DOCTYPE,"re")) AND (LIMIT-TO (PUBYEAR,2022) OR LIMIT-TO (PUBYEAR,2023) OR LIMIT-TO (PUBYEAR,2024) OR LIMIT-TO (PUBYEAR,2025))	98
Web of Science	1. TS=("bioremediation" AND ("heavy metals" OR cadmium OR lead OR chromium OR nickel OR mercury OR arsenic OR copper OR zinc)) AND PY=(2001-2025)	11.646
Web of Science	2. TS=(("microbiota" OR bacteria OR microorganism*) AND ("heavy metals" OR cadmium OR lead OR chromium OR nickel OR mercury OR arsenic OR copper OR zinc)) AND PY=(2001-2025)	161.040
Web of Science	3. TS=((microbial OR bacteria OR microorganism* OR microbiota) AND bioremediation AND ("heavy metals" OR cadmium OR lead OR chromium OR nickel OR mercury OR arsenic OR copper OR zinc)) AND PY=(2001-2025)	7.529
Web of Science	4. TI=(microbial OR bacteria OR microorganism* OR microbiota) AND TI=(bioremediation) AND TI=("heavy metals" OR cadmium OR lead OR chromium OR nickel OR mercury OR arsenic OR copper OR zinc) NOT TS=(aquaculture OR marine OR dye* OR textile* OR "organic pollutant*" OR nanoparticle* OR "rare earth*" OR photocatalys* OR antibiotic*) AND PY=(2021-2025)	86
Web of Science	5. TS=((*Pseudomonas* OR *Bacillus* OR *Rhodococcus* OR *Acinetobacter* OR *Shewanella* OR *Geobacter*) AND (microbial OR bacteria OR microorganism* OR microbiota) AND bioremediation AND ("heavy metals" OR cadmium OR lead OR chromium OR nickel OR mercury OR arsenic OR copper OR zinc)) NOT TS=(phytoremediation OR aquaculture OR dye* OR textile* OR "organic pollutant*" OR nanoparticle* OR "rare earth*" OR photocatalys* OR antibiotic*) AND PY=(2022-2025)	636
Web of Science	6. TS=((*Pseudomonas* OR *Bacillus* OR *Rhodococcus* OR *Acinetobacter* OR *Shewanella* OR *Geobacter*) AND (microbial OR bacteria OR microorganism* OR	86

	microbiota) AND (soil OR dirt) AND bioremediation AND ("heavy metal*" OR cadmium OR lead OR chromium OR nickel OR mercury OR arsenic OR copper OR zinc) AND (biosorption OR bioaccumulation OR biomineralization OR bioprecipitation OR "redox transformation")) NOT TS=(phytoremediation OR aquaculture OR dye* OR textile* OR "organic pollutant*" OR nanoparticle* OR "rare earth*" OR photocatalys* OR antibiotic*) AND PY=(2022-2025)	
PubMed	1. (bioremediation[MeSH Terms] OR bioremediation[Title/Abstract]) AND ("heavy metals"[MeSH Terms] OR "heavy metals"[Title/Abstract] OR cadmium[Title/Abstract] OR lead[Title/Abstract] OR chromium[Title/Abstract] OR nickel[Title/Abstract] OR mercury[Title/Abstract] OR arsenic[Title/Abstract] OR copper[Title/Abstract] OR zinc[Title/Abstract])AND ("2000/01/01"[Date - Publication] : "2025/12/31"[Date - Publication])	11.271
PubMed	2. ("microbiota"[MeSH Terms] OR microbiota[Title/Abstract] OR bacteria[Title/Abstract] OR microorganism*[Title/Abstract]) AND ("heavy metals"[MeSH Terms] OR "heavy metals"[Title/Abstract] OR cadmium[Title/Abstract] OR lead[Title/Abstract] OR chromium[Title/Abstract] OR nickel[Title/Abstract] OR mercury[Title/Abstract] OR arsenic[Title/Abstract] OR copper[Title/Abstract] OR zinc[Title/Abstract]) AND ("2000/01/01"[Date - Publication] : "2025/12/31"[Date - Publication])	43.915
PubMed	3. (microbial[Title/Abstract] OR bacteria[Title/Abstract] OR microorganism*[Title/Abstract] OR microbiota[Title/Abstract]) AND (bioremediation[MeSH Terms] OR bioremediation[Title/Abstract]) AND ("heavy metals"[MeSH Terms] OR "heavy metals"[Title/Abstract] OR cadmium[Title/Abstract] OR lead[Title/Abstract] OR chromium[Title/Abstract] OR nickel[Title/Abstract] OR mercury[Title/Abstract] OR arsenic[Title/Abstract] OR copper[Title/Abstract] OR zinc[Title/Abstract])AND ("2000/01/01"[Date - Publication] : "2025/12/31"[Date - Publication])	4.230
PubMed	4. (microbial[Title] OR bacteria[Title] OR microorganism*[Title] OR microbiota[Title]) AND (bioremediation[Title]) AND ("heavy metals"[Title] OR cadmium[Title] OR lead[Title] OR chromium[Title] OR nickel[Title] OR mercury[Title] OR arsenic[Title] OR copper[Title] OR zinc[Title]) NOT (aquaculture[Title/Abstract] OR marine[Title/Abstract] OR dye*[Title/Abstract] OR textile*[Title/Abstract] OR "organic pollutant*"[Title/Abstract] OR nanoparticle*[Title/Abstract] OR "rare earth*"[Title/Abstract] OR photocatalys*[Title/Abstract] OR antibiotic*[Title/Abstract]) AND ("2021/01/01"[Date - Publication] : "2025/12/31"[Date - Publication])	47

PubMed	5. (*Pseudomonas*[MeSH Terms] OR *Bacillus*[MeSH Terms] OR *Rhodococcus*[Title/Abstract] OR *Acinetobacter*[MeSH Terms] OR *Shewanella*[MeSH Terms] OR *Geobacter*[MeSH Terms] OR *Pseudomonas*[Title/Abstract] OR *Bacillus*[Title/Abstract] OR *Acinetobacter*[Title/Abstract] OR *Shewanella*[Title/Abstract] OR *Geobacter*[Title/Abstract]) AND (microbial[Title/Abstract] OR bacteria[Title/Abstract] OR microorganism*[Title/Abstract] OR microbiota[Title/Abstract]) AND (bioremediation[MeSH Terms] OR bioremediation[Title/Abstract]) AND ("heavy metals"[MeSH Terms] OR "heavy metals"[Title/Abstract] OR cadmium[Title/Abstract] OR lead[Title/Abstract] OR chromium[Title/Abstract] OR nickel[Title/Abstract] OR mercury[Title/Abstract] OR arsenic[Title/Abstract] OR copper[Title/Abstract] OR zinc[Title/Abstract]) NOT (phytoremediation[Title/Abstract] OR aquaculture[Title/Abstract] OR dye*[Title/Abstract] OR textile*[Title/Abstract] OR "organic pollutant*"[Title/Abstract] OR nanoparticle*[Title/Abstract] OR "rare earth*"[Title/Abstract] OR photocatalys*[Title/Abstract] OR antibiotic*[Title/Abstract]) AND ("2022/01/01"[Date - Publication] : "2025/12/31"[Date - Publication])	74
PubMed	6. (*Pseudomonas*[Title/Abstract] OR *Bacillus*[Title/Abstract] OR *Rhodococcus*[Title/Abstract] OR *Acinetobacter*[Title/Abstract] OR *Shewanella*[Title/Abstract] OR *Geobacter*[Title/Abstract])AND (microbial[Title/Abstract] OR bacteria[Title/Abstract] OR microorganism*[Title/Abstract] OR microbiota[Title/Abstract]) AND (soil[Title/Abstract] OR dirt[Title/Abstract]) AND (bioremediation[MeSH Terms] OR bioremediation[Title/Abstract]) AND ("heavy metals"[MeSH Terms] OR "heavy metals"[Title/Abstract] OR cadmium[Title/Abstract] OR lead[Title/Abstract] OR chromium[Title/Abstract] OR nickel[Title/Abstract] OR mercury[Title/Abstract] OR arsenic[Title/Abstract] OR copper[Title/Abstract] OR zinc[Title/Abstract]) AND (biosorption[Title/Abstract] OR bioaccumulation[Title/Abstract] OR biomineralization[Title/Abstract] OR bioprecipitation[Title/Abstract] OR "redox transformation"[Title/Abstract]) NOT (phytoremediation[Title/Abstract] OR aquaculture[Title/Abstract] OR dye*[Title/Abstract] OR textile*[Title/Abstract] OR "organic pollutant*"[Title/Abstract] OR nanoparticle*[Title/Abstract] OR "rare earth*"[Title/Abstract] OR photocatalys*[Title/Abstract] OR antibiotic*[Title/Abstract]) AND ("2022/01/01"[Date - Publication] : "2025/12/31"[Date - Publication])	4

Table A3.3

Eligibility criteria and rationale for inclusion and exclusion applied in the systematic review. The table details the methodological boundaries used to determine study eligibility, including study type, biological system, target metals, environmental matrices, quantitative evidence, analytical validation, taxonomic identification, and mechanistic requirements. Criteria were established a priori in accordance with the PRISMA 2020 guidelines to ensure transparency, reproducibility, and methodological consistency across the study selection process.

Category	Inclusion criteria	Exclusion criteria / rationale for exclusion
Study type and publication features	Original experimental research articles published in peer-reviewed journals (2022–2025). Written in English. Contain reproducible methodology and quantitative results.	Review, mini-review, opinion, or conceptual papers without new data. Book chapters, proceedings, or non-peer-reviewed publications. Duplicate or inaccessible full texts.
Biological system	Microbial bioremediation in which bacteria, actinomycetes, or mixed microbial consortia represent the primary remediation agents.	Plant-centered phytoremediation or plant–microbe synergy where the main mechanism is plant-based. Purely abiotic or enzymatic systems lacking living cells.
Target pollutants	Experiments addressing at least one toxic heavy metal (Cd, Pb, Cr, Ni, Cu, Zn, Hg, As).	Studies limited to non-metal pollutants (dyes, hydrocarbons, antibiotics, microplastics, pesticides, organics, rare-earths).
Environmental matrix	Environmentally relevant matrices: soil, sediment, wastewater, effluent, sludge, or simulated soil systems.	Aquatic or laboratory systems with no soil relevance (e.g., pure-culture in liquid medium without environmental context).
Quantitative evidence required	At least one measurable outcome: metal-removal percentage, adsorption capacity (q_{max}), ecc.	Only qualitative or descriptive observations with no numerical metrics.
Analytical validation	Robust analytical techniques: AAS, ICP-OES/ICP-MS, XRF, SEM/EDS, FTIR, XRD, or equivalent.	Indirect colorimetric or unvalidated assays lacking instrumental confirmation.
Taxonomic identification	Identification to at least the genus level (preferably 16S rRNA-based or WGS).	Unidentified microbial sources or unclassified mixed cultures.

Mechanistic or molecular characterization	Presence of biochemical or genetic evidence supporting detoxification (EPS, biofilm, enzymes, siderophores, biomineralization, resistance genes.	Absence of mechanistic data or purely descriptive tolerance assays.
Metagenomic and omics studies	Included only when quantitative gene/pathway data directly linked to metal detoxification or resistance are reported.	Omics studies lacking quantitative association between genes and detoxification performance.

Table A3.4

NOS assessment of the included works for review according to PRISMA 2020 protocol.

Author (year)	Title	Journal	NOS score
Wang et al., 2025	Lead biosorption by *Bacillus tequilensis* FB-6: characterization of resistance mechanisms and remediation potential	Journal of the Science of Food and Agriculture	9
Kaushal and Pati, 2024	*Bacillus altitudinis* Mediated Lead Bioremediation for Enhanced Growth of Rice Seedlings	Current Microbiology	8
Kashyap et al., 2022	Biosorption efficiency of nickel by various endophytic bacterial strains for removal of nickel from electroplating industry effluents: an operational study	Ecotoxicology	8
Mtengai et al., 2022	Existence of a novel heavy metal–tolerant *Pseudomonas aeruginosa* strain Zambia SZK-17 Kabwe 1: the potential bioremediation agent in the heavy metal–contaminated area	Environmental Monitoring and Assessment	7
Henagamage et al., 2022	Fungal-bacterial biofilm mediated heavy metal rhizo-remediation	World Journal of Microbiology and Biotechnology	8
Ye et al., 2024	Mechanism of Cr(VI) removal by efficient Cr(VI)-resistant *Bacillus mobilis* CR3	World Journal of Microbiology and Biotechnology	9
Monga et al., 2022	Isolation and Identification of Novel Chromium Tolerant Bacterial Strains From a Heavy Metal Polluted Urban Creek: An Assessment of Bioremediation Efficiency and Flocculant Production	Thalassas: International Journal of Marine Sciences	8
Shaaban Emara et al., 2023	Mechanistic action of lead removal by the native isolate *Bacillus amyloliquefaciens* ON261680.1	Arabian Journal of Chemistry	9
Ghosh et al., 2024	Plant growth-promoting *Bacillus cereus* MCC3402 facilitates rice seedling growth under arsenic-spiked soil	Biocatalysis and Agricultural Biotechnology	8
Sahu et al., 2022	Bacterial strains found in the soils of a municipal solid waste dumping site facilitated phosphate solubilization along with cadmium remediation	Chemosphere	8

Ali et al., 2022	Cadmium tolerant microbial strains possess different mechanisms for cadmium biosorption and immobilization in rice seedlings	Chemosphere	8
Lin et al., 2022	Construction of bifunctional bacterial community for co-contamination remediation: Pyrene biodegradation and cadmium biomineralization	Chemosphere	9
Zuo et al., 2022	Using *Bacillus thuringiensis* HM-311 hydroxyapatite biochar beads to remediate Pb and Cd contaminated farmland soil	Chemosphere	9
Gao et al., 2024	Contribution of Cd passivating functional bacterium H27 to tobacco growth under Cd stress	Chemosphere	8
Kaur et al., 2024	Removal of cadmium through biomineralization using halophilic and ureolytic bacteria under saline conditions	International Biodeterioration & Biodegradation	9
Soto-Ramírez et al., 2024	Engineering the cell wall reactive groups of Plant Growth Promoting Rhizobacteria by culture strategy for heavy metal removal.	Journal of Biotechnology	9
Mondal et al., 2025	Bioprotective mechanisms of *Enterobacter* sp. against arsenic, cadmium, and lead toxicity and its potential role in soil bioremediation.	Journal of Environmental Chemical Engineering	9
Huang et al., 2024	Immobilization of Cd^{2+} in an aqueous environment using a two-step microbial-induced carbonate precipitation method.	Journal of Environmental Management	8
Yan et al., 2024	Cadmium biosorption and mechanism investigation using two cadmium-tolerant microorganisms isolated from rhizosphere soil of rice	Journal of Hazardous Materials	9
Cai et al., 2025	A cooperation mechanism between *Bacillus thuringiensis* and *Citrobacter freundii* that enhances cadmium biomineralization	Journal of Hazardous Materials	9
Chen et al., 2025	Integrated analyses of characterization and transcriptome reveal the adaptive response mechanism of *Bacillus cereus* FCHN 7–1 in cadmium adsorption	Journal of Hazardous Materials	8
Peng et al., 2023	Mixed bacteria passivation for the remediation of arsenic, lead, and cadmium: Medium optimization and mechanisms.	Process Safety and Environmental Protection	9

Su et al., 2022	Characterization of the simultaneous degradation of pyrene and removal of Cr(VI) by a bacteria consortium YH	Science of the Total Environment	9
Zhang et al., 2023	Cadmium-tolerant *Bacillus cereus* 2–7 alleviates the phytotoxicity of cadmium exposure in banana plantlets	Science of the Total Environment	9
Zhang et al., 2024a	Bioremediation of paddy soil with amphitropic mixture markedly attenuates rice cadmium: Effect of soil cadmium removal and Fe/S-cycling bacteria in rhizosphere	Science of the Total Environment	9
Zhang et al., 2024b	Biogenic calcium improved Cd2+ and Pb^{2+} immobilization in soil using the ureolytic bacteria *Bacillus pasteurii*.	Science of the Total Environment	9
Elahi et al., 2022	Isolation and characterization of a highly effective bacterium *Bacillus cereus b-525k* for hexavalent chromium detoxification	Saudi Journal of Biological Sciences	8
Mitra et al., 2025	Halotolerant bacteria isolated from the soils of Indian mangrove ecosystem for metal removal and NPK enhancement.	Scientific Reports	9
Manikandan and Nair, 2023	Developing a biocatalyst showcasing the synergistic effect of rice husk biochar and bacterial cells for the removal of heavy metals.	New Journal of Chemistry	8
Shan et al., 2024	Bioremediation Potential of Cr(VI) by *Lysinibacillus cavernae* CR-2 Isolated from Chromite-Polluted Soil: A Promising Approach for Cr(VI) Detoxification.	Geomicrobiology Journal	9
Surabhi et al., 2025	Multi-metal Tolerance Efficiency and Bioremediation Capabilities of *Bacillus aerius* from Mangrove Rhizosphere	Geomicrobiology Journal	9
Satyapal et al., 2024	Gamma irradiation in modulating arsenic bioremediation potential of *Pseudomonas* sp. AK1 and AK9	International Journal of Radiation Biology	
Bhandari et al., 2024	Microbial bioremediation: unraveling the potential for cleaner environments through comparative analysis	Bioremediation Journal	8
Sundarraj et al., 2023	Bioremediation of hexavalent chromium by transformation of *Escherichia coli* DH5α with	Journal of Applied Microbiology	8

	chromate reductase (ChrR) genes of *Pseudomonas putida* isolated from tannery effluent		
Yasmin et al., 2022	Biosorptive Potential of *Pseudomonas* species RY12 Toward Zinc Heavy Metal in Agriculture Soil Irrigated with Contaminated Waste Water	Dose–Response	8
Sizentsov et al., 2025	In vitro assessment of the biosorption potential of some representatives of THE genus bacillus during interaction with lead cations	Applied Ecology and Environmental Research	7
Liang et al., 2025	Isolation and characterization of cadmium-resistant *Bacillus cereus* strains from Cd-contaminated mining areas for potential bioremediation applications	Frontiers in Microbiology	9
Firincă et al., 2023	Microbial Removal of Heavy Metals from Contaminated Environments Using Metal-Resistant Indigenous Strains	Journal of Xenobiotics	9
Arce-Inga et al., 2022	Bioremediation Potential of Native *Bacillus* sp. Strains as a Sustainable Strategy for Cadmium Accumulation of Theobroma cacao in Amazonas Region	Microorganisms	9
Mungla et al., 2022	Assessing the Potential of Mechanical Aeration Combined with Bioremediation Process in Soils and Coastal Sediments Impacted by Heavy Metals Bioremediation Process in Soils and Coastal Sediments Impacted by Heavy Metals	AIMS Environmental Science	8
Dahnoun et al., 2024	Characterization and bioremediation potential of heavy metal resistant bacteria isolated from agricultural soil	Turkish Journal of Agriculture and Forestry	9

Table A3.5

Top 50 keywords identified by VOSviewer in the literature on microbial heavy metal bioremediation (2020–2025). Keywords are ranked by occurrence and total link strength.

Keyword	Occurrences	Total link strength
bioremediation	10427	253412
biodegradation, environmental	4373	134323
metabolism	3626	111758
heavy metal	3523	102341
bacteria	3523	101981
bacterium	3514	106733
controlled study	3267	109929
heavy metals	2964	74765
soil pollution	2886	88036
chemistry	2537	84746
soil pollutants	2389	81450
cadmium	2298	73013
soil pollutant	2258	77430
microbiology	2190	73644
microbial community	2117	73815
soil	2074	68798
bacteria (microorganisms)	2029	56677
biodegradation	1863	51631
metals, heavy	1751	58137
phytoremediation	1739	49203
soils	1687	55272
chromium	1679	49020
pH	1617	53271
copper	1550	50679
biotechnology	1524	39017
lead	1489	49019
zinc	1406	47921
biomass	1325	42641
genetics	1321	41617
soil microbiology	1295	45335
enzyme activity	1261	42738
arsenic	1253	37189

microbial activity	1216	37123
bioaccumulation	1197	38282
water pollutants, chemical	1196	40156
bacterial strain	1188	38708
toxicity	1152	34752
water pollutant	1147	38784
rna 16s	1061	38235
adsorption	1044	31365
contamination	1040	31238
unclassified drug	1027	33732
pollutant removal	1006	30548
microorganisms	1002	26144
iron	945	32534
plant growth	931	35295
wastewater treatment	928	26115
heavy metal removal	920	29488
nitrogen	876	31347
pollution	874	24573

References

Ali, Q., Ayaz, M., Yu, C., Wang, Y., Gu, Q., Wu, H., & Gao, X. (2022). Cadmium tolerant microbial strains possess different mechanisms for cadmium biosorption and immobilization in rice seedlings. *Chemosphere*, *303*, 135206. https://doi.org/10.1016/j.chemosphere.2022.135206

Arce-Inga, M., González-Pérez, A. R., Hernandez-Diaz, E., Chuquibala-Checan, B., Chavez-Jalk, A., Llanos-Gomez, K. J., Leiva-Espinoza, S. T., Oliva-Cruz, S. M., & Cumpa-Velasquez, L. M. (2022). Bioremediation potential of native *Bacillus* sp. Strains as a sustainable strategy for cadmium accumulation of *Theobroma cacao* in Amazonas region. *Microorganisms*, *10*(11), 2108. https://doi.org/10.3390/microorganisms10112108

Bhandari, D., Sharma, P., & Dwivedi, V. (2024). Microbial bioremediation: Unravelling the potential for cleaner environments through comparative analysis. *Bioremediation Journal*, 1–9. https://doi.org/10.1080/10889868.2024.2357136

Cai, Q., Zhao, W., Wang, J., Yang, G., Amils, R., Martínez, J. M., Mateos, G., Carrasco-Ropero, I., Wu, J., & Xu, M. (2025). A cooperation mechanism between *Bacillus thuringiensis* and *Citrobacter freundii* that enhances cadmium biomineralization. *Journal of Hazardous Materials*, *488*, 137354. https://doi.org/10.1016/j.jhazmat.2025.137354

Chen, Y., Fang, Z., Iddrisu, L., Ye, J., Pan, X., Liang, Y., & Gooneratne, R. (2025). Integrated analyses of characterization and transcriptome reveal the adaptive response mechanism of *Bacillus cereus* FCHN 7–1 in cadmium adsorption. *Journal of Hazardous Materials*, *489*, 137525. https://doi.org/10.1016/j.jhazmat.2025.137525

Dahnoun, K., Djadouni, F., Essghaier, B., Naccache, C., Zitouna, N., Zehdi-Azouzi, S., BayyiĞiT, İs., Latif, H. R., Mezghani-Khemakhem, M., & Bourguiba, H. (2024). Characterization and bioremediation potential of heavy-metal resistant bacteria isolated from agricultural soil. *Turkish Journal of Agriculture and Forestry*, *48*(4), 607–617. https://doi.org/10.55730/1300-011X.3205

Elahi, A., Rehman, A., Zajif Hussain, S., Zulfiqar, S., & Shakoori, A. R. (2022). Isolation and characterization of a highly effective bacterium *Bacillus cereus* b-525k for hexavalent chromium detoxification. *Saudi Journal of Biological Sciences*, *29*(4), 2878–2885. https://doi.org/10.1016/j.sjbs.2022.01.027

Firincă, C., Zamfir, L.-G., Constantin, M., Răut, I., Capră, L., Popa, D., Jinga, M.-L., Baroi, A. M., Fierăscu, R. C., Corneli, N. O., Postolache, C., Doni, M., Gurban, A.-M., Jecu, L., & Șesan, T. E. (2023). Microbial removal of heavy metals from contaminated environments using metal-resistant indigenous strains. *Journal of Xenobiotics*, *14*(1), 51–78. https://doi.org/10.3390/jox14010004

Gao, Y., Zhang, X., Wang, L., Guan, E., Zhu, L., Wang, J., Kim, Y. M., & Wang, J. (2024). Contribution of Cd passivating functional bacterium H27 to tobacco growth under Cd stress. *Chemosphere*, *362*, 142552. https://doi.org/10.1016/j.chemosphere.2024.142552

Ghosh, P. K., Pramanik, K., Mahapatra, K., Mondal, S., Ghosh, S. K., Ghosh, A., & Maiti, T. K. (2024). Plant growth-promoting *Bacillus cereus* MCC3402 facilitates rice seedling growth under arsenic-spiked soil. *Biocatalysis and Agricultural Biotechnology*, *61*, 103405. https://doi.org/10.1016/j.bcab.2024.103405

Henagamage, A. P., Peries, C. M., & Seneviratne, G. (2022). Fungal-bacterial biofilm mediated heavy metal rhizo-remediation. *World Journal of Microbiology and Biotechnology*, *38*(5), 85. https://doi.org/10.1007/s11274-022-03267-8

Huang, X., Zhang, R., Xu, Y., & Zheng, J. (2024). Immobilization of Cd2+ in an aqueous environment using a two-step microbial-induced carbonate precipitation method. *Journal of Environmental Management*, *351*, 119868. https://doi.org/10.1016/j.jenvman.2023.119868

Kashyap, S., Chandra, R., Kumar, B., & Verma, P. (2022). Biosorption efficiency of nickel by various endophytic bacterial strains for removal of nickel from electroplating industry effluents: An

operational study. *Ecotoxicology*, *31*(4), 565–580. https://doi.org/10.1007/s10646-021-02445-y

Kaur, M., Sidhu, N., & Reddy, M. S. (2024). Removal of cadmium through biomineralization using halophilic and ureolytic bacteria under saline conditions. *International Biodeterioration & Biodegradation*, *191*, 105805. https://doi.org/10.1016/j.ibiod.2024.105805

Kaushal, P., & Pati, A. M. (2024). *Bacillus altitudinis* mediated lead bioremediation for enhanced growth of rice seedlings. *Current Microbiology*, *81*(12), 410. https://doi.org/10.1007/s00284-024-03934-z

Liang, B., Feng, Y., Ji, X., Li, C., Li, Q., Zeng, Z., & Wang, Y. (2025). Isolation and characterization of cadmium-resistant *Bacillus cereus* strains from Cd-contaminated mining areas for potential bioremediation applications. *Frontiers in Microbiology*, *16*, 1550830. https://doi.org/10.3389/fmicb.2025.1550830

Lin, H., Shi, J., Dong, Y., Li, B., & Yin, T. (2022). Construction of bifunctional bacterial community for co-contamination remediation: Pyrene biodegradation and cadmium biomineralization. *Chemosphere*, *304*, 135319. https://doi.org/10.1016/j.chemosphere.2022.135319

Manikandan, S. K., & Nair, V. (2023). Developing a biocatalyst showcasing the synergistic effect of rice husk biochar and bacterial cells for the removal of heavy metals. *New Journal of Chemistry*, *47*(46), 21199–21213. https://doi.org/10.1039/D3NJ02889E

Mitra, S., Dey, J., Sarkar, S., & Banik, P. (2025). Halotolerant bacteria isolated from the soils of Indian mangrove ecosystem for metal removal and NPK enhancement. *Scientific Reports*, *15*(1), 20804. https://doi.org/10.1038/s41598-025-07839-0

Mondal, S., Mondal, T., Pal, P., Mitra, S., Ghosh, S. K., Soren, T., & Maiti, T. K. (2025). Bioprotective mechanisms of *Enterobacter* sp. Against arsenic, cadmium, and lead toxicity and its potential role in soil bioremediation. *Journal of Environmental Chemical Engineering*, *13*(2), 115432. https://doi.org/10.1016/j.jece.2025.115432

Monga, A., Fulke, A. B., Gaud, A., Sharma, A., Ram, A., & Dasgupta, D. (2022). Isolation and identification of novel chromium tolerant bacterial strains from a heavy metal polluted urban creek: An assessment of bioremediation efficiency and flocculant production. *Thalassas: An International Journal of Marine Sciences*, *38*(2), 1233–1244. https://doi.org/10.1007/s41208-022-00458-w

Mtengai, K., Ramasamy, S., Msimuko, P., Mzula, A., & Mwega, E. D. (2022). Existence of a novel heavy metal–tolerant *Pseudomonas aeruginosa* strain Zambia SZK-17 Kabwe 1: The potential bioremediation agent in the heavy metal–contaminated area. *Environmental Monitoring and Assessment*, *194*(12), 887. https://doi.org/10.1007/s10661-022-10565-z

Mungla, G., Facknath, S., & Lalljee, B. (2022). Assessing the potential of mechanical aeration combined with bioremediation process in soils and coastal sediments impacted by heavy metals. *AIMS Environmental Science*, *9*(5), 692–707. https://doi.org/10.3934/environsci.2022039

Peng, C., Zhao, X., Ji, X., Wu, J., Liang, W., Song, H., Zhang, W., & Wang, X. (2023). Mixed bacteria passivation for the remediation of arsenic, lead, and cadmium: Medium optimization and mechanisms. *Process Safety and Environmental Protection*, *170*, 720–727. https://doi.org/10.1016/j.psep.2022.12.037

Sahu, S., Rajbonshi, M. P., Gujre, N., Gupta, M. K., Shelke, R. G., Ghose, A., Rangan, L., Pakshirajan, K., & Mitra, S. (2022). Bacterial strains found in the soils of a municipal solid waste dumping site facilitated phosphate solubilization along with cadmium remediation. *Chemosphere*, *287*, 132320. https://doi.org/10.1016/j.chemosphere.2021.132320

Satyapal, G. K., Haque, R., & Kumar, N. (2024). Gamma irradiation in modulating arsenic bioremediation potential of *Pseudomonas* sp. AK1 and AK9. *International Journal of Radiation Biology*, *100*(6), 934–939. https://doi.org/10.1080/09553002.2024.2345137

Shaaban Emara, N., Elwakil, B. H., Zakaria, M., & Olama, Z. A. (2023). Mechanistic action of lead removal by the native isolate *Bacillus amyloliquefaciens* ON261680.1. *Arabian Journal of Chemistry*, *16*(8), 104962. https://doi.org/10.1016/j.arabjc.2023.104962

Shan, B., Hao, R., Zhang, J., Li, J., Ye, Y., Xu, H., & Lu, A. (2024). Bioremediation potential of Cr(VI) by *Lysinibacillus cavernae* CR-2 isolated from chromite-polluted soil: A promising approach for Cr(VI) detoxification. *Geomicrobiology Journal*, *41*(4), 459–473. https://doi.org/10.1080/01490451.2023.2246035

Sizentsov, A. N., Galaktionova, L. V., Davydova, O. K., & Nikiyan, H. N. (2025). In vitro assessment of the biosorption potential of some representatives of the genus *Bacillus* during interaction with lead cations. *Applied Ecology and Environmental Research*, *23*(3), 4335–4349. https://doi.org/10.15666/aeer/2303_43354349

Soto-Ramírez, R., Vlatten, N., Ruz, F., Tavernini, L., & Lobos, M.-G. (2024). Engineering the cell wall reactive groups of Plant Growth Promoting Rhizobacteria by culture strategy for heavy metal removal. *Journal of Biotechnology*, *394*, 125–134. https://doi.org/10.1016/j.jbiotec.2024.08.015

Su, Y., Sun, S., Liu, Q., Zhao, C., Li, L., Chen, S., Chen, H., Wang, Y., & Tang, F. (2022). Characterization of the simultaneous degradation of pyrene and removal of Cr(VI) by a bacteria consortium YH. *Science of The Total Environment*, *853*, 158388. https://doi.org/10.1016/j.scitotenv.2022.158388

Sundarraj, S., Sudarmani, D. N. P., Samuel, P., & Sevarkodiyone, S. P. (2023). Bioremediation of hexavalent chromium by transformation of *Escherichia coli* DH5α with chromate reductase (ChrR) genes of *Pseudomonas putida* isolated from tannery effluent. *Journal of Applied Microbiology*, *134*(1), lxac019. https://doi.org/10.1093/jambio/lxac019

Surabhi, A., Sundaramanickam, A., Barathan, V., & Praveena, S. M. (2025). Multi-metal tolerance efficiency and bioremediation capabilities of *Bacillus aerius* from mangrove rhizosphere. *Geomicrobiology Journal*, *42*(8), 737–744. https://doi.org/10.1080/01490451.2025.2523818

Wang, X., Xu, W., Lu, Y., Cao, L., Tian, M., Shang, Y., Han, N., & Ding, J. (2025). Lead biosorption by *Bacillus tequilensis*: Characterization of resistance mechanisms and its potential for remediation of contaminated soil. *Journal of the Science of Food and Agriculture*, *105*(13), 7095–7102. https://doi.org/10.1002/jsfa.14408

Yan, Z., Li, Y., Peng, S., Wei, L., Zhang, B., Deng, X., Zhong, M., & Cheng, X. (2024). Cadmium biosorption and mechanism investigation using two cadmium-tolerant microorganisms isolated from rhizosphere soil of rice. *Journal of Hazardous Materials*, *470*, 134134. https://doi.org/10.1016/j.jhazmat.2024.134134

Yasmin, R., Zafar, M. S., Tahir, I. M., Asif, R., Asghar, S., & Raza, S. K. (2022). Biosorptive potential of *Pseudomonas* species RY12 toward zinc heavy metal in agriculture soil irrigated with contaminated wastewater. *Dose-Response*, *20*(3), 15593258221117352. https://doi.org/10.1177/15593258221117352

Ye, Y., Hao, R., Shan, B., Zhang, J., Li, J., & Lu, A. (2024). Mechanism of Cr(VI) removal by efficient Cr(VI)-resistant *Bacillus mobilis* CR3. *World Journal of Microbiology and Biotechnology*, *40*(1), 21. https://doi.org/10.1007/s11274-023-03816-9

Zhang, F., Deng, Y., Peng, R., Jiang, H., & Bai, L. (2024). Bioremediation of paddy soil with amphitropic mixture markedly attenuates rice cadmium: Effect of soil cadmium removal and Fe/S-cycling bacteria in rhizosphere. *Science of The Total Environment*, *915*, 169876. https://doi.org/10.1016/j.scitotenv.2024.169876

Zhang, L., Hu, Y., Chen, Y., Qi, D., Cai, B., Zhao, Y., Li, Z., Wang, Y., Nie, Z., Xie, J., & Wang, W. (2023). Cadmium-tolerant *Bacillus cereus* 2–7 alleviates the phytotoxicity of cadmium exposure in banana plantlets. *Science of The Total Environment*, *903*, 166645. https://doi.org/10.1016/j.scitotenv.2023.166645

Zhang, L., Wang, W., Yue, C., & Si, Y. (2024). Biogenic calcium improved Cd2+ and Pb2+ immobilization in soil using the ureolytic bacteria *Bacillus pasteurii*. *Science of The Total Environment*, *921*, 171060. https://doi.org/10.1016/j.scitotenv.2024.171060

Zuo, W., Song, B., Shi, Y., Zupanic, A., Guo, S., Huang, H., Jiang, L., & Yu, Y. (2022). Using *Bacillus thuringiensis* HM-311 hydroxyapatite biochar beads to remediate Pb and Cd contaminated farmland soil. *Chemosphere*, *307*, 135797.

Annex B: Supplementary material for chapter 4

Table B4.1

Elemental concentrations (mg/kg) of major, trace, and potentially toxic elements detected in the twelve soil samples. The dataset includes macro-elements (e.g., Ca, Mg, Fe, K), micronutrients (e.g., B, Mn, Zn), and heavy metals (e.g., Pb, Cd, Cu, Cr, Ni, As).

	Al	As	B	Ba	Ca	Cd	Cr	Cu	Fe	K	Mg	Mn	Na	Ni	P	Pb	S	Si	Sr	Ti	V	Zn
1	9970.62	3.31	19.65	176.62	139126.43	0.19	24.10	34.42	13392.91	7413.33	6498.86	648.04	1720.43	10.58	1397.93	45.09	3473.61	34647.03	224.47	1167.79	32.46	4061.68
2	18297.79	11.14	52.11	280.83	133429.38	1.75	58.14	106.78	33293.28	6765.33	6240.56	562.82	6473.71	41.54	8741.46	176.84	2162.12	34809.26	232.05	2550.66	52.39	648.09
3	4053.84	3.55	11.77	64.33	109781.36	0.71	15.13	40.94	20590.33	3053.44	11834.21	304.47	657.26	11.50	585.76	18.70	9835.14	14797.64	88.32	735.95	18.82	6340.72
4	33428.49	6.22	30.44	302.75	130327.66	0.38	31.79	42.23	21882.47	13744.84	12421.21	666.00	3036.71	17.32	944.75	25.53	2188.15	54343.02	178.92	1981.42	48.17	76.20
5	5918.62	4.09	25.32	203.78	142198.64	0.16	109.38	50.65	12318.63	8240.77	5319.78	593.33	2988.59	13.08	710.40	25.11	2772.67	48564.90	219.95	1498.36	34.31	183.60
6	5066.77	4.33	30.37	180.30	136459.81	0.22	22.20	216.27	9374.76	7030.28	5074.07	482.19	2017.21	12.07	783.73	35.57	5200.16	39934.60	254.75	1267.66	30.12	729.05
7	9087.66	8.53	33.30	212.75	123404.69	0.35	28.64	30.30	14574.45	9631.72	6595.09	681.16	2191.20	16.86	1249.86	72.64	2671.33	51882.27	233.71	1561.47	39.28	128.28
8	11223.64	5.81	27.59	316.96	139847.91	0.22	27.04	25.27	15170.29	10211.74	8222.62	664.45	3164.65	13.33	708.09	210.83	2648.52	56635.78	238.31	1698.17	43.36	140.60
9	4407.36	3.83	18.63	221.56	144394.66	0.11	26.67	13.46	12958.57	9631.62	6420.65	942.21	2695.08	14.73	373.85	8.51	1752.40	57420.56	276.13	1136.79	38.02	30.85
10	4637.46	5.01	32.72	237.10	121098.86	0.59	23.59	31.44	9001.81	8046.08	4265.55	489.19	1984.56	11.17	887.35	40.42	2933.51	35879.87	197.85	1948.42	32.42	3572.49
11	10771.61	5.31	40.58	593.43	140950.32	0.84	100.58	1002.15	25105.36	10630.21	8554.10	1268.09	5518.58	72.60	2108.14	467.30	12312.86	37506.31	313.84	3106.96	31.25	473.02
12	27294.63	9.70	30.02	507.77	83776.48	1.11	42.92	63.12	34884.27	22389.64	8554.05	900.81	4825.39	15.10	1867.21	30.86	1567.90	76863.79	274.40	2646.17	67.82	111.18

Table B4.2

IPERI index values for seven HMs across 12 soil samples.

	As	Cd	Cr	Cu	Ni	Pb	Zn	Σ
1	4.38	21.50	1.43	5.38	1.68	10.20	65.83	110.40
2	14.74	202.37	3.46	16.69	6.59	40.01	10.50	294.36
3	4.70	81.44	0.90	6.40	1.83	4.23	102.77	202.26
4	8.23	44.06	1.89	6.60	2.75	5.78	1.23	70.54
5	5.42	19.02	6.51	7.91	2.08	5.68	2.98	49.60
6	5.73	25.53	1.32	33.79	1.92	8.05	11.82	88.15
7	11.28	40.84	1.70	4.73	2.68	16.43	2.08	79.75
8	7.69	25.35	1.61	3.95	2.12	47.70	2.28	90.70
9	5.06	12.92	1.59	2.10	2.34	1.93	0.50	26.43
10	6.63	67.78	1.40	4.91	1.77	9.14	57.90	149.54
11	7.02	96.45	5.99	156.59	11.52	105.72	7.67	390.96
12	12.83	127.99	2.55	9.86	2.40	6.98	1.80	164.42

Table B4.3

SPERI index values for seven HMs across 12 soil samples.

	As	Cd	Cr	Cu	Ni	Pb	Zn	Σ
1	0.00	0.05	0.10	0.02	0.00	0.08	0.64	0.126
2	1.00	1.00	0.46	0.09	0.50	0.37	0.10	0.502
3	0.03	0.36	0.00	0.03	0.01	0.02	1.00	0.208
4	0.37	0.16	0.18	0.03	0.11	0.04	0.01	0.128
5	0.10	0.03	1.00	0.04	0.04	0.04	0.02	0.182
6	0.13	0.07	0.08	0.21	0.02	0.06	0.11	0.096
7	0.67	0.15	0.14	0.02	0.10	0.14	0.02	0.176
8	0.32	0.07	0.13	0.01	0.04	0.44	0.02	0.147
9	0.07	0.00	0.12	0.00	0.07	0.00	0.00	0.037
10	0.22	0.29	0.09	0.02	0.01	0.07	0.56	0.179
11	0.26	0.44	0.91	1.00	1.00	1.00	0.07	0.668
12	0.82	0.61	0.29	0.05	0.07	0.05	0.01	0.272

Figure B4.1

Correlogram showing Spearman's rs correlation coefficients among soil physicochemical parameters, bacterial family-level abundances, and elemental concentrations. Positive correlations are shown in blue, negative correlations in red, with the intensity and size of ellipses proportional to correlation strength. Black frames indicate statistically significant correlations ($p < 0.05$).

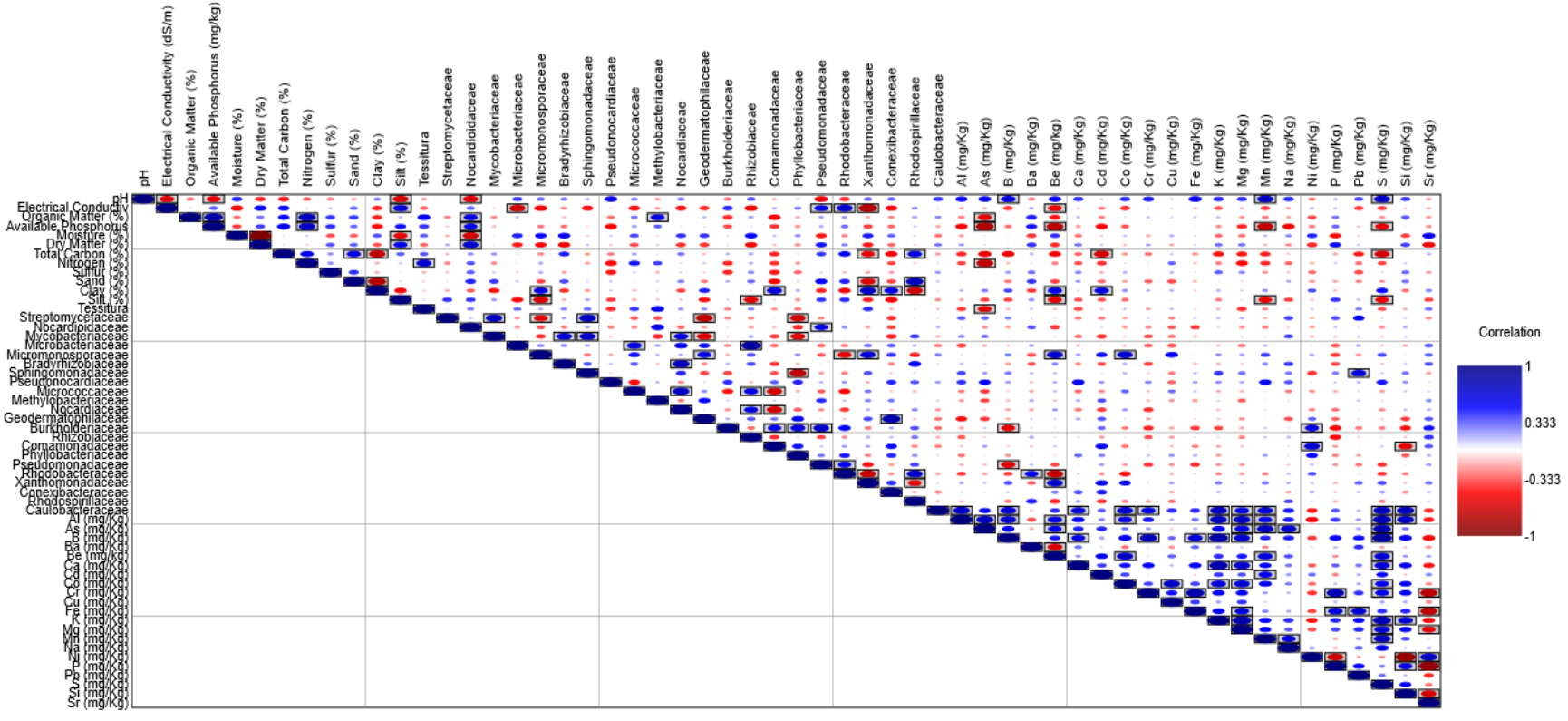

Figure B4.2

Decision classification/regression tree model (C&RT) based on the IPERI index. Values on the branches represent the abundance of microbial families, while the boxes contain mean values (mu) and variance (var) of IPERI.

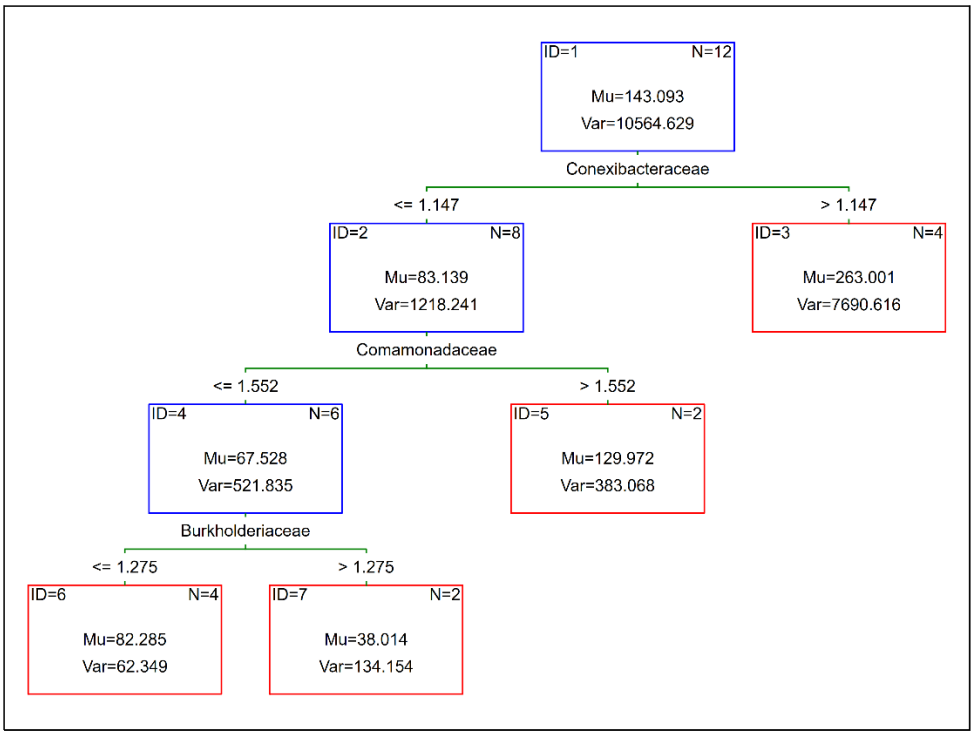

Figure B4.3

Scatter plot with linear regression between IPERI and SPERI indices ($R^2 = 0.896$)

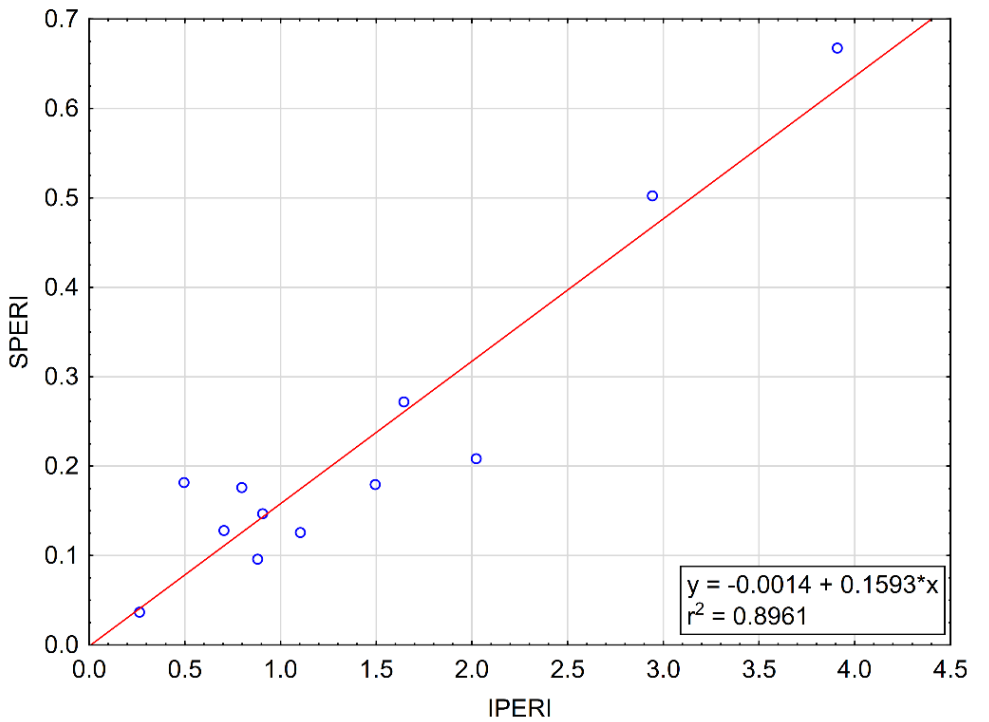

Annex C: Supplementary material for chapter 6

Table C6.1.

Coordinates (WGS84) of the 12 environmental sampling sites in the peri-urban area of Foggia, Italy. Each site is associated with a set of bacterial strains (n = 100), sequentially numbered according to the sampling location.

Sampling Site	Longitude	Latitude	Strains (from – to)
1	15.585849	41.422099	FG1-FG9
2	15.608232	41.444830	FG10-FG19
3	15.604090	41.466206	FG20-FG27
4	15.584307	41.477667	FG28-FG35
5	15.545304	41.477356	FG36-FG43
6	15.528977	41.482316	FG44-FG51
7	15.492058	41.474061	FG52-FG59
8	15.496651	41.452132	FG60-FG66
9	15.505415	41.433294	FG67-FG73
10	15.508348	41.413625	FG74-FG82
11	15.535685	41.421741	FG83-FG91
12	15.523417	41.370251	FG92-FG100

Table C6.2

Growth Index (GI, %) of *Pseudomonas* isolates after 48 h of incubation in liquid medium supplemented with 200mg/L of HMs: zinc (Zn), lead (Pb), chromium (Cr), arsenic (As), and copper (Cu).

Zn					Pb					Cr					As					Cu				
Strain	48h	48h II	Mean	Std. Dev.	Strain	48h	48h II	Mean	Std. Dev.	Strain	48h	48h II	Mean	Std. Dev.	Strain	48h	48h II	Mean	Std. Dev.	Strain	48h	48h II	Mean	Std. Dev.
1	110.87	110.93	110.90	0.03	1	58.42	58.57	58.50	0.07	1	81.25	81.48	81.37	0.12	1	89.13	89.32	89.22	0.09	1	139.67	139.74	139.71	0.03
2	43.87	44.00	43.93	0.07	2	75.68	75.80	75.74	0.06	2	61.12	61.25	61.19	0.06	2	58.21	58.40	58.31	0.10	2	108.11	108.29	108.20	0.09
4	120.63	120.74	120.69	0.05	4	104.76	104.88	104.82	0.06	4	53.97	54.17	54.07	0.10	3	20.40	20.57	20.49	0.08	3	86.10	86.18	86.14	0.04
5	82.58	82.77	82.68	0.10	5	84.68	84.87	84.78	0.09	5	46.25	46.33	46.29	0.04	4	140.74	140.94	140.84	0.10	4	126.45	126.63	126.54	0.09
7	52.88	52.96	52.92	0.04	6	141.33	141.49	141.41	0.08	6	23.47	23.67	23.57	0.10	5	104.80	104.97	104.89	0.08	5	137.24	137.45	137.34	0.11
8	2.02	2.23	2.13	0.11	7	47.64	47.73	47.69	0.04	8	42.75	42.97	42.86	0.11	6	130.10	130.23	130.17	0.06	6	128.57	128.64	128.60	0.03
12	57.74	57.83	57.79	0.05	8	52.11	52.29	52.20	0.09	10	31.08	31.26	31.17	0.09	7	21.99	22.08	22.03	0.04	8	53.58	53.72	53.65	0.07
15	63.18	63.32	63.25	0.07	9	84.02	84.10	84.06	0.04	11	50.25	50.35	50.30	0.05	8	27.16	27.27	27.21	0.06	9	27.40	27.46	27.43	0.03
20	35.11	35.22	35.16	0.06	10	58.46	58.61	58.53	0.07	12	21.26	21.45	21.35	0.09	9	96.35	96.48	96.41	0.07	10	67.23	67.37	67.30	0.07
26	31.42	31.56	31.49	0.07	11	81.86	82.03	81.94	0.08	13	20.63	20.72	20.68	0.04	10	46.00	46.21	46.10	0.10	12	18.90	19.04	18.97	0.07
27	33.23	33.29	33.26	0.03	12	27.03	27.28	27.16	0.12	15	24.83	24.95	24.89	0.06	12	85.30	85.47	85.38	0.08	13	53.57	53.66	53.61	0.04
28	140.68	140.89	140.79	0.10	13	65.87	66.04	65.96	0.08	20	2.13	2.24	2.18	0.05	13	21.30	21.48	21.39	0.09	15	76.69	76.78	76.73	0.05
32	102.46	102.57	102.51	0.06	14	78.42	78.56	78.49	0.07	27	88.00	88.11	88.06	0.06	15	75.34	75.53	75.44	0.10	16	62.28	62.37	62.33	0.04
56	45.91	46.11	46.01	0.10	15	41.89	41.97	41.93	0.04	28	13.69	13.84	13.76	0.08	18	59.05	59.12	59.08	0.04	20	89.06	89.18	89.12	0.06
57	47.76	47.90	47.83	0.07	16	55.02	55.09	55.05	0.04	30	12.93	13.16	13.04	0.11	20	95.29	95.51	95.40	0.11	23	57.83	58.01	57.92	0.09
59	132.30	132.46	132.38	0.08	18	27.75	27.94	27.84	0.09	31	33.46	33.59	33.52	0.06	23	58.67	58.76	58.72	0.04	24	55.13	55.31	55.22	0.09
60	20.00	20.12	20.06	0.06	19	44.75	44.89	44.82	0.07	33	23.06	23.29	23.17	0.11	24	62.30	62.44	62.37	0.07	25	74.31	74.41	74.36	0.05
62	16.17	16.34	16.25	0.09	20	75.99	76.06	76.03	0.04	34	33.07	33.28	33.18	0.11	25	72.05	72.19	72.12	0.07	27	26.77	26.92	26.85	0.08

70	32.42	32.63	32.52	0.10	22	109.09	109.19	109.14	0.05	35	22.54	22.63	22.59	0.04	26	46.01	46.20	46.10	0.10	28	40.68	40.93	40.81	0.12
77	76.47	76.66	76.57	0.09	25	99.84	99.96	99.90	0.06	39	77.78	77.88	77.83	0.05	27	87.38	87.56	87.47	0.09	29	46.42	46.62	46.52	0.10
78	93.55	93.76	93.65	0.11	26	69.79	70.00	69.90	0.10	40	5.88	5.97	5.93	0.04	28	26.62	26.86	26.74	0.12	30	4.16	4.31	4.23	0.08
93	51.31	51.49	51.40	0.09	27	102.46	102.62	102.54	0.08	41	10.41	10.61	10.51	0.10	29	150.51	150.74	150.62	0.11	31	103.61	103.71	103.66	0.05
94	60.15	60.21	60.18	0.03	28	86.31	86.41	86.36	0.05	43	55.49	55.71	55.60	0.11	30	42.73	42.87	42.80	0.07	33	78.31	78.38	78.35	0.03
95	87.55	87.76	87.65	0.10	29	45.39	45.48	45.44	0.04	47	34.85	34.91	34.88	0.03	31	70.72	70.84	70.78	0.06	35	73.66	73.80	73.73	0.07
97	148.11	148.26	148.19	0.08	30	40.18	40.43	40.31	0.12	48	91.03	91.21	91.12	0.09	33	60.73	60.96	60.85	0.12	36	125.92	126.03	125.97	0.06
					31	34.79	35.02	34.91	0.12	53	15.63	15.74	15.68	0.06	34	88.33	88.43	88.38	0.05	40	25.21	25.33	25.27	0.06
					32	85.26	85.47	85.37	0.11	56	5.28	5.37	5.32	0.05	35	43.30	43.41	43.36	0.05	41	136.16	136.37	136.27	0.10
					33	85.16	85.25	85.21	0.05	57	3.59	3.76	3.67	0.08	36	125.46	125.67	125.57	0.11	43	5.27	5.48	5.38	0.10
					34	95.72	95.96	95.84	0.12	62	46.24	46.49	46.36	0.12	37	77.32	77.52	77.42	0.10	46	77.86	78.02	77.94	0.08
					35	39.06	39.24	39.15	0.09	63	85.92	86.00	85.96	0.04	39	61.46	61.66	61.56	0.10	47	83.30	83.48	83.39	0.09
					36	27.98	28.12	28.05	0.07	76	15.38	15.45	15.42	0.03	40	42.30	42.49	42.39	0.10	48	110.76	110.95	110.85	0.09
					37	51.76	51.98	51.87	0.11	78	46.24	46.40	46.32	0.08	42	35.00	35.16	35.08	0.08	50	105.82	106.01	105.92	0.10
					38	86.29	86.44	86.37	0.07	83	10.46	10.59	10.53	0.07	43	35.86	35.96	35.91	0.05	53	168.75	168.99	168.87	0.12
					39	57.64	57.75	57.69	0.06	88	69.81	69.92	69.87	0.05	47	12.70	12.92	12.81	0.11	56	81.00	81.10	81.05	0.05
					40	33.61	33.73	33.67	0.06	89	6.67	6.88	6.77	0.11	48	123.77	123.86	123.81	0.05	57	46.41	46.59	46.50	0.09
					41	68.77	68.99	68.88	0.11	90	14.43	14.61	14.52	0.09	50	80.95	81.14	81.05	0.09	58	175.30	175.37	175.34	0.03
					42	167.50	167.70	167.60	0.10	91	50.97	51.06	51.02	0.05	52	60.00	60.20	60.10	0.10	59	189.49	189.67	189.58	0.09
					43	85.65	85.89	85.77	0.12	92	90.29	90.54	90.41	0.12	53	150.78	150.96	150.87	0.09	60	73.33	73.42	73.38	0.04
					44	25.88	26.00	25.94	0.06	93	15.36	15.43	15.39	0.03	54	99.00	99.09	99.04	0.05	61	148.26	148.41	148.34	0.08
					46	32.63	32.72	32.68	0.04	94	60.15	60.23	60.19	0.04	55	171.07	171.26	171.16	0.10	62	12.78	12.88	12.83	0.05
					47	58.98	59.17	59.08	0.09	96	8.89	9.06	8.97	0.08	56	179.16	179.23	179.19	0.04	63	160.56	160.80	160.68	0.12
					48	60.99	61.06	61.02	0.04	98	41.67	41.86	41.76	0.10	57	93.50	93.59	93.54	0.05	64	12.92	13.16	13.04	0.12

	50	112.70	112.88	112.79	0.09		59	106.22	106.29	106.26	0.03	65	6.57	6.67	6.62	0.05
	52	81.50	81.65	81.58	0.08		60	157.04	157.28	157.16	0.12	67	85.98	86.09	86.03	0.06
	56	84.17	84.25	84.21	0.04		61	161.00	161.12	161.06	0.06	69	122.43	122.60	122.52	0.09
	57	77.80	77.89	77.84	0.04		62	81.20	81.44	81.32	0.12	70	115.93	116.06	116.00	0.07
	60	141.48	141.70	141.59	0.11		63	109.39	109.60	109.50	0.11	71	112.99	113.19	113.09	0.10
	61	98.07	98.16	98.11	0.05		64	88.28	88.47	88.37	0.10	73	6.01	6.17	6.09	0.08
	64	45.22	45.44	45.33	0.11		65	60.90	61.05	60.97	0.07	76	35.63	35.75	35.69	0.06
	65	68.86	69.00	68.93	0.07		66	136.57	136.80	136.69	0.12	77	48.74	48.88	48.81	0.07
	67	104.26	104.48	104.37	0.11		67	110.98	111.12	111.05	0.07	78	159.13	159.38	159.26	0.12
	69	44.16	44.34	44.25	0.09		68	69.91	70.12	70.02	0.11	79	15.26	15.33	15.30	0.03
	73	125.14	125.27	125.20	0.07		69	98.83	99.03	98.93	0.10	81	63.37	63.50	63.43	0.06
	75	97.92	98.02	97.97	0.05		70	108.24	108.37	108.30	0.06	83	131.70	131.87	131.79	0.09
	76	55.87	56.11	55.99	0.12		71	134.57	134.68	134.63	0.05	85	14.71	14.82	14.77	0.05
	78	140.86	141.06	140.96	0.10		72	34.29	34.49	34.39	0.10	86	143.75	143.89	143.82	0.07
	82	50.89	50.99	50.94	0.05		73	118.58	118.70	118.64	0.06	87	114.63	114.76	114.70	0.06
	83	135.29	135.38	135.34	0.05		74	84.72	84.81	84.77	0.04	89	84.85	84.93	84.89	0.04
	84	55.53	55.70	55.61	0.09		75	123.61	123.75	123.68	0.07	90	70.49	70.71	70.60	0.11
	85	145.23	145.38	145.30	0.07		76	57.49	57.59	57.54	0.05	91	9.73	9.92	9.83	0.10
	86	161.87	162.07	161.97	0.10		77	101.68	101.86	101.77	0.09	92	104.85	104.99	104.92	0.07
	87	96.95	97.17	97.06	0.11		78	158.06	158.13	158.10	0.03	93	143.45	143.65	143.55	0.10
	88	93.71	93.80	93.75	0.04		81	86.14	86.22	86.18	0.04	94	125.56	125.65	125.61	0.04
	89	96.97	97.09	97.03	0.06		82	52.38	52.62	52.50	0.12	96	109.52	109.59	109.55	0.03
	90	52.13	52.34	52.23	0.10		83	119.61	119.86	119.73	0.12	97	114.05	114.22	114.14	0.09
	92	135.92	136.12	136.02	0.10		84	67.34	67.41	67.37	0.03	98	59.87	59.96	59.91	0.04

	94	56.02	56.13	56.07	0.06		86	120.63	120.86	120.74	0.12	100	51.88	51.99	51.93	0.05
	95	86.31	86.41	86.36	0.05		88	161.01	161.21	161.11	0.10					
	96	96.19	96.27	96.23	0.04		89	51.52	51.72	51.62	0.10					
	97	122.70	122.86	122.78	0.08		90	120.66	120.88	120.77	0.11					
	98	38.16	38.24	38.20	0.04		91	198.44	198.51	198.48	0.03					
							92	128.15	128.22	128.19	0.04					
							93	110.49	110.68	110.59	0.10					
							94	121.43	121.49	121.46	0.03					
							95	118.67	118.92	118.80	0.12					
							96	56.51	56.58	56.55	0.04					
							97	163.24	163.38	163.31	0.07					
							98	97.15	97.34	97.24	0.09					
							99	115.91	116.02	115.97	0.06					
							100	110.82	110.96	110.89	0.07					

Table C6.3

Growth Index (GI, %) of *Pseudomonas* isolates after 48 h of incubation in liquid medium supplemented with 300mg/L of HMs: zinc (Zn), lead (Pb), chromium (Cr), arsenic (As), and copper (Cu).

Zn					Pb					Cr					As					Cu				
Strain	48h	48h II	Mean	Std. Dev.	Strain	48h	48h II	Mean	Std. Dev.	Strain	48h	48h II	Mean	Std. Dev.	Strain	48h	48h II	Mean	Std. Dev.	Strain	48h	48h II	Mean	Std. Dev.
1	26.56	26.69	26.63	0.06	4	38.06	38.31	38.19	0.12	27	51.30	51.45	51.37	0.08	1	29.24	29.37	29.30	0.06	1	66.07	66.19	66.13	0.06
4	81.59	81.75	81.67	0.08	5	57.03	57.22	57.13	0.10	63	16.03	16.16	16.09	0.06	2	18.34	18.53	18.44	0.10	2	45.27	45.43	45.35	0.08
5	71.88	72.05	71.96	0.09	6	22.75	22.98	22.86	0.12						4	108.39	108.45	108.42	0.03	3	42.50	42.57	42.54	0.04
7	15.37	15.49	15.43	0.06	8	18.43	18.55	18.49	0.06						5	85.16	85.27	85.21	0.05	4	126.45	126.55	126.50	0.05
12	6.65	6.82	6.74	0.09	9	51.97	52.08	52.02	0.05						6	67.45	67.66	67.56	0.11	5	78.13	78.24	78.18	0.06
15	36.02	36.23	36.13	0.10	10	26.06	26.29	26.17	0.12						9	33.69	33.81	33.75	0.06	10	25.87	26.08	25.97	0.10
28	89.12	89.01	89.07	0.05	11	14.13	14.29	14.21	0.08						12	50.36	50.48	50.42	0.06	13	21.63	21.77	21.70	0.07
32	4.30	4.47	4.38	0.08	13	28.53	28.64	28.58	0.05						15	59.32	59.44	59.38	0.06	15	91.30	91.55	91.43	0.12
59	67.20	67.30	67.25	0.05	14	54.46	54.52	54.49	0.03						18	90.85	90.92	90.89	0.03	20	35.85	36.08	35.97	0.11
77	50.72	50.78	50.75	0.03	16	45.99	46.13	46.06	0.07						20	55.93	56.07	56.00	0.07	25	36.95	37.09	37.02	0.07
78	41.44	41.59	41.52	0.07	20	6.39	6.47	6.43	0.04						23	57.19	57.30	57.25	0.06	31	18.68	18.84	18.76	0.08
93	28.09	28.31	28.20	0.11	22	17.77	18.00	17.88	0.12						24	72.16	72.40	72.28	0.12	36	15.51	15.61	15.56	0.05
94	24.94	25.19	25.07	0.12	25	75.86	76.04	75.95	0.09						25	71.59	71.76	71.68	0.08	41	61.46	61.66	61.56	0.10
95	23.20	23.44	23.32	0.12	26	81.92	82.11	82.02	0.10						27	97.93	98.15	98.04	0.11	53	7.64	7.83	7.74	0.09
97	141.11	141.22	141.17	0.06	27	103.11	103.31	103.21	0.10						29	35.94	36.14	36.04	0.10	56	40.51	40.59	40.55	0.04
					28	54.65	54.72	54.69	0.03						31	74.54	74.70	74.62	0.08	58	59.87	60.00	59.93	0.06
					32	52.34	52.43	52.39	0.04						33	56.36	56.51	56.44	0.07	59	48.62	48.79	48.71	0.08
					33	47.27	47.45	47.36	0.09						34	41.80	42.02	41.91	0.11	60	22.02	22.23	22.12	0.10
					34	21.96	22.14	22.05	0.09						36	51.51	51.66	51.58	0.08	61	59.44	59.60	59.52	0.08

37	46.95	47.10	47.02	0.08	37	57.75	57.85	57.80	0.05	63	76.72	76.81	76.76	0.05
39	12.77	13.00	12.89	0.12	39	39.28	39.38	39.33	0.05	69	17.94	18.07	18.01	0.06
41	16.70	16.93	16.81	0.11	42	60.07	60.19	60.13	0.06	70	73.81	73.90	73.85	0.05
42	37.00	37.20	37.10	0.10	48	68.36	68.43	68.40	0.03	71	44.40	44.59	44.49	0.10
43	134.48	134.72	134.60	0.12	50	90.04	90.13	90.09	0.04	89	100.40	100.56	100.48	0.08
47	96.00	96.13	96.07	0.07	52	52.63	52.78	52.71	0.08	93	29.03	29.12	29.07	0.05
48	22.52	22.60	22.56	0.04	53	67.52	67.71	67.61	0.10	94	63.47	63.67	63.57	0.10
50	36.36	36.58	36.47	0.11	54	90.49	90.70	90.60	0.11	97	103.33	103.53	103.43	0.11
52	30.77	30.86	30.81	0.05	55	69.96	70.13	70.05	0.09	98	48.48	48.71	48.60	0.11
56	73.32	73.47	73.39	0.07	56	66.60	66.67	66.64	0.04	100	27.29	27.49	27.39	0.10
57	45.68	45.90	45.79	0.11	57	69.38	69.47	69.43	0.04					
60	15.51	15.67	15.59	0.08	59	39.22	39.34	39.28	0.06					
61	41.77	41.83	41.80	0.03	60	41.01	41.08	41.05	0.04					
65	107.95	108.01	107.98	0.03	61	125.30	125.39	125.35	0.04					
67	17.28	17.42	17.35	0.07	62	69.25	69.43	69.34	0.09					
73	71.03	71.20	71.12	0.08	63	84.35	84.47	84.41	0.06					
75	34.40	34.49	34.45	0.05	64	57.00	57.09	57.04	0.05					
76	64.56	64.70	64.63	0.07	65	45.48	45.56	45.52	0.04					
78	90.99	91.22	91.11	0.12	66	71.03	71.18	71.11	0.08					
82	22.63	22.73	22.68	0.05	67	53.46	53.57	53.51	0.06					
83	97.50	97.70	97.60	0.10	68	42.37	42.60	42.49	0.11					
84	65.82	65.91	65.86	0.05	69	80.66	80.78	80.72	0.06					
85	16.09	16.34	16.22	0.12	70	155.24	155.44	155.34	0.10					
86	48.65	48.85	48.75	0.10	71	96.92	97.15	97.04	0.12					
87	30.08	30.23	30.15	0.07	73	124.83	124.91	124.87	0.04					
89	39.36	39.48	39.42	0.06	74	62.26	62.43	62.35	0.08					

	90	99.03	99.19	99.11	0.08		75	55.96	56.13	56.05	0.08	
	92	136.84	136.92	136.88	0.04		76	43.96	44.05	44.00	0.05	
	94	24.72	24.94	24.83	0.11		77	55.50	55.56	55.53	0.03	
	95	64.99	65.08	65.04	0.04		78	146.85	147.03	146.94	0.09	
	96	57.53	57.65	57.59	0.06		81	42.17	42.28	42.23	0.06	
	97	118.33	118.57	118.45	0.12		82	37.33	37.58	37.46	0.12	
							83	77.71	77.85	77.78	0.07	
							84	31.82	31.92	31.87	0.05	
							86	67.12	67.18	67.15	0.03	
							88	63.99	64.05	64.02	0.03	
							89	44.18	44.30	44.24	0.06	
							90	121.04	121.18	121.11	0.07	
							91	124.33	124.41	124.37	0.04	
							92	118.20	118.32	118.26	0.06	
							93	40.45	40.67	40.56	0.11	
							94	49.00	49.18	49.09	0.09	
							95	46.00	46.13	46.06	0.07	
							96	30.33	30.43	30.38	0.05	
							97	132.22	132.42	132.32	0.10	
							98	61.40	61.52	61.46	0.06	
							99	50.00	50.20	50.10	0.10	
							100	61.23	61.31	61.27	0.04	

Table C6.4

Residual concentrations (mg/L) of individual HMs measured in culture supernatants after 48 h of incubation with *Pseudomonas* isolates.

Cr			Zn			Cu			As			Pb		
Sample	**Mean**	**Std. Dev.**	**Sample**	**Mean**	**Std. Dev.**	**Sample**	**Mean**	**Std. Dev.**	**Sample**	**Mean**	**Std. Dev.**	**Sample**	**Mean**	**Std. Dev.**
1	61.42	0.04	1	47.48	0.04	1	101.06	0.04	4	60.62	0.04	5	56.69	0.09
2	63.94	0.04	4	49.50	0.08	4	100.90	0.10	5	61.64	0.10	9	60.38	0.06
4	63.02	0.04	5	48.42	0.14	5	100.15	0.09	6	59.02	0.06	14	56.74	0.04
11	65.11	0.03	7	46.09	0.05	15	100.66	0.04	12	61.50	0.12	25	64.16	0.10
27	57.68	0.08	12	50.16	0.14	41	90.45	0.09	15	59.42	0.12	26	43.20	0.06
39	61.41	0.03	15	48.88	0.10	58	90.59	0.11	18	61.74	0.04	27	14.69	0.11
43	56.38	0.14	28	45.12	0.02	61	98.26	0.06	20	63.19	0.07	28	33.60	0.04
48	65.49	0.05	32	47.13	0.13	63	94.43	0.09	23	61.57	0.05	32	46.36	0.08
63	60.36	0.08	59	47.48	0.08	70	96.07	0.13	24	65.67	0.07	43	30.04	0.08
88	58.63	0.09	77	42.20	0.12	89	81.77	0.11	25	76.01	0.13	47	47.97	0.09
91	65.42	0.12	78	45.11	0.09	94	87.87	0.07	27	63.59	0.07	57	33.05	0.11
92	63.98	0.02	93	50.52	0.14	97	97.65	0.05	31	62.67	0.03	65	60.56	0.06
94	57.30	0.12	94	62.83	0.09				33	62.41	0.03	73	51.86	0.12
			95	44.39	0.13				36	61.41	0.11	76	19.70	0.04
			97	44.46	0.14				37	62.61	0.09	78	35.35	0.03
									42	61.35	0.11	83	69.90	0.04
									48	61.66	0.02	84	38.55	0.07
									50	61.47	0.07	90	53.73	0.03
									52	61.55	0.07	92	59.50	0.14
									53	62.39	0.13	95	67.40	0.06
									54	62.75	0.13	96	86.30	0.10
									55	0.30	0.08	97	68.27	0.13
									56	60.76	0.06			
									57	61.07	0.05			
									61	61.55	0.03			
									62	60.66	0.04			
									63	59.79	0.07			
									64	57.14	0.10			
									66	57.50	0.10			
									67	60.91	0.13			
									69	60.41	0.11			
									70	59.58	0.08			
									71	60.60	0.12			
									73	59.84	0.08			

			74	61.95	0.09	
			75	62.84	0.04	
			77	59.23	0.07	
			78	61.19	0.03	
			83	59.98	0.08	
			86	58.60	0.02	
			88	60.99	0.13	
			90	58.29	0.07	
			91	55.94	0.06	
			92	57.34	0.14	
			97	59.19	0.13	
			98	60.48	0.02	
			99	59.97	0.13	
			100	54.27	0.05	

Table C6.5

List of bacterial isolates obtained from contaminated soil samples, with corresponding GenBank accession numbers for 16S rRNA gene sequences.

Isolate	Accession Number
FG1	PX352722
FG4	PX352723
FG12	PX352724
FG15	PX352725
FG25	PX352726
FG27	PX352727
FG28	PX352728
FG32	PX352729
FG43	PX352730
FG48	PX352731
FG55	PX352732
FG57	PX352733
FG61	PX352734
FG63	PX352735
FG73	PX352736
FG76	PX352737
FG77	PX352738
FG78	PX352739
FG83	PX352740
FG88	PX352741
FG90	PX352742
FG91	PX352743
FG92	PX352744
FG94	PX352745
FG95	PX352746
FG97	PX352747

Figure C6.1

Heatmap showing Growth Index (GI) (%) values of *Pseudomonas* isolates under osmotic stress induced by PEG at concentrations of 5%, 10%, 15%, and 20%. Isolates are grouped in numerical order and displayed along the x-axis (A from strain 1 to 33, B: from strain 34 to 66, C: from strain 67 to 100). GI values are color-coded from dark green (strong inhibition, GI = –100) to dark red (slightly enhanced growth, GI = +60).